RADIO ASTRONOMY

Journal of the Society of Amateur Radio Astronomers
May - June 2023

Detecting Vela Pulsar Glitches with Steve Olney
Southern Hemisphere Contributor

Dr. Richard A. Russel
SARA President and Editor

Bogdan Vacaliuc
Contributing Editor

Radio Astronomy is published bimonthly as the official journal of the Society of Amateur Radio Astronomers. Duplication of uncopyrighted material for educational purposes is permitted but credit shall be given to SARA and to the specific author. Copyrighted materials may not be copied without written permission from the copyright owner.

Radio Astronomy is available for download only by SARA members from the SARA web site and may not be posted anywhere else.

It is the mission of the Society of Amateur Radio Astronomers (SARA) to: Facilitate the flow of information pertinent to the field of Radio Astronomy among our members; Promote members to mentor newcomers to our hobby and share the excitement of radio astronomy with other interested persons and organizations; Promote individual and multi station observing programs; Encourage programs that enhance the technical abilities of our members to monitor cosmic radio signals, as well as to share and analyze such signals; Encourage educational programs within SARA and educational outreach initiatives. Founded in 1981, the Society of Amateur Radio Astronomers, Inc. is a membership supported, non-profit [501(c) (3)], educational and scientific corporation.

Cover Photo:
Steve Olney

Contents

President's Page

The second half of 2023 is full of exciting opportunities!

The SARA Annual Conference at the Green Bank Observatory will be held 20-22 August. This will be a combined live and virtual conference and is already full of excellent speakers.

The SARA elections will also be held during the conference. There are two officer positions open, (secretary and treasurer), plus 2 director and 2 director at large positions. This is your chance to get involved with operating a multi-national organization!

We are also looking to fill the education and membership chair positions. They will lead the organization in training and mentoring in all aspects of SARA.

Membership success: The SARA membership has increased 20% in the past 12 months. The YouTube Channel has increased 185%.

The SARA Hydrogen Observing Overall Survey (SHOOS) observation program is the first major hydrogen data collection effort made by SARA. This program will allow members to develop their hydrogen observing telescopes and procedures as well as developing a repository of Northern and Southern hemisphere hydrogen data that can be shared by members, scientists, and students.

Three zoom meetings a month provide ready access to fellow radio astronomers as well as tie the organization in with worldwide members located in North America, Europe, Asia, and Australia.

Thanks!

Rich
SARA President

Editor's Notes

We are always looking for basic radio astronomy articles, radio astronomy tutorials, theoretical articles, application and construction articles, news pertinent to radio astronomy, profiles and interviews with amateur and professional radio astronomers, book reviews, puzzles (including word challenges, riddles, and crossword puzzles), anecdotes, expository on "bad astronomy," articles on radio astronomy observations, suggestions for reprint of articles from past journals, book reviews and other publications, and announcements of radio astronomy star parties, meetings, and outreach activities.

Subscribe to the SARA YouTube Channel

SARA has a YouTube channel at: https://www.youtube.com/channel/UC-SzptAQZ-20c9CkRb9ZPxw/videos

We are also looking to add content to the site. Anyone who wants to help produce a series of 5 - minute videos relating to radio astronomy technology or observations please contact me. (drrichrussel@netscape.net)

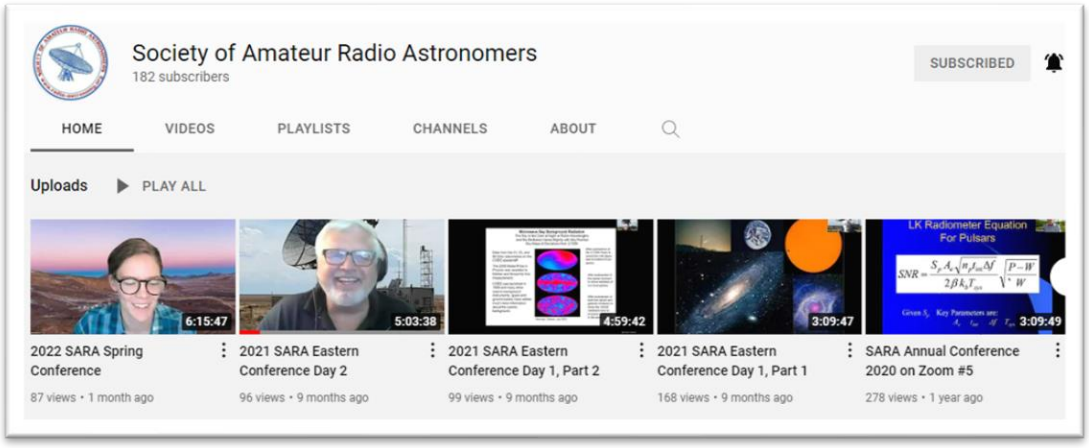

Observation Reports

We are now accepting 1-2 page observation reports. These reports should include the astronomical object's RA/DEC plus UTC of the observation. Also include the telescope configuration, process used to observe the object and results. Picture of the setup and plots of the observation are a plus to the report.

If you would like to write an article for Radio Astronomy, please follow **the newly updated Author's Guide** on the SARA web site:
http://www.radio-astronomy.org/publicat/RA-JSARA_Author's_Guide.pdf.

Let us know if you have questions; we are glad to assist authors with their articles and papers and will not hesitate to work with you. You may contact your editors any time via email here: edit@radio-astronomy.org.

The editor(s) will acknowledge that they have received your submission within two days. If they do not reply, assume they did not receive it and please try again.

Please consider submitting your radio astronomy observations for publication: any object, any wavelength. Strip charts, spectrograms, magnetograms, meteor scatter records, space radar records, photographs; examples of radio frequency interference (RFI) are also welcome.
Guidelines for submitting observations may be found here: http://www.radio-astronomy.org/publicat/RA-JSARA_Observation_Submission_Guide.pdf

SARA NOTES

2023 Request for Nominations for Officers and Directors

As required by Section 3 of SARA By-Laws (see below), this is the official call for nominations for SARA officers and board members. If you are interested in running for office and would like to know more about the positions, please contact a board member or SARA President Rich Russel. The requirement to be on the board is to attend the board meetings at the annual meeting and to actively participate in board-related activities. If you are unable to attend the annual meetings, then the director at large position may be for you. This position is a full board position except that attending the annual meeting is not required. The following positions will be up for election in Aug 2023: Secretary, Treasurer, two Directors at Large and two regular Directors. If you would like to run for one of the available SARA officer or board positions, please send a note to Secretary Bruce Randall copying President Rich Russel.

Contact information:
Bruce Randall: brandall@comporium.net
Dr. Rich Russel: drrichrussel@netscape.net

Please Note: It is important to get someone's permission before nominating them!

Text from the By-Laws: SECTION 3:
Elections of Directors and Officers will be accomplished by the President placing an initial call for nominations in "The Journal" no less than ninety (90) days prior to the regular scheduled meeting. Two (2) nominations from different members will be required to nominate a member for an office. No less than thirty (30) days prior to this meeting (in a newsletter issued prior to the meeting), the President will place a notice of the results of the nominations in "The Journal", along with a ballot for the members to use to vote for the nominee of their choice. This ballot will be forwarded to the Secretary for collection and counting at the regular meeting.

Responsibilities of Directors:
The Director needs to respond to and vote on business brought before the BOD. This includes the SARA annual meeting, email meetings, and teleconference meetings such as Zoom.

Responsibilities of Secretary:
A. Record minutes of all SARA BOD meetings at annual meeting, and other meetings as needed.
B. Send minutes to all BOD members for corrections and approval.
C. Publish minutes on SARA web site through web master.
D. Make call for nominations.
E. Record nominations and prepare ballot.
F. Tally election result with assistance and observation of two other members.
G. Record election results.

Responsibilities of Treasurer:
A. Deposit funds into bank account in a timely fashion.
B. Manage PayPal account.
C. Record all financial transaction.

D. Pay all SARA bills on time.
E. Reconcile bank and PayPal statements.
F. File Form 990EZ with IRS by November 15th
G. Maintain membership records.
H. Send renewal notice to members.
I. Email members when a new Journal is available.
J. Send list of new members to be in next Journal.
K. Handle sales of SARA items.

SARA Student & Teacher Grant Program

All, SARA has a grant program that is, sad to say very underutilized. We will provide kits or money to students and teachers including college students to help them with a radio telescope project. SARA can supply any of the following kits:

[1] SuperSID
[2] Scope in a Box
[3] IBT (Itty Bitty Telescope)
[4] Radio Jove kit
[5] Inspire
[6] Sky Scan

We can also provide up to five hundred dollars ($500.00 USD) for an approved radio telescope project.

We have on occasion provided more money based on the merits of the project and the SARA Grant Committee approval.

More information on the grant program can be found at the URL below.
SARA Student and Teacher Project Grants | Society of Amateur Radio Astronomers (radio-astronomy.org)

All that is required is the SARA grant request form be filled out and sent in. If it needs more work for approval, we will work with the student to help ensure their success.

Please pass the word that SARA will fund any legitimate radio telescope project anywhere in the world.

If you have a question, contact me at crowleytj at hotmail dot com.
Tom Crowley - SARA Grant Program Administrator

NEW Drake's Lounge Australia

This new zoom forum is geared to the Melbourne, Australia time zone (UTC+10) in order to improve coordination with our Australia, New Zealand, and Japanese members. The meetings are scheduled for the 4rth Friday of every month, 9 AM Melbourne time (2000 UTC December 23). A zoom announcement will be sent out to all SARA members before the meeting.

Radio Telescope Observation Party (RTOP)

RTOP is designed to demonstrate how to take observations using various radio telescopes. It will also cover how to record and analyze data.

RTOP is every month on the 1st Sunday at 2 pm Eastern time (1800 UTC). ZOOM email notifications will be sent to all members.

Drake's Lounge

Join the SARA community as we discuss the latest astronomy and radio astronomy news. The lounge also provides a forum to share and get advice on your radio astronomy projects from very experienced amateur radio astronomers.

Drake's Lounge is every month on the 3rd Sunday at 2 pm Eastern time (1800 UTC). ZOOM email notifications will be sent to all members.

SARA 2023 Eastern/Annual Conference

2023 SARA Eastern Conference
and
Global Radio Astronomy Symposium
Green Bank Observatory
Green Bank, West Virginia, 2023
20-22 August 2023

The 2023 SARA Eastern Conference and Global Radio Astronomy Symposium will be held at the Green Bank Observatory, West Virginia, Sunday through Tuesday, 20-22 August 2023. The conference will also be available as a fully interactive online event.

SARA has traditionally held our Eastern Conferences at GBO, and we are very pleased to return following a two-year hiatus due to the pandemic.

The first trailblazers of American radio astronomy called Green Bank Observatory (GBO) home over 60 years ago. Today, GBO is a world leader in advancing research, innovation, and education. Nestled in the mountain ranges and farmland of West Virginia, within the National Quiet Zone, radio astronomers are listening to the remote whispers of the universe, in order to discover answers to our most astounding astronomical questions.

Schedule: Conference meetings will be held in the main auditorium of the Jansky Laboratory at Green Bank Observatory with presentations by SARA members, GBO staff and distinguished speakers. Security and COVID restrictions permitting, tours of the facility, radio telescopes and laboratories will be conducted. Certain locations are open only to U.S. citizens who submit for a security review two weeks prior; however, other areas will be open to all attendees. ***Fully interactive online participation will be available for those who cannot attend in person.***

Key advantages of in-person attendance are training and hands-on use of the historical 40-foot radio telescope as well as user tutorial on the 20 Meter radio telescope.

Sunday through Tuesday evenings, round table discussions and refreshments are scheduled in the Drake's Lounge, and there will be space outside for attendees to set up and display their own portable radio astronomy systems and optical telescopes.

Meals in the GBO cafeteria are included in the registration fee for in-person attendees.

Virtual online sessions are available for those who cannot attend in person.

Lodging is not included in the conference registration fee. No-frills rooms and RV/camping sites are available at the nearby Boyer Station Motel and Campground. The Elk Springs Resort is about 12 miles away. Numerous VRBO / Airbnb properties and private rentals are nearby. A list of many properties is at https://pocahontascountywv.com/lodging/ . Many chain accommodations are located about 30 miles away in Elkins, but that drive takes at least an hour due to mountainous roads. (A few on-site dormitory rooms may become available for conference presenters and SARA officers, but additional rooms for other conference attendees are not expected.)

Registration: Registration for in-person attendance by SARA members at the Conference is $275.00 (USD) if received by July 20, 2023, which includes meals but not lodging. The fee for family members or other guests who do not participate in conference sessions is $75.00, which includes meals amd evening activities. Registration by July 20th for non-members is $295.00, which includes a year's membership in SARA. SARA members wishing to renew their membership at the same time as they register may also pay $295 and should include a renewal comment with their payment.

Late registration after July 20, 2023, is $325.00. Walk-in registration at the conference is $350.00.

Online participation is $35.00

Payment can be made through PayPal, www.paypal.com by sending payment to treasurer@radio-astronomy.org Please include in comments that the payment is for the **2023 Eastern Conference.**

Registration is also available on the SARA Store at these links:

On-Site Participation or **Online Participation**

Keynote Address: Dr. James M. Jackson

Dr. Jackson has served as Director of Green Bank Observatory since 2021. Previously, he served as Associate Director for Research for the Stratospheric Observatory for Infrared Astronomy (SOFIA) with the Universities Space Research Association (USRA). Dr. Jackson has also led administration and research in astronomy and astrophysics for the University of Newcastle (Australia) and Boston University and served as Assistant Director for the Center for Astrophysical Research in Antarctica. He has co-authored 148 journal articles, with over 12,000 total citations.

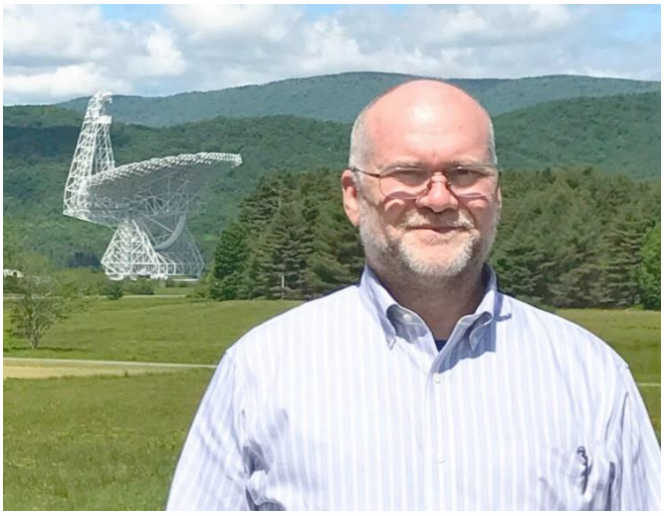

Dr. James M. Jackson, Director of Green Bank Observatory

Dr. Jackson is widely recognized for his research into star formation, galactic processes and the study of deep-space molecular emissions. He has published extensive research on the observation and analysis of molecular clouds and has done in-depth study of the Milky Way's Central Molecular Cloud Zone.

At ALMA, he was part of a distinguished research team that investigated G0.253+0.016, aka 'the Brick', one of the most massive (> 10^5 Msun) and dense (> 10^4 cm-3) molecular clouds in the Milky Way's Central Molecular Zone. Previous observations had detected tentative signs of active star formation, most notably a water maser that is associated with a dust continuum source. His team reported unambiguous evidence of active star formation within G0.253+0.016. They concluded that the sources are young and rapidly accreting and may potentially form intermediate and high-mass stars in the future. The masses and projected spatial distribution of the cores are generally consistent with thermal fragmentation, suggesting that the large-scale turbulence and strong magnetic field in the cloud do not dominate on these scales, and that star formation on the scale of individual protostars is similar to that in Galactic disc environments.

His Boston University lectures on "Fundamentals of Radio Astronomy" provide a foundation for understanding principles of antenna design and signal analysis. Of particular relevance is his explanations of beam patterns, directivity, gain, effective area, antenna temperature and sources of side lobes.

In his keynote address, Dr. Jackson will outline exciting new projects and research strategies now being undertaken at Green Bank and discuss long-term opportunities for the observatory.

Featured Presentation: Dr. Wolfgang Herrmann
President, Astropeiler Stockert, e.V., Germany

Dr. Herrmann's presentation will be on practical considerations for building small and medium-sized radio telescopes.

In recent years, the team at Astropeiler Stockert has been building and commissioning several radio telescopes varying in diameter from 3.2 meters to 1.2 meter. These are used mainly as instruments for lab courses and are designed to cover L-band to allow observation of hydrogen emission. The talk will cover the approach taken for each of these instruments for mount, feed horn, LNA and backend. Also, software designs will be discussed as well as performance parameters achieved for each design.
Dr. Herrmann received his PhD from the University of Bonn, where his thesis investigated laser spectroscopy, which was also the subject of his subsequent work at the IBM research labs in Zurich and the GKSS research center in Hamburg. He moved on to work in the telecommunication industry where he served as member of the board of a company that developed and produced advanced communication systems. Afterwards, he founded his own successful consulting company that supported major telecommunication carriers in the implementation of specialized radio and fixed line communication networks for the railway and aviation industry as well as high security networks for public administrations.

Currently, Dr. Herrmann serves as president of the Astropeiler Stockert group which operates one of the world's largest radio telescopes available to amateurs.

Conference Presentations

Introduction to Radio Astronomy
Ed Harfmann

The Sunday afternoon workshop session begins with an engaging and highly interactive presentation on the fundamentals of radio astronomy. Ed's presentation gives beginners all they need to know to get started yet will be informative to those who have spent years working in the field. This is both a "why to do it" and "how to do it" session.

Ed brings shares years of professional experience as he inspires and guides beginners and old-hands alike.

Hints and Kinks for Radio Astronomy
Charles Osborne

Immediately following the introductory session, Charles presents helpful guidance on how to set up and operate amateur radio telescopes with a view to avoiding the pitfalls which have frustrated many. Charles has managed large radio telescope research facilities and has designed and built his own amateur radio telescope systems at home, so his insight and advice can benefit everyone in the field.

40-Foot Radio Telescope Introduction and Operation
Hands-On Training and Workshop
Skip Crilly

For decades, the famous 40-foot radio telescope at GBO has been an important research and teaching instrument. Skip Crilly is one of the key volunteers at GBO responsible for maintaining this telescope and training others in its use. After a brief classroom introduction, Skip will move the session to the telescope control room where he will demonstrate how everything works before guiding the group as they learn to operate the telescope and interpret the data that is collected.

Twenty Meter Radio Telescope Introduction and Demonstration
Steve Tzikas

SARA has a user agreement with GBO which allows SARA members to remotely access and control the 20 Meter Radio Telescope. Certain security restrictions apply, but this telescope allows SARA members to conduct individual projects. Steve will cover:

- 20m Project Updates
- 20m Dish Demo

- 20m Useful Comments
- Raster Scans and Considerations
- 20m Observing Podcasts
- How to register and use the instrument

Easy Radio Astronomy
ezRA
Radio Astronomy Team, Little Thompson Observatory
Berthoud, Colorado

The software suite called ezRA (easy radio astronomy) is a free and easy way to get started in amateur radio astronomy. Ted Cline, N0RQV, developed this software and is a regular participant in SARA's online Drake's Lounge, where he is happy to answer questions and provide assistance.

Within minutes of powering on the system, an ezRA user can tell if her antenna is receiving HI (neutral Hydrogen emissions on 1420 MHz). Within a day, she may see the pattern of the Milky Way crossing overhead and verify antenna pointing accuracy and stability.

From a beginner's standpoint, it would be hard to make one's entry into radio astronomy easier.

As one gets more experienced with the software, ezRA has advanced features that allow researchers to plot complex galactic motions, structures, and anomalies.

The beauty of ezRA's graphics is dramatic and encouraging, even for a beginner in their first days.

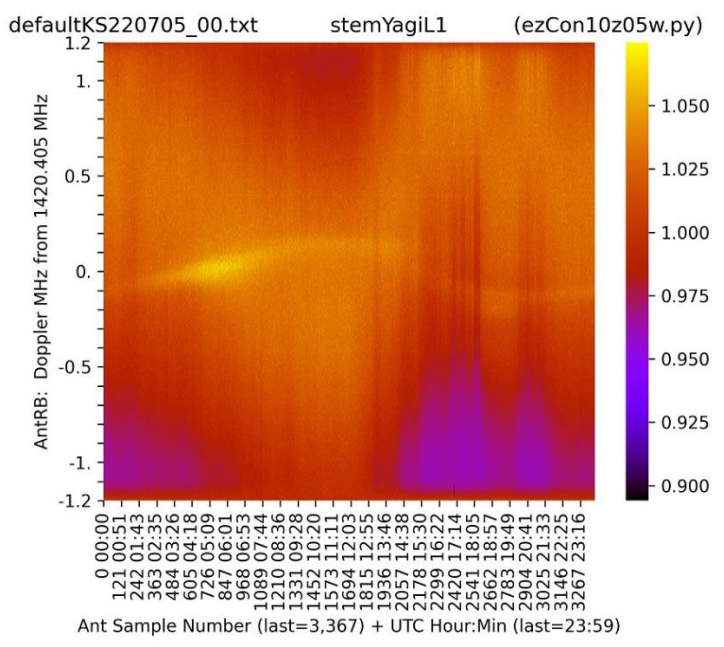

ezRA sky map made on the first day by students with $5 antenna and $80 receiver

STEMSAT-1 Project Update
Dr. J. Wayne McCain, Athens State University

STEMSAT-1 (formerly known as SARA-SAT1) is manifested for launch late fourth quarter 2023 on a Vaya Space hybrid rocket from Cape Canaveral Space Force Station along with another commercial satellite.

First announced at the 2017 Western Conference, the primary objective of this 3U cubesat is to involve students from kindergarten through college level in various aspects of designing, building, launch, and mission control of the satellite as a STEM learning activity. The secondary scientific mission is to monitor VLF (50-200 KHz range) radio signals that won't otherwise penetrate the Earth's atmosphere and translate that data to a UHF, 430 MHz that is transmitted to ground stations world-wide. This paper will update the progress on STEMSAT including the project's collaboration with SARA and opportunities for global amateur radio astronomy participation and ground station support.

Modeling a Three-Element Interferometer System
Dr. Richard Russel

Dr. Russel presents a method for modeling interferometer systems which may be useful for planning small to medium-size systems and explains how this method can be applied.

Dr. Rich Russel is SARA president and science lead for the Deep Space Exploration Society. He is a retired Northrop Grumman Senior Systems Engineer and served as the Chief Architect for the Satellite Control Network Contract (SCNC). In this capacity he was charged with planning the future architecture of the Air Force Satellite Control Network (AFSCN) and extending the vision to the Integrated Satellite Control Network (ISCN). Dr. Russel has been the lead architect and integrator for the Space-Based Blue Force Tracking project for U.S Space Command, the Center for Y2K Strategic Stability, and CUBEL Peterson. Dr. Russel also has led the SPAWAR Factory team in the deployment of the UHF Follow-On Satellite system. He has a Doctorate in Computer Science, an Engineers Degree in Aeronautics and Astronautics, a Master’s in Astronautical Engineering, and a Bachelor’s in Electrical Engineering. He is also certified as a Navy Nuclear Engineer and he is a retired Navy nuclear fast attack submariner and Navy Space Systems Engineer.

Antenna Arrays in Interstellar Communication
Skip Crilly

A hypothesis has been proposed and tested suggesting that interstellar communication signals might contain pairs of close frequency/time-spaced narrow bandwidth pulses. In addition to detectability, an important requirement in interstellar communication systems is the measurement of angle of signal arrival. Phased array receiving antennas, and interferometry, provide a method to make and calibrate these measurements, and to reduce confounding radio interference.

A twelve-element phased array system is under construction to search for hypothesized pulsed signals, anomalous given an RFI-augmented random noise model. This presentation will summarize the presenter’s past multi-telescope observations and reports, describe the phased array radio telescope

system under construction, explain reasoning behind the experimental methods, and seek ideas from conference attendees.

Skip presents both theoretical and practical approaches to radio astronomers interested in searching for evaluating signals that might indicate interstellar communications.

The Big Problem with Little c
B.J. Wilson, Little Thompson Observatory

Almost every calculation in astrophysics depends on an accurate determination of the speed of light, or "c." The problem is that the one-way speed of light has never been measured, and many theorize that it can never be measured by any means.

The importance of this issue was raised during a recent SARA conference when a high school STEM student in the audience asked our speaker, Nobel Laureate Dr. John C. Mather, challenging questions about distance to the source of cosmic microwave background radiation and whether conventional assumptions regarding the one-way speed of light in space could be defended scientifically. If, for instance, the one-way speed of light approached infinity, could the entire universe indeed be younger than 6,000 years? Without any reliable measurement of the one-way speed of light in space, the student asked, how could such a contrarian hypothesis of the universe be discounted?

This paper discusses the problem and proposes a global scientific initiative to find a method to definitively measure the one-way speed of light in deep space. The proposed mechanism is a "Reber Device."

Field Measurements and Front End Electronics for LWA Antennas
Whitham D. Reeve

Whit's presentation covers field measurements taken in New Mexico on the Long Wavelength Array system and provides technical and operational details for front end electronics.

What Green Bank Observatory Visitors Need to Know

COVID Restrictions. GBO reserves the right to impose requirements for vaccinations and masks. SARA will notify all registrants should GBO issue a policy statement. Should GBO policies adversely impact a conference registrant, they may change their registration from in-person to virtual / online and receive a refund for the difference. Should GBO close the campus for any reason, all registrations will be changed to virtual / online.

No Cellular Phone Service. GBO is in the National Radio Quiet Zone and there is no wireless phone service in the area. Use of wi-fi devices and satellite phones such as Iridium or Globalstar near the facility is not allowed, and severe restrictions are placed on digital cameras, although film cameras without electronic flash are allowed. There is a computer lab available during the day.

Pre-Conference Activities. Suggested pre-conference activities include free self-guided tours of the Green Bank Observatory Science Center and reasonably priced guided tours of the radio telescope area. Full details with a link for ticket purchase: https://greenbankobservatory.org/visit/
An overall guide to other activities and attractions in the area: https://pocahontascountywv.com/things-to-do/

Contact: Please contact the conference coordinator, B.J. Wilson, if you have any questions or if you would like to help with the conference: vicepresident@radio-astronomy.org

Additional Information: Additional details and updates will be published online at www.radio-astronomy.org and in the SARA journal, *Radio Astronomy*, as we get closer to the conference date.

National Radio Quiet Zone and Major Roads to Green Bank

Green Bank Observatory Site Map

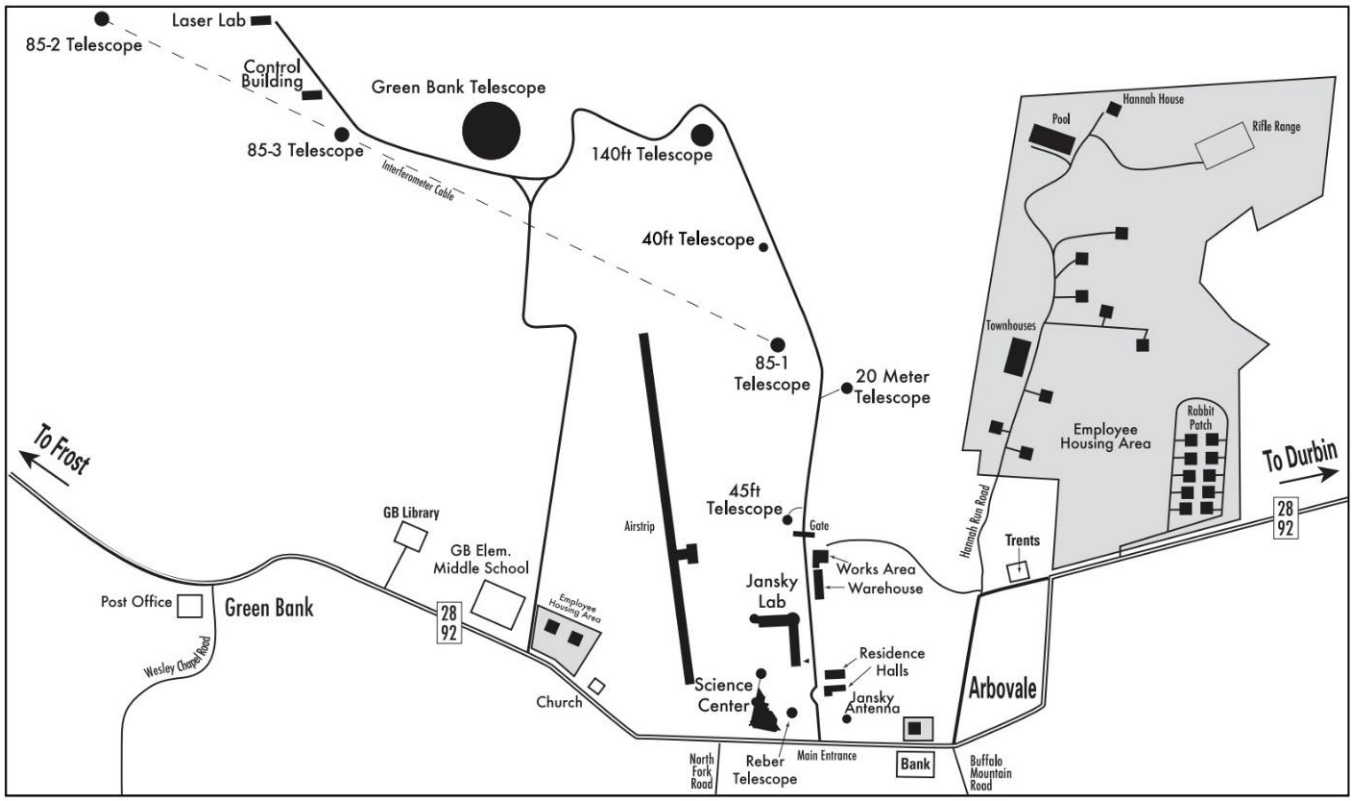

2023 SARA Annual Conference
and
Global Radio Astronomy Symposium

DAY	TIME	SPEAKER	TITLE
Sunday 8/20/2023	**Preconference Activities and Workshops** ***In-Person Only: Not Streamed Online***		
	8:30-11:30 AM	On-your-own no-cost tours of Green Bank Observatory Science Center, exhibits, gift shop. Suggested lunch at the GBO Starlight Café. Bus tour tickets are sold at the gift shop, but online advance purchase is highly recommended.	
	12:00 Noon	Registration at Jansky Lab Building, just down the hill from Science Center. Ask at gift shop if you need directions.	
	12:30 PM	Jay Wilson, Chair	Administrative Announcements Safety, RFI Rules and Security Reminder
	12:45 PM	Dr. Rich Russel SARA President	Welcome and Workshop Opening
	1:00 PM	Ed Harfmann	Introduction to Radio Astronomy
	2:15 PM	Charles Osborne	Radio Astronomy Hints and Kinks
	2:45 PM	Break	
	3:00 PM	Skip Crilly	40 Ft. Radio Telescope Overview
	3:20 PM	Skip Crilly	40 Ft. Radio Telescope Hands-On Workshop
	5:15 PM	Dinner at GBO Cafeteria	
	6:30 PM	Set Up Outside Experiments and Demonstrations	
	6:30 PM	Steve Tzikas	20m GBO Skynet Robotic Radio Telescope Workshop
	8:00 PM	Social at Drake's Lounge Informal technical roundtable Outside equipment demonstrations. 40-foot radio telescope available for individual use.	

Note: Times are for Green Bank, WV, which is U.S. Eastern Daylight Time (UTC minus 4).

Monday 8/21/2019	**SARA Annual Conference and Global Radio Astronomy Symposium** *In-Person at Green Bank Observatory with Interactive Online Sessions*		
	7:45 AM	Breakfast at GBO Cafeteria	
	8:30 AM		Registration at Jansky Lab Building
	9:00 AM	Jay Wilson, Chair	Administrative Announcements Safety, RFI Rules and Security Reminders
	9:15 AM	Dr. Rich Russel SARA President	Welcome and Conference Opening
	9:30 AM	Steve Tzikas	SARA Section Updates
	9:45 AM	David Westman	Western Conference Recap
	10:00 AM	Dr. Rich Russel	SARA Online Programs Online Drake's Lounge -- SARA RTOP SARA Drake's Lounge for Australia/New Zealand
	10:15 AM	Refreshment Break and Poster Session	
	10:30 AM	Dr. Wolfgang Hermann Astropeiler Stockert	Building Small and Medium Sized Radio Telescopes
	12:00 PM	Lunch at GBO Cafeteria	
	1:00 PM	Dr. James Jackson Director, Green Bank Observatory	Keynote Address
	3:00 PM	Refreshment Break and Poster Session	
	3:15 PM	Dr. Rich Russel	Modeling a 3-Element Interferometer System
	4:00	Dr. Wayne McCain	Radio Astronomy STEMSAT Progress Repot
	4:45 PM	Dr. Rich Russel SARA President	SARA Announcements
	5:00 PM	Bruce Randall SARA Secretary	Call for Nominations (End of online session)
	5:15 PM	Dinner at GBO Cafeteria	
	6:15 PM	Flea Market in Dorm Parking Lot	
	6:15 PM	Setup Outside Experiments	
	7:00 PM	Social at Drake's Lounge. Outdoor experiments 40-foot radio telescope available for individual use	

SARA Annual Conference and International Radio Astronomy Symposium *In-Person at Green Bank Observatory with Interactive Online Sessions*			
Tuesday 8/22/2023	7:45 AM	Breakfast at GBO Cafeteria	
	9:00 AM	Jay Wilson	Administrative Announcements
	9:10 AM	Charles Osborne	Remembering Recently Passed Members and Friends Adrian Howell Bill Lord Paul Oxley Frank Drake Others we should honor? Please share.
	9:15 AM	Dr. Rich Russel SARA President	SARA Elections conducted by Bruce Randall Installation of Officers Business Meeting
	10:00 AM	Coffee Break and Poster Session	
	10:15 AM	Jay Wilson	The Big Problem with Little c
	10:30 AM	Skip Crilly	Antenna Arrays for Interstellar Communications
	11:15 AM	LTO Staff	ezRA Easy Radio Astronomy
	11:45 AM	Open Mic	Open Mic
	12:30 PM	Lunch at GBO Cafeteria	
	1:30 PM	Group Picture	
	1:45 PM	Whitham Reeve	Field Measurements and Front End Electronics for LWA Antennas
	2:30 PM	DSES Science Team	Plishner Radio Telescope
	3:15 PM	Refreshment Break and Poster Session	
	3:30 PM	Open Mic	Open Mic
	4:00 PM	Dr. Rich Russel	Online Conference Wrap-up
	4:15 PM	SARA Officers	SARA Board of Directors Meeting
	5:15 PM	Dinner at GBO Cafeteria	
	6:15 PM	Flea Market in Dorm Parking Lot	
	6:15 PM	Set Up Outside Experiments	

	8:00 PM	Social at Drake Lounge. Outdoor experiments 40 foot radio telescope available for individual use

Note: Times are for Green Bank, WV, which is U.S. Eastern Daylight Time (UTC minus 4).

SARA Annual Conference and International Radio Astronomy Symposium *In-Person at Green Bank Observatory Only*			
Wednesday 8/23/2023	7:45 AM		Breakfast at GBO Cafeteria
	9:00 AM	Jay Wilson	Administrative Announcements
	9:15 AM	Sue Ann Heatherly	Technical Area Tours
	11:45 AM	Dr. Rich Russel	Conference Wrap-Up
	12:30 PM		Lunch at GBO Cafeteria

Note: Times are for Green Bank, WV, which is U.S. Eastern Daylight Time (UTC minus 4).

News: (May-June 2023)

EarthSky.org ~ *New supernova! Closest in a decade*
https://earthsky.org/todays-image/supernova-in-m101-pinwheel-galaxy-closest-in-a-decade-how-to-see/

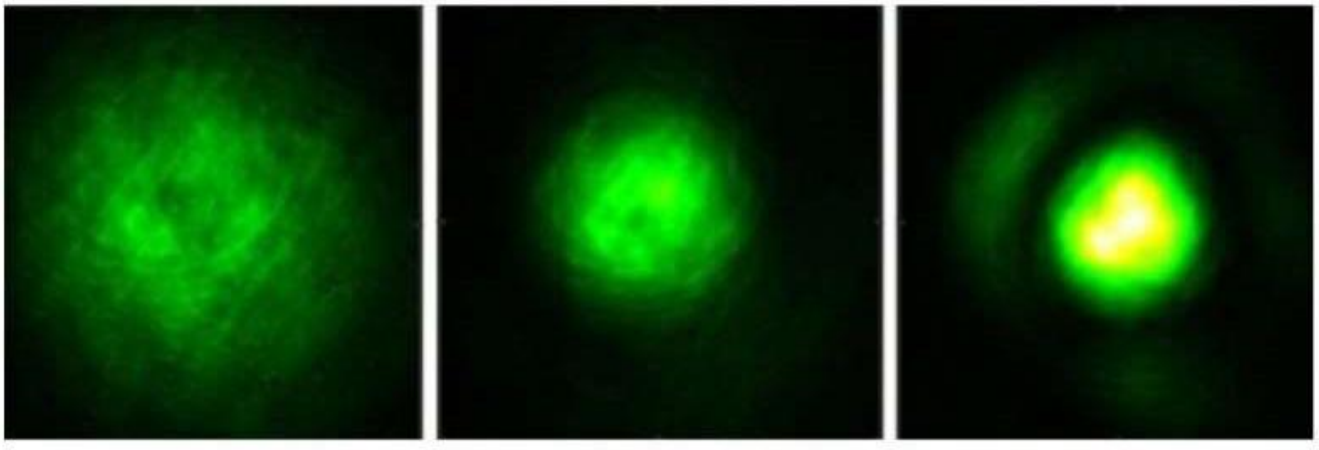

University of Maryland ~ *Experiment demonstrates continuously operating optical fiber made of thin air*
https://phys.org/news/2023-05-optical-fiber-thin-air.html

https://dx.doi.org/10.1364/OPTICA.487292

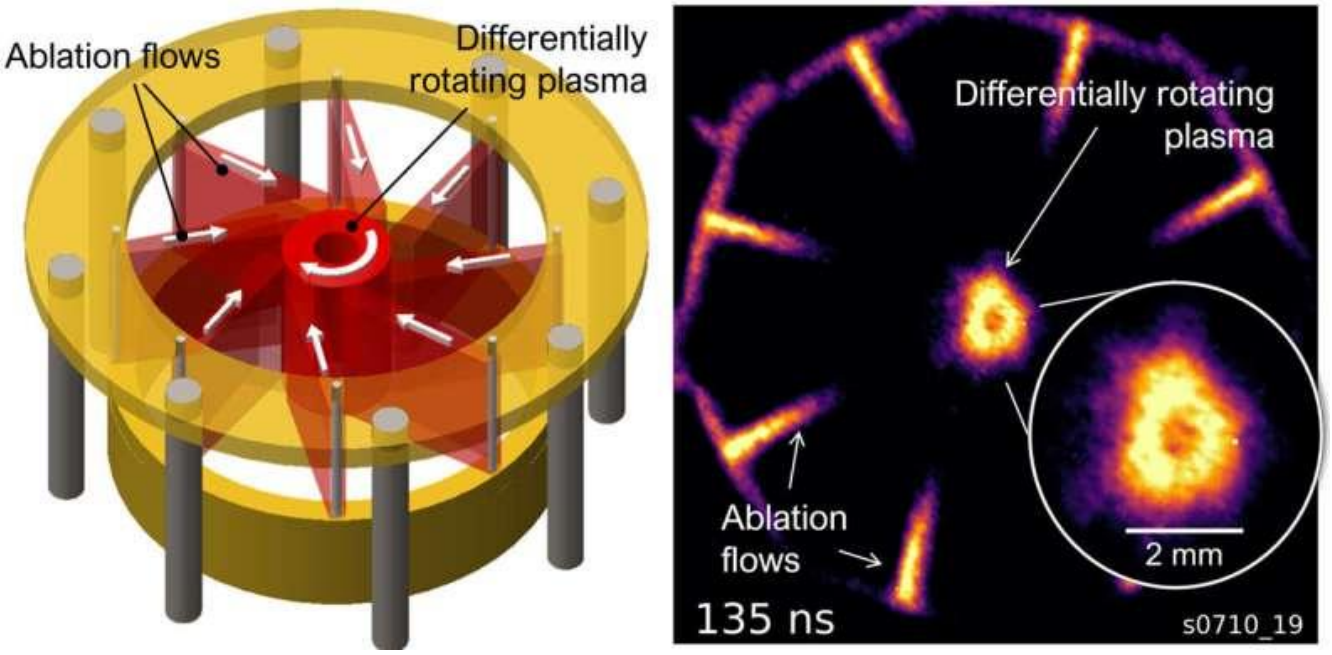

Imperial College of London ~ *Accretion disk around black holes recreated in the lab*
https://phys.org/news/2023-05-accretion-disk-black-holes-recreated.html
https://dx.doi.org/10.1103/PhysRevLett.130.195101

Universe Today ~ *NASA: We'd Have a 30-Minute Warning Before a Killer Solar Storm Hits Earth*
https://www.universetoday.com/161355/nasa-thinks-they-can-give-us-30-minutes-of-warning-before-a-killer-solar-storm-hits-earth/

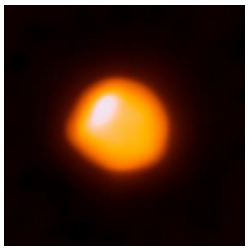

Universe Today ~ *Betelgeuse is Almost 50% Brighter Than Normal. What's Going On?*
https://www.universetoday.com/161751/betelgeuse-is-almost-50-brighter-than-normal-whats-going-on/
https://arxiv.org/pdf/2306.00287.pdf
Image Credit: ALMA (ESO/NAOJ/NRAO)/E. O'Gorman/P. Kervella

Amri Wandel ~ *The Fermi Paradox revisited: Technosignatures and the Contact Era*
https://arxiv.org/abs/2211.16505

Live Science ~ *Hundreds of ancient, invisible structures discovered near our galaxy's center*
https://www.livescience.com/space/black-holes/hundreds-of-ancient-invisible-structures-discovered-near-our-galaxys-center
https://iopscience.iop.org/article/10.3847/2041-8213/acd54b

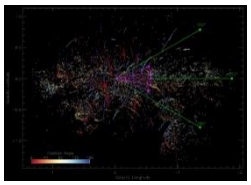

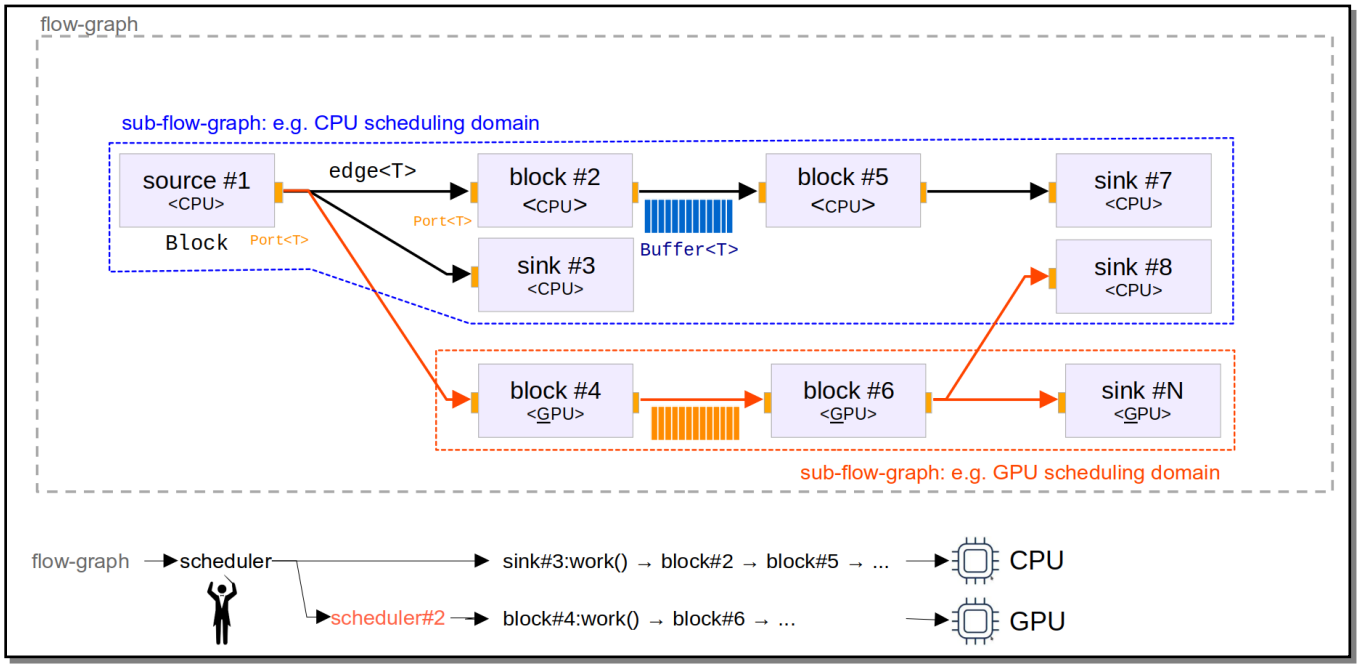

GNU Radio ~ *Further Evolving GNU Radio 4.0*
https://www.gnuradio.org/blog/2022-12-03-low_level_api/

Facialix ~ Google offers a free course to learn Rust: The programming language of the future

https://facialix.com/en/google-offers-a-free-course-to-learn-rust-the-programming-language-of-the-future/
https://google.github.io/comprehensive-rust/welcome.html

Whitney Knitter ~ FPGA and Pi in Space: Lattice Certus NX Space Dev Board
https://www.hackster.io/news/fpga-and-pi-in-space-lattice-certus-nx-space-dev-board-3e7f4a4d5fe7
https://www.adiuvoengineering.com/boards/lattice-certus-nx-space-dev-board

RTL-SDR.com ~ *uSDR: A TX/RX 300-3700 MHz, 30.72 MSPS Capable SDR with M.2 Interface and Web Browser Control*
https://www.rtl-sdr.com/usdr-a-tx-rx-300-3700-mhz-30-72-msps-capable-sdr-with-m-2-interface-and-web-browser-control/
https://www.crowdsupply.com/wavelet-lab/usdr

Raspberry Pi ~ *Bugg.xyz acoustic monitoring for conservationists*
https://www.raspberrypi.com/news/bugg-xyz-acoustic-monitoring-for-conservationists/
https://sarabsethi.github.io/autonomous_ecosystem_monitoring/
https://www.pnas.org/content/117/29/17049

Technical Knowledge & Education: (May-June 2023)

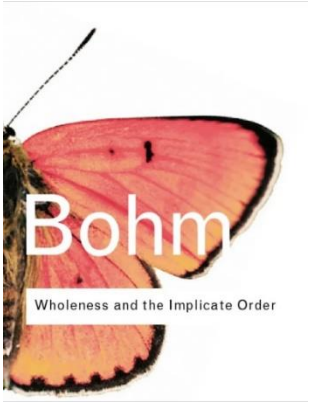

The Marginalian ~ *Wholeness and the Implicate Order: Physicist David Bohm on Bridging Consciousness and Reality*
https://www.themarginalian.org/2023/05/25/wholeness-and-the-implicate-order-david-bohm/

https://worldcat.org/title/35572685

Nature ~ *Don't feed the physicists*
https://www.nature.com/articles/d41586-023-01835-y

SARA ~ ezRA – Easy Radio Astronomy Analysis Tutorials:
- *Analysis 1- Introduction and Data Collectors*: https://youtu.be/ig_jPTuS8ZA
- *Analysis 2- Spreadsheet Analysis*: https://youtu.be/HkrIN9d6Hd8
- *Analysis 3- Signal Progression*: https://youtu.be/VIp7L6gIZPY
- *Analysis 4- More Plots and ezb file*: https://youtu.be/K02MADafOhc
- *Analysis 5- Interference Filters*: https://youtu.be/FeFk9EvITtc

SARA ~ *Radio Astronomy Video Series: Constants, Variables and Formulas, Radio Astronomy Formulas:*
- *Lesson 1- Parabolic Dish Gain*: https://www.youtube.com/watch?v=2bx5K9jUc_w
- *Lesson 2 -Parabolic Dish Half Power Beamwidth*: https://www.youtube.com/watch?v=XWOMRrwjkl8
- *Lesson 3 -Thermal Noise*: https://youtu.be/MMJ6Xvapt10
- *Lesson 4 -Focal Length and f/D*: https://youtu.be/Am6t06KqFPE
- *Lesson 5 -Feed Illumination Angle*: https://youtu.be/4RZzPzVBSJ4
- *Lesson 6 -Pointing Offset Gain Loss*: https://youtu.be/dQ8wAaTtm40
- *Lesson 7 -Measuring System Temperature (TSys)*: https://youtu.be/4gVUFFxra-U
- *Lesson 8 -Coax Attenuation Interpolation*: https://youtu.be/3B8hV6vFyo8
- *Lesson 9 -Pulsar math including electron density, distance, and age*: https://youtu.be/Bymdp--_3JU
- *Lesson 10 -Distance Math - AU, Parallax, Parsecs and Light Years*: https://youtu.be/6fo0y3fDOZs
- *Lesson 11 -Doppler Frequency and Relative Velocity Calculations*: https://youtu.be/8zKloAVpnJc
- *Lesson 12 -Pointing to the Milky Way using a Compass and Protractor*: https://youtu.be/33xeUSji94U
- *Lesson 13 -Radiometer Equation Basics*: https://youtu.be/vAyypJ8f2z8
- *Lesson 14 -Noise Figure and Noise Factor Calculations*: https://youtu.be/GD6wZhW5NPA
- *Lesson 15 -Interpreting Stokes Parameters*: https://youtu.be/wUVsbfURIsg

ASTROPEILER STOCKERT e.V.
Historische Radiosternwarte

European Conference on Amateur Radio Astronomy
EUCARA

Bad Münstereifel-Eschweiler, Germany
September 16th - 17th, 2023

Conference Announcement and Call for Papers

Background
EUCARA has been initiated in 2014 and has been held at the Astropeiler Stockert.
The next conferences took place in 2016 in Dwingeloo, 2018 again at Stockert, and 2021 as a virtual conference organized by the Dwingeloo team. Now it is time again to meet at Stockert.

The structure of the conference

EUCARA will be a two days conference on the weekend of September 16th and 17th, 2023. Saturday morning will be devoted to talks and the keynote speech by Dr. Laura Spitler from the Max-Planck Institute for Radio Astronomy. After lunch, we will depart by bus to a visit of the Effelsberg radio telescope. In the evening, there will be a conference dinner.

On Sunday, there will be talks in the morning. After lunch, in the afternoon there will be tours of the Stockert site with various demonstrations of the telescopes as well as individual discussions. The conference will close in the late afternoon on Sunday. For attendants arriving earlier on Friday, the conference site will be open for informal discussions and site tours.

The venue
The venue will be the facilities of the "Astropeiler Stockert" radio telescope, which comprises of several buildings and 6 radio telescopes (25-m, 10-m, 3-m, 2.3-m, 1.2m and a Ku-band interferometer). Presentations will be held in our conference room. Another room is available for lunch, coffee and individual discussions.

The site is located near the town of Bad Münstereifel in the west of Germany. The distance to Cologne and Bonn is about 50km.

For transportation and lodging information, please see the attached information sheet.

Registration
Important notice:
Due to the limited space at the Astropeiler Stockert and based on the experience from the previous conference, the number of attendants will be limited to a maximum of 40. Confirmation of registration will be on a first come,

first serve basis. After reaching the maximum number of registrations, further requests will be put on a waiting list.

Registration is now open. Registrations are requested by sending an email to eucara2023@astropeiler.de, giving the following information:

- Full name
- Affiliation (if any)
- Full postal address
- Email address
- Ham callsign (if any)

Registration fee

Please note that the conference fee still has to be determined based on incoming quotations. You can expect that the conference fee will be 100 EUR or less. This will cover the transportation by bus for the visit to Effelsberg, lunch, coffee and drinks for both days and some material needed. Please note that the conference dinner is not included and will be paid individually.

The conference fee shall be paid (once finally determined) via bank transfer to the account of Astropeiler Stockert e.V. Bank details are:

Raiffeisenbank Rheinbach Voreifel e.G.
IBAN DE88 3706 9627 0071 7580 10
BIC GENODED1RBC

Please give your name in the transfer so that we can allocate payments.

Conference language

The conference language will be English. Assistance on site in other languages can be provided in German and French.

Website

A conference website has been set up at
https://www.astropeiler.de/eucara/european-conference-on-amateur-radioastronomy-2023/
Additional information will be provided there as they become available.

Call for papers / presentations

We are asking for papers for presentation at the conference. If you are interested to present, please notify us by July 16th giving the title of the paper.

In the schedule, we have allocated time for a total of 12 presentations of 20 min each. Should the number of submissions exceed this limit, we will need to make a selection.
We will inform you about the acceptance of your paper by July 23rd.

If your paper is accepted, you are requested to submit an abstract for inclusion in the detailed program by August 6th. We are also requesting to provide your slides at least one week before the conference so that we can upload it to our presentation server.

We are planning to put the presentations on a web site after the conference. If you prefer not to make your material publicly available please indicate so.

Potential video streaming
Should the number of registration requests substantially exceed the number of available places, we are considering to provide a live stream of the talks. We are presently investigating the feasibility of this but cannot make a promise at this point in time.

Covid-19
At this time, there are no restrictions due to Covid-19.

Hotels

The town of Bad Münstereifel and the surrounding area has suffered a severe flooding in the summer of 2021. Still, a lot of restauration work is ongoing and as a consequence the choice of Hotels in Bad Münstereifel is limited. Additional opportunities are in the town of Euskirchen. One of the options there is:

Welcome Park Hotel
Alleestraße 1
53879 Euskirchen
Phone: +49 2251 7750
Mail: reservierung.eus@welcome-hotels.com

Furthermore, a few rooms are available at the “Hotel Kurhaus Uhlenberg” in Bad Münstereifel. Prices vary between 89 EUR and 149 EUR depending on size. For booking, contact is:

Hotel Kurhaus Uhlenberg
Uhlenbergweg 3
53902 Bad Münstereifel
Phone +49 2253 54270
Mail: info@kurhaus-uhlenberg.de

Other options can be found through booking.com or other hotel reservations services.

Transportation
The railway line between Euskirchen and Bad Münstereifel is not yet operational again after the flooding. However, there is a bus line instead running every 30 minutes. We will provide a shuttle service from the bus stop in Iversheim to the Astropeiler Stockert. If you stay in the Welcome Park Hotel, the bus stop in Euskirchen would be an easy walking distance from the hotel. If you stay in Bad Münstereifel, you can also catch a bus to Iversheim where we will pick you up.

Transportation to the Effelsberg telescope will be provided by bus. A shuttle service will also be available for going from the conference site to the conference dinner location and back.

SuperSID

SuperSID
Collaboration of Society of Amateur Radio Astronomers and Stanford Solar Center

- Stanford provides data hosting, database programming, and maintains the SuperSID website
- Society of Amateur Radio Astronomers (SARA) sells the SuperSID monitors for 48 USD to amateur radio astronomers and the funds are then used to support free distribution to students all over the world (image below as of Fall 2017)
-
- Jonathan Pettingale at SARA is responsible for building and shipping the SuperSID monitor kits: SuperSID@radio-astronomy.org
- SuperSID kits may be ordered through the SARA SuperSID webpage: http://radio-astronomy.org/node/210
- Questions about the SuperSID project may be directed to Steve Berl at Stanford: steveberl@gmail.com
- Jaap Akkerhuis at Stanford is responsible for the SuperSID software and SARA has provided financial support for his efforts
- SuperSID website hosted by Stanford: http://solar-center.stanford.edu/SID/sidmonitor/
- SuperSID database: http://sid.stanford.edu/database-browser/
- The data is searchable by time, station, date, and multiple plots may be placed on the same graph for comparison.
-

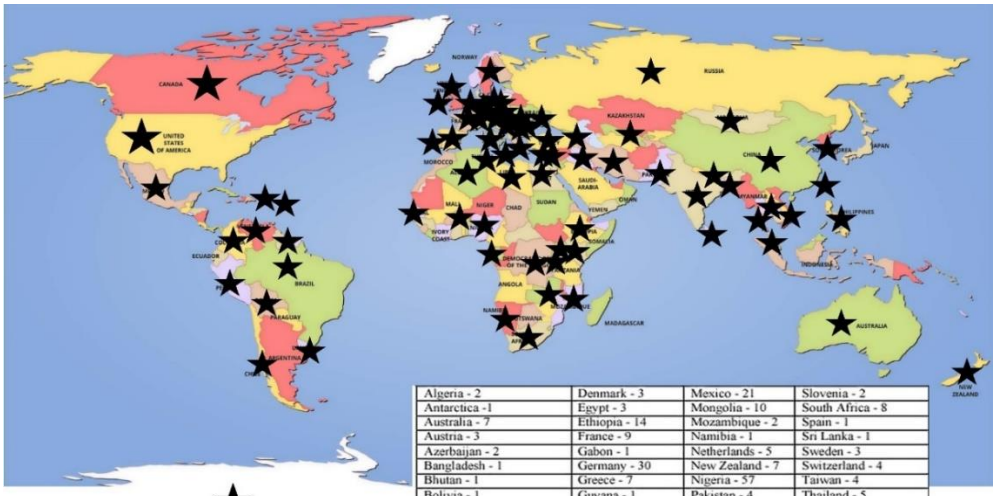

Algeria - 2	Denmark - 3	Mexico - 21	Slovenia - 2
Antarctica -1	Egypt - 3	Mongolia - 10	South Africa - 8
Australia - 7	Ethiopia - 14	Mozambique - 2	Spain - 1
Austria - 3	France - 9	Namibia - 1	Sri Lanka - 1
Azerbaijan - 2	Gabon - 1	Netherlands - 5	Sweden - 3
Bangladesh - 1	Germany - 30	New Zealand - 7	Switzerland - 4
Bhutan - 1	Greece - 7	Nigeria - 57	Taiwan - 4
Bolivia - 1	Guyana - 1	Pakistan - 4	Thailand - 5
Bosnia-Herzegovina - 2	Hungary - 1	Peru - 10	Tunisia - 9
Brazil - 11	India - 33	Philippines - 3	Turkey - 2
British Virgin Islands - 1	Indonesia - 2	Poland - 2	Uganda - 5
Bulgaria - 2	Iran - 4	Portugal - 3	UK - 32
Burkino Faso - 1	Iraq - 1	Rep of Congo - 3	Uruguay - 9
Canada - 33	Ireland - 9	Romania - 4	US Virgin Islands - 2
Chile - 1	Italy - 42	Russia - 3	USA - 491
China - 38	Kenya - 23	Rwanda - 1	Uzbekistan - 2
Columbia - 9	Korea (South) - 2	S Africa - 4	Venezuela - 2
Croatia - 7	Lebanon - 11	Senegal - 1	Vietnam - 1
Cypress - 1	Libya - 1	Serbia - 1	Zambia - 2
Czech Republic - 1	Malaysia - 19	Singapore - 3	
D Rep of Congo - 4	Malta - 1	Slovak Repub - 2	

For official use only
Monitor assigned: _____
Site name: _____
Country: _____

SuperSID Space Weather Monitor

Request Form

	Your information here		
Name of site/school *(if an institution)*:			
Choose a site name: *(3-6 characters) No Spaces*			
Primary contact person:			
Email:			
Phone(s):			
Primary Address:	Name School or Business Street Street City State/Province Country Postal Code		
Shipping address, if different:	Name School or Business Street Street City State/Province Country Postal Code		
Shipping phone number:			
Latitude & longitude of site:	Latitude: _____ Longitude: _____		

I understand that neither Stanford nor the Society of Amateur Radio Astronomers is responsible for accidents or injuries related to monitor use. I will assure that a surge protector and other lightning protection devices are installed if necessary.

Signature: _____ **Date:** _____

I will need:

What	*Cost*	*How many?*
SuperSID distribution USB Power	$48 (assembled)	
USB Sound card 96 kHz sample rate *(or provide this yourself)*	$40 *(optional)*	
Antenna wire (120 meters) *(or you can provide this yourself)*	$23 *(optional) with connectors attached and tested*	
RG 58 Coax Cable (9 meters) *(or provide this yourself)*	$14 *(optional) with connectors attached and tested*	
Shipping	US $12 Canada & Mexico $40 all other $60	
	TOTAL	$

____ **I have included a $_____ check** (payable to SARA)

____ **I will make payment thru** www.paypal.com to treas@radio-astronomy.org

or

____ If you are a Minority-serving institution, in a Developing or economically deprived nation, and/or you are using the monitor with students for educational purposes, you may qualify for obtaining a monitor at reduced or no cost. Check here if you wish to apply for this designation. Then tell us how you want to use the SuperSID monitor. Include type of site, number of students involved, whether public or private school, grade levels, etc. and describe your program. The goal of the SuperSID project is to provide as many students with systems as possible. If you are able to pay for a system, even if you qualify for a free one, please do so and help support our goal.

_____

_____

_____

For more details on the Space Weather Monitor project, see: **http://sid.stanford.edu**

To set up a SuperSID monitor you will need:

1. Access to power and an antenna location that is relatively free of electric interference (could be indoors or out)
2. A **PC**** with the following minimal specifications:
    a. A sound card that can record (sample) up to 96 kHz, or a USB port to connect such a sound card (for North and South America)
        i. All other countries can use AC97 sound card with 48 kHz record (sample) rate. Most computers made after 1997 will have AC97.
    b. Windows 2000 or more recent operating system
    c. 1 GHz Processer with 128 mb RAM
    d. Ethernet connection & internet browser (desirable, but not required)
    e. Standard keyboard, mouse, monitor, etc.
3. An inexpensive antenna that you build yourself. You'll need about 120 meters (400 feet) of **insulated** wire. Solid wire is easier to wind than stranded. Magnet wire will work but be more fragile. You can use anything from #18 to #26 size wire. The antenna frame can be made of wood, PVC pipe, or similar materials. We'll provide instructions. You can purchase the wire from us or obtain your own.
4. RG58 coax cable with a BNC connector at one end to run from the antenna to the SuperSID receiver. 9 meters is recommended, but the length will depend on where you place the antenna. You can purchase the coax from us or obtain your own.
5. Surge protector and other protection against a lightning strike

---

Return this form to: SuperSID@radio-astronomy.org
or mail to: SARA
Brian O'Rourke, SARA Treasurer
337 Meadow Ridge Rd,
Troy, VA 22974-3256

Announcing Radio JOVE 2.0

The Radio JOVE Team

Radio JOVE students and amateur scientists from around the world observe and analyze natural radio emissions of Jupiter, the Sun, and our galaxy using their own easy to construct radio telescopes.

Our Project announces Radio JOVE 2.0, where participants assemble a 16-24 MHz radio spectrograph to observe solar, Jupiter, Galactic, and Earth-based natural radio emissions and share their observations with fellow participants.

In the Beginning

Radio JOVE started as a NASA sponsored educational outreach project in 1999. We developed a radio telescope kit suitable for receiving signals from Jupiter, the Sun, the Galaxy, and Earth-based radio emissions. The original kit comprised a radio receiver (RJ1.1) and a dual dipole antenna for 20.1 MHz. An important goal was to teach electronic principles including how to build, solder, and assemble the radio receiver and antenna.

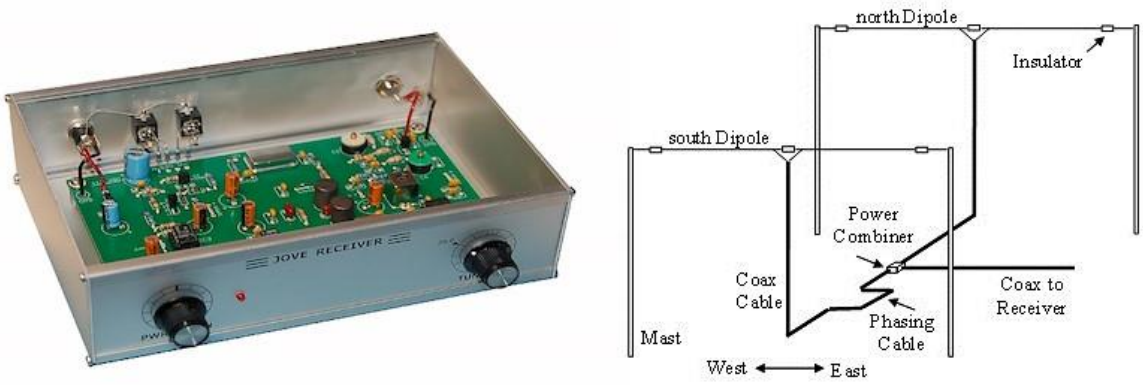

Figure 1. A Radio JOVE RJ1.1 receiver and a schematic of the dual-dipole antenna.

In addition to the hardware, three software packages were developed. These were Radio Jupiter Pro (Jupiter emission prediction program), Radio-SkyPipe (strip chart program) and Radio Sky Spectrograph (control and display of radio spectrograph data).

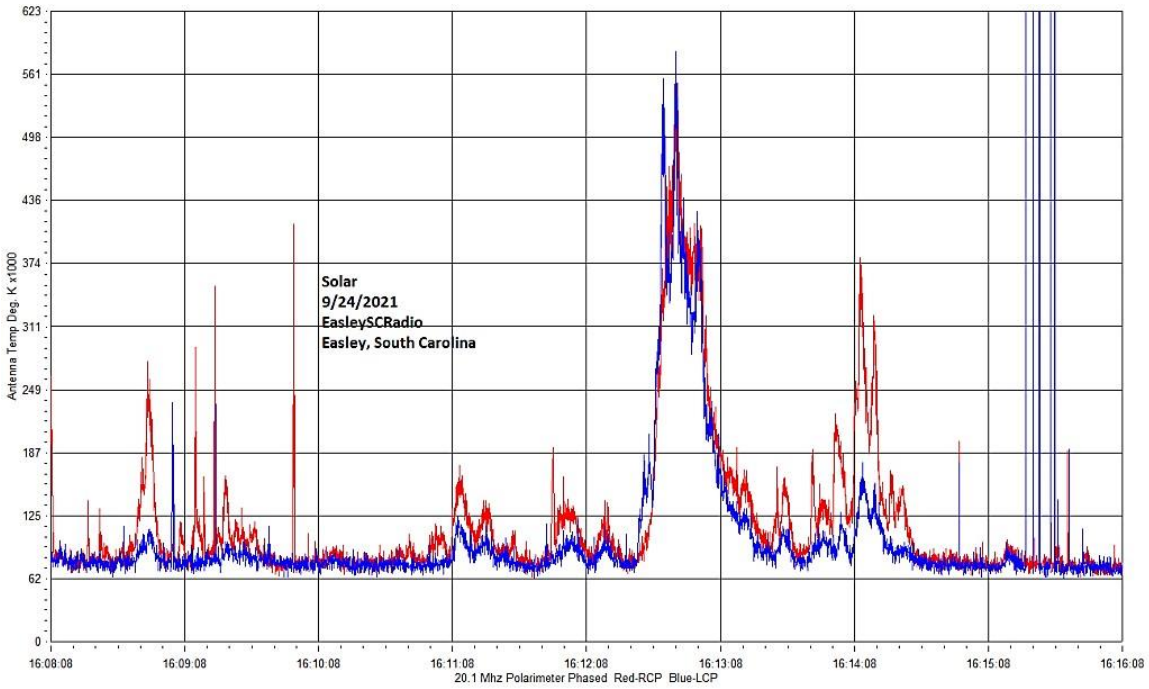

Figure 2. A SkyPipe strip chart showing multiple solar bursts using a JOVE receiver. John Cox, SC.

The Growth of Radio JOVE

As of Autumn 2021, over 2,500 kits have been sold at cost to schools and individuals around the world. Thousands of data submissions from observers have been made to the Radio JOVE data archive.

The Radio JOVE web site has always provided a wealth of information describing observation methods and various educational materials intended to teach radio astronomy techniques and scientific methods. Biannual newsletters are produced and several telephone help sessions are held each year.

A sub-group of experienced observers known as the Spectrograph Users Group (SUG) evolved from the core JOVE group. These observers developed data collection and analysis techniques using more advanced equipment and techniques. SUG members have contributed to articles published in peer-reviewed scientific journals. This group remains active under the Radio JOVE listserv at https://groups.io/g/radio-jove/.

Moving Forward with New Technology

In the past, Radio JOVE provided the hands-on experience of building a radio kit. We have many RJ1.1 receivers in operation successfully contributing scientifically valuable data. It has, however, become increasingly difficult to obtain parts for the RJ1.1 receiver kits and we therefore decided to replace the RJ1.1 receiver with a new SDR-based design for the receiver portion of our radio telescope kits. While we continue to support the hardware and software for the original RJ1.1 receivers, the only kits now available for purchase from Radio JOVE contain this newly designed system.

In recent years, new technologies have made software defined radios (SDRs) ever more affordable. These radios can operate on a single frequency like the original JOVE receiver but can also generate spectrograms which depict radio activity as a function of both time and frequency. Such displays offer new insights into our studies of the Sun, Jupiter, the Galaxy, and both natural and artificial Earth-based radio emissions.

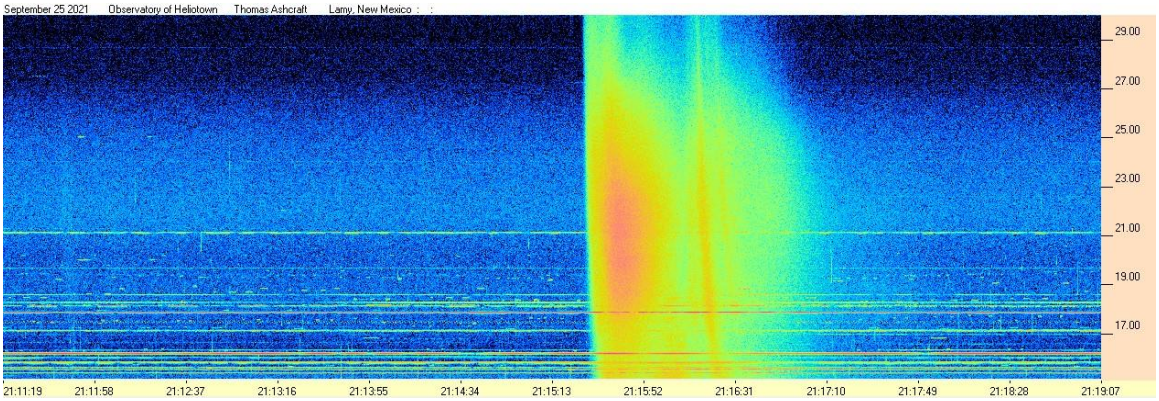

Figure 3. Radio spectrogram showing multiple solar bursts received by Tom Ashcraft in New Mexico. Horizontal scale is time, and the vertical scale is frequency. Amplitude is displayed using different colors corresponding to the strength of signals.

Radio JOVE continues to sell radio telescope packages including an antenna, receiver, and software; however, the receiver is now a commercially built SDR.

Figure 4. The JOVE team has had considerable success with the SDRPlay RSP1A unit and will provide support for using this instrument for our radio astronomy program. Not all SDR types can be supported, but it is our intent to provide support for some other SDRs as they become available during this period of rapid SDR development.

It continues to be our goal to introduce new observers to the scientific method and help them experience the thrill of receiving cosmic radio signals. Through a series of educational training modules and observing and analysis projects we aim to guide new observers to levels where they can contribute to Citizen Science projects.

We continue to support our large user base that uses JOVE RJ1.1 receivers – both in terms of technical support for the receivers but also with new and exciting observing projects for both RJ1.1 and SDR users.

We welcome both new and experienced observers to the JOVE 2.0 program as we share the excitement of receiving, studying, and understanding radio signals from our corner of the galaxy.

Please see the Radio JOVE web site at https://radiojove.gsfc.nasa.gov for more information.

RADIO JOVE 2.0 RADIO TELESCOPE KIT ORDER FORM

Order Online using PayPal™

* * * Please allow 2 to 3 weeks for delivery. * * *

IMPORTANT: Before you order the Jove receiver kit and/or the antenna kit, we suggest that you read the on-line manuals. You will need to provide additional materials and tools to complete the antenna. The cost of additional materials for the antenna support structure (masts, etc.) may be in the range of US$75 to US$100. Also note that the optimal antenna height can be up to 20ft, depending upon your latitude.

Item # RJK2u – Complete 2.0 Kit: Receiver + Unbuilt Antenna Kit + Software This kit includes an SDRplay RSP1A, USB Cable, SMA/BNC cable, F-adapter, unbuilt Antenna Kit (RJA), printed assembly manuals, and Radio-Sky Spectrograph (RSS) software. Note: Kit does not include antenna support structure. **Price: $215 + Shipping (See reverse for shipping)**	**Item # RJK2p** – Complete 2.0 Kit: Receiver + Professionally Built Antenna Kit + Software This kit includes an SDRplay RSP1A, USB Cable, SMA/BNC cable, F-adapter, Professionally Built Antenna Kit (RJA2), printed assembly manuals, and Radio-Sky Spectrograph (RSS) software. Note: Kit does not include antenna support structure. **Price: $384 + Shipping (See reverse for shipping)**
Item # RJA – Unbuilt Antenna Kit The RJA Radio JOVE Antenna Kit includes a printed construction manual, stranded copper easy-to-solder antenna wire, ceramic insulators, RG-59 easy-to-solder coax cable, screw-on Fconnectors, and a power combiner. Note: Kit does not include antenna support structure. Assembly requires a soldering gun and other tools. **Price: $90 + Shipping (See reverse for shipping)**	**Item # RJA2** – Professionally Built Antenna Kit The RJA2 Radio JOVE Antenna Kit includes a printed installation manual, two professionally assembled dipole antennas constructed of #14 Copperweld wire with Budwig center insulators and center support rope attachment points, high quality RG-6 coax with pre-installed commercial grade connectors, and a power combiner. Note: Kit does not include antenna support structure. **Price: $249 + Shipping (See reverse for shipping)**
Item # LTJ2 – Listening to Jupiter, 2nd Ed. by R. S. Flagg PDF download of Richard Flagg's book "Listening to Jupiter, 2nd Ed., 2005". The file is downloaded from a secure website. **Price: $10 + $0 shipping (PDF file download)**	**Item # RJR2** – Radio JOVE 2.0 Receiver-Only Kit This kit includes one SDRplay RSP1A SDR receiver, USB Cable, SMA/BNC cable, and F-adapter, printed assembly manuals, and Radio-Sky Spectrograph (RSS) software. **Price: $135 + Shipping (See reverse for shipping)**

RADIO JOVE 2.0 RADIO TELESCOPE KIT ORDER FORM (continued)

Order Online at https://radiojove.net/kit/order_form.html OR
Complete this form and mail with payment

Payment may be made by Credit Card via PayPal™, U.S. Check, U.S. Money Order, International Money Order in U.S. funds drawn on a U.S. bank, or Western Union Money Transfer made payable to **The Radio JOVE Project**. No bank-to-bank wire transfers are accepted. Purchase Orders are accepted from U.S. Institutions.

Send to: The Radio JOVE Project
1301 East Main St
MTSU Box 412
Murfreesboro, TN 37132, USA
email: chiggins@mtsu.edu
FEIN: 20-5239863

Item	Description	Quantity	Item Price	Shipping (see below)	Subtotal
RJK2u	Complete Radio JOVE 2.0 Kit Receiver + unbuilt Antenna		$215		
RJK2p	Complete Radio JOVE 2.0 Kit Receiver + Professionally Built Antenna		$384		
RJA2	Professionally Built Antenna-Only Kit		$249		
RJA	Unbuilt Antenna-Only Kit		$90		
RJR2	Receiver-Only Kit		$135		
LTJ2	Listening to Jupiter, 2nd Ed., by R.S. Flagg (PDF download)		$10	$0	
				Total:	

Shipping Fees for Radio JOVE: We ship all packages using USPS Priority Mail flat rate boxes.
U.S.A.: $17.00
Canada: $57.00
All Other International Shipping: $85.00

Ship to: (Please print clearly)

Name: _____
Address: _____
City, State, Postal Code: _____
Province, Country: _____
Email: _____

Visit the Radio JOVE web site and fill out the team application form at https://radiojove.net/sign_up_form.php even if you are just an interested individual so that you can receive important information about kit updates, online services, and activities within the project as they occur!

Founded in 1890

The British Astronomical Association
A company limited by guarantee
Registered Charity No. 210769
Burlington House, Piccadilly, London, W1J 0DU
Telephone: 020 7734 4145 Fax No.: 020 7439 4629
Email: office@britastro.org Website: www.britastro.org

Please send questions, reports and observations to John Cook: jacook@jacook.plus.com

John Cook's VLF Report

BAA Radio Astronomy Section, Director: Paul Hearn

RADIO SKY NEWS **2023 MARCH**

VLF SID OBSERVATIONS

The sun has been a little less active in March, with fewer strong flares. There were 9 of M-class compared with 28 in February, and just a single X-class compared with two in February. The SIDs have however remained quite complex with multiple peaks making them tricky to analyse. The 23.4kHz has also been very unreliable, off-air from the 16th with just a short active period over night on the 29th – 30th. The X2.1 flare was rather late in the afternoon, peaking at 17:54UT, on the 3rd, and so lost in the sunset for most signals.

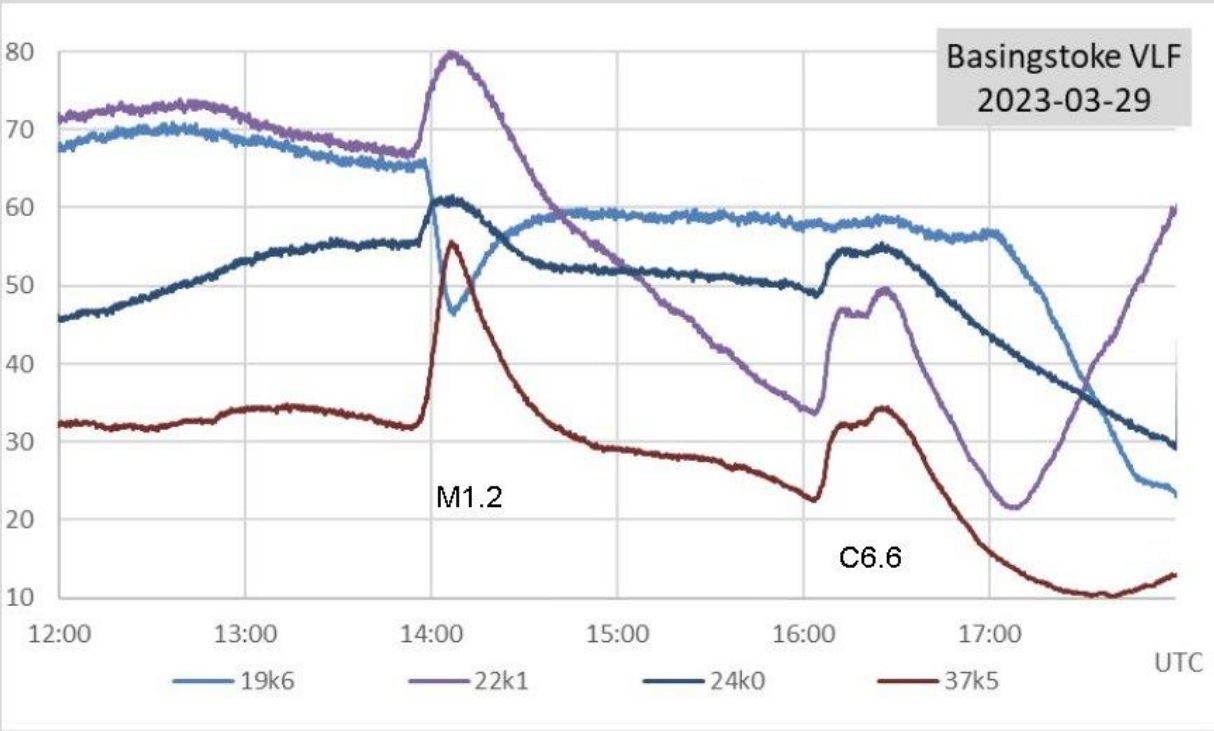

Paul Hyde recorded the very clean M1.2 flare on the 29th, followed by the twin peaked C6.6 flare just before the sunset started. 19.6 kHz shows an inverted SID for the M1.2 flare compared to the other signals, but a very small

response to the C6.6 flare in the same direction as the other signals. The difference in path length at 19.6 and 22.1kHz is very small, and both in the same direction, and so the difference in response is quite surprising.

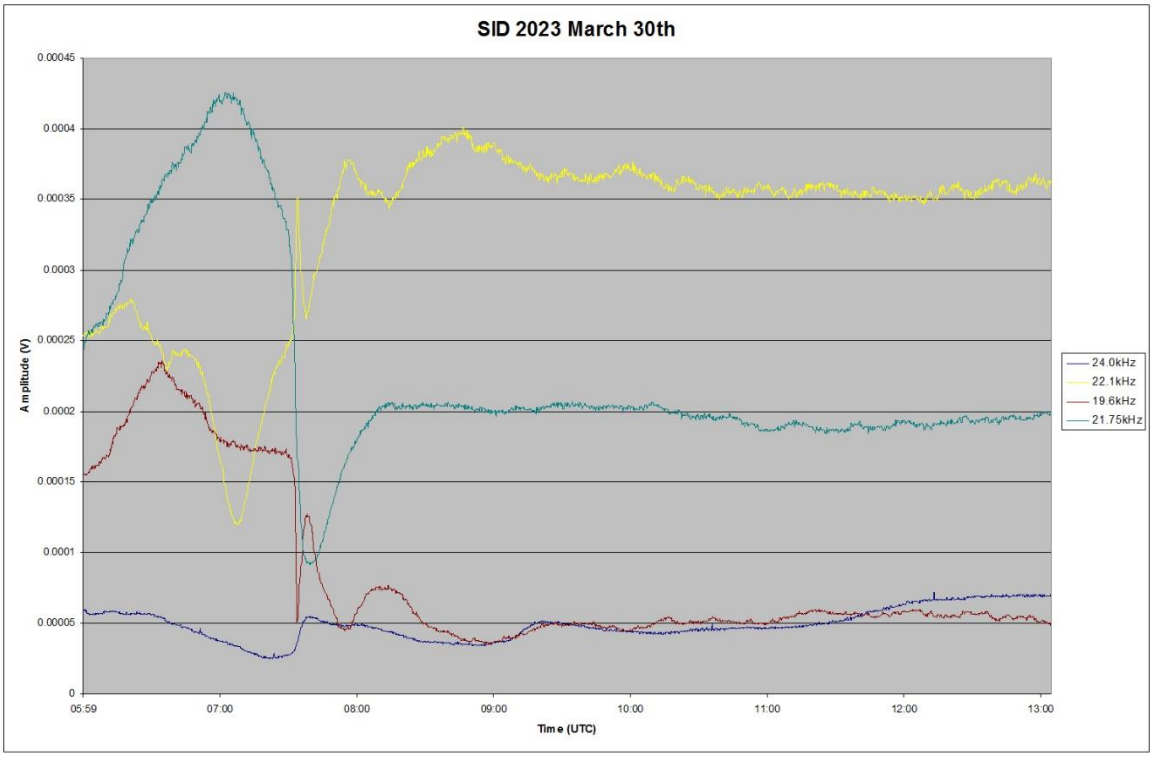

The strong M5.4 flare peaking at 07:40UT on the 30th was more widely recorded, shown here by Mark Edwards. The 22.1 and 19.6kHz signals again show SIDs in opposing directions, both spike-and-wave in this case. 24kHz also shows a small SID, despite the relatively early timing.

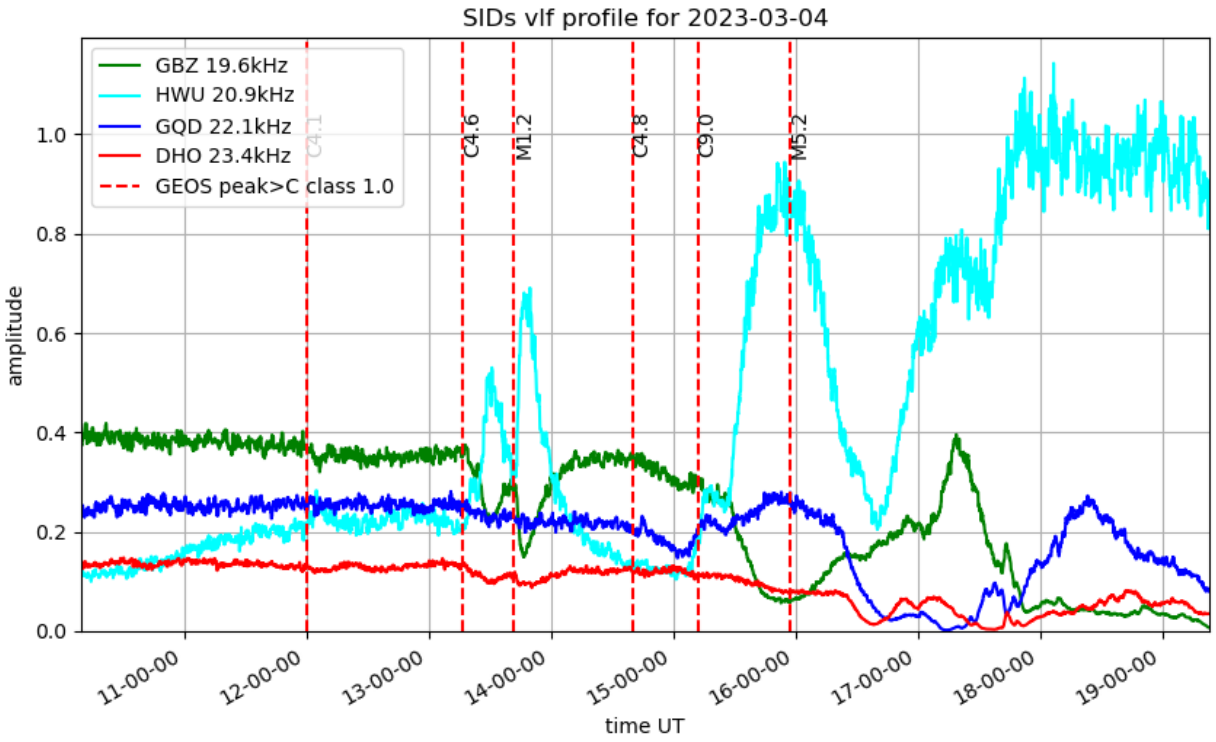

This recording by Mark Prescott shows activity on the 4th, showing a very complex series of SIDs. 20.1 and 19.6kHz also show opposing responses, 19.6kHz being the more responsive to the flares. The M5.2 flare was very slow and has produced a strong SID on the southerly path at 20.9kHz shortly before the local sunset.

SOLAR EMISSIONS

The sun is now within sight of Colin Clements' VHF and UHF aerials, with some strong activity recorded. The M1.2 flare on the 29th produced a strong emission at 151MHz (red), with a much smaller signal at 610MHz (black). 408MHz (blue) has not been affected:

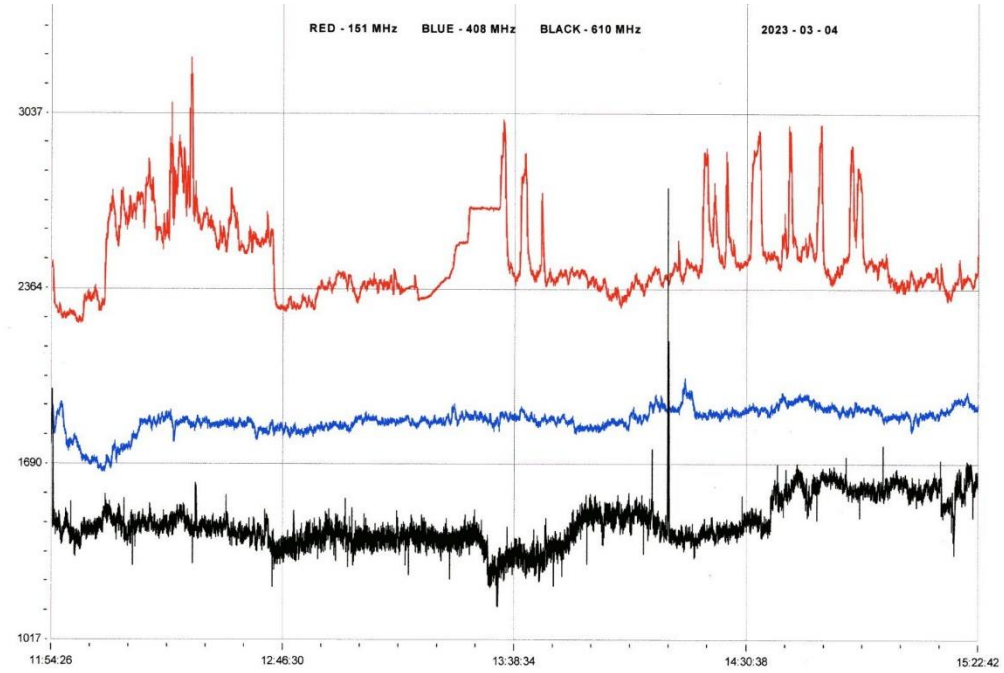

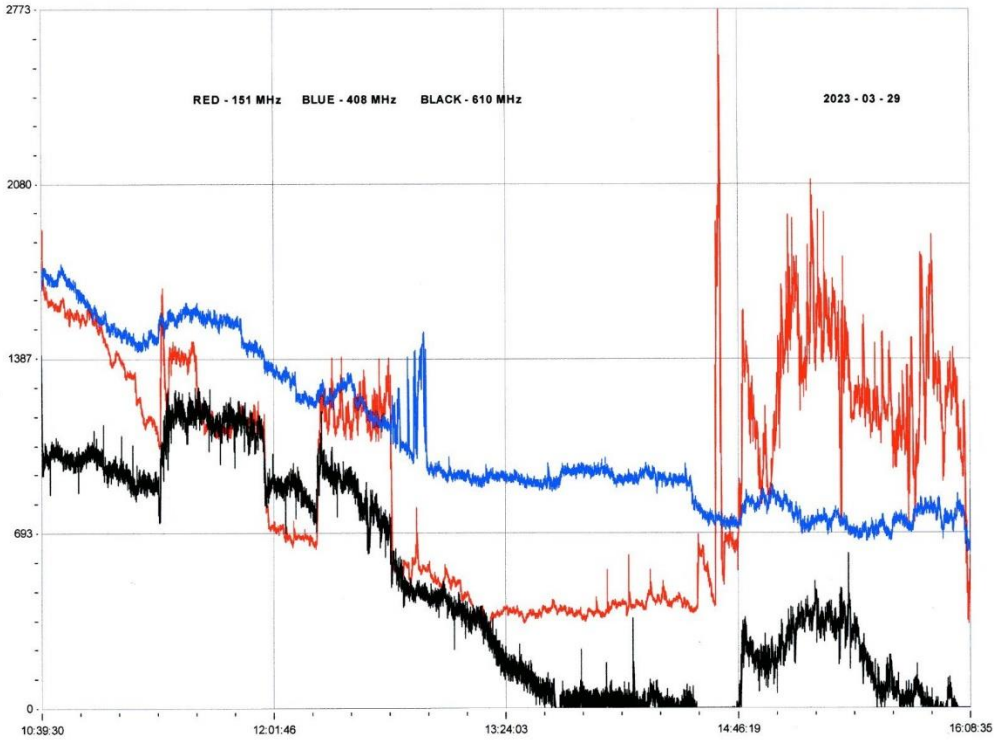

Colins's recording from the 4th again shows 408MHz and 610MHz quiet, but with strong emissions at 151MHz matching the C4.1, M1.2 and C4.8 flares. A strong 151MHz emission was also recorded all day on the 22nd. The SWPC bulletin lists only minor C-flares on the 22nd, none recorded as SIDs.

MAGNETIC OBSERVATIONS

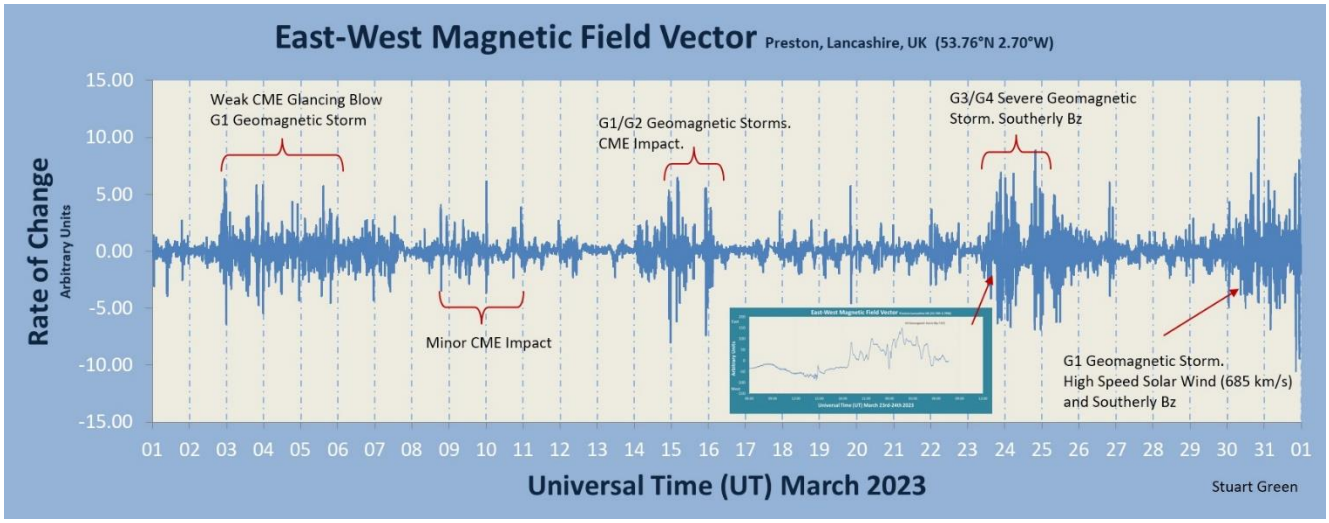

Stuart Green's summary of magnetic activity in March shows a few minor CME impacts. Most of the stronger flares were produced near the Sun's limb, and so produced only glancing blows. The most active period was overnight on the 23rd/24th, shown here by Nick Quinn and Callum Potter:

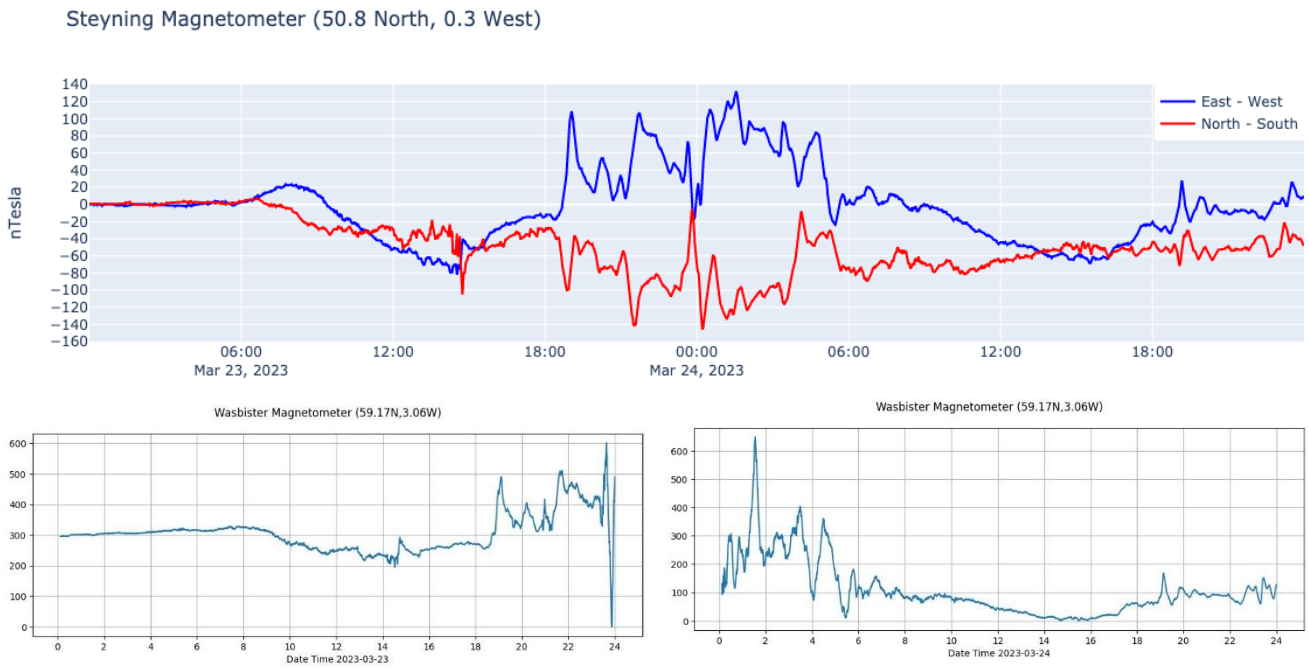

Nick Quinn (top panel) is near the south coast of England, location shown on the chart. Callum Potter is now our most northerly magnetic observer, having moved to the Orkney Island of Rousay, location again shown on the chart (lower panel). The STCE bulletin lists solar flares on the 20th as the source of the disturbance, combining to produce a magnetic storm. Both recordings show an initial pulse at 14:30UT, which may be from the initial impact. Roger Blackwell's Mull magnetometer shows this pulse to be about 100nT, with +/-250nT recorded overnight. For those lucky enough to have clear skies, there was a widespread Aurora seen overnight. Mark Edwards also recorded effects at 37.5kHz related to this storm.

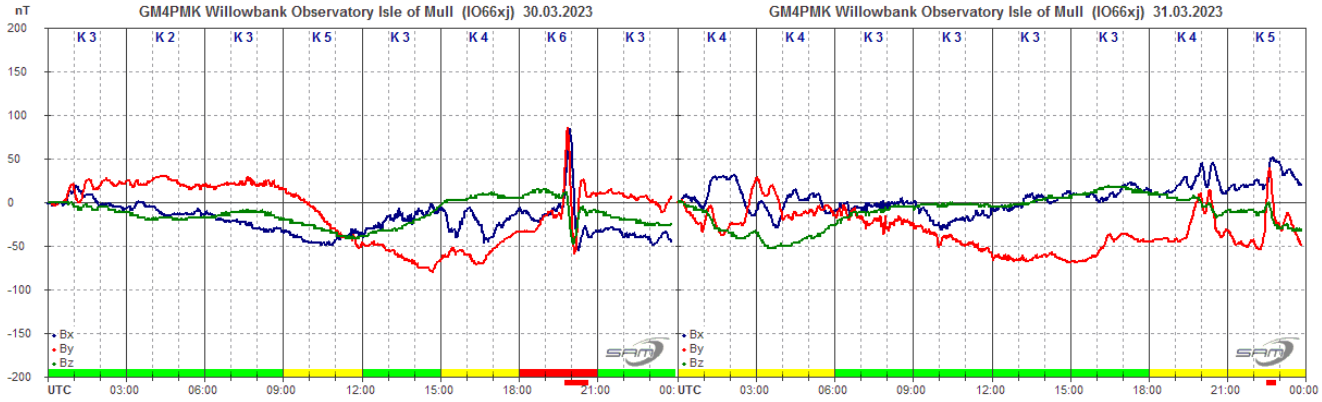

There was also a fairly strong disturbance on the evening of the 30th, shown in Roger Blackwell's recording. This is listed as due to the high-speed wind from an equatorial coronal hole. The strong pulse at 20:00UT looks like a sudden impulse, and also shows in the recordings from Nick and Callum.

The 14th and 15th were also fairly active with disturbance from a filament eruption on the 12th. Nick Quinn's recordings show the activity:

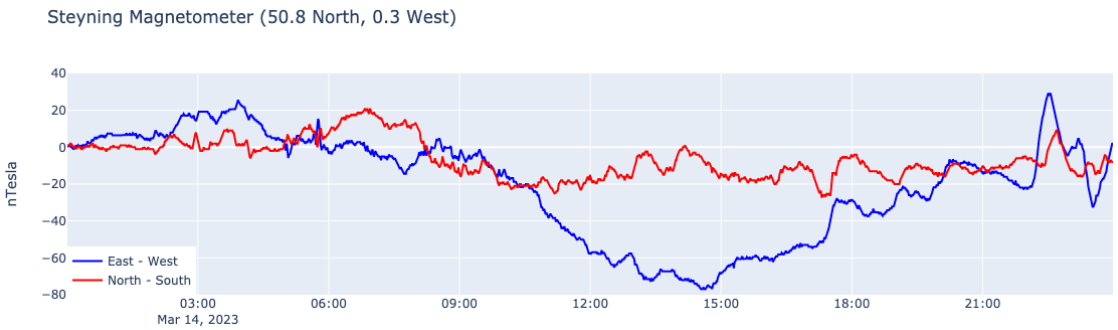

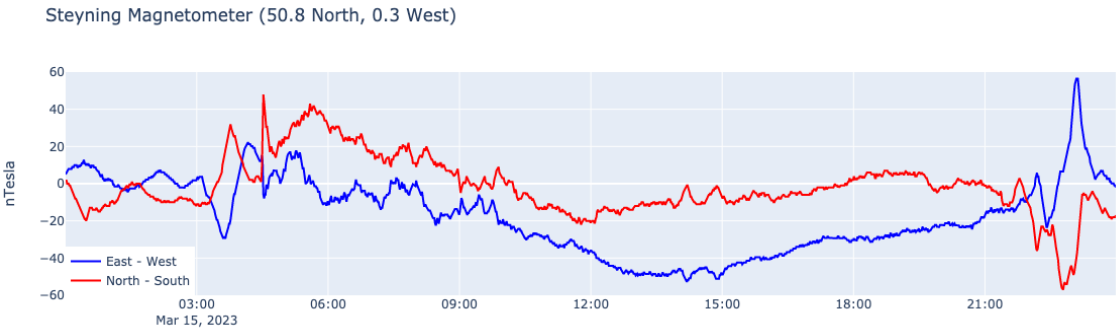

This activity faded out in the morning of the 16th, followed by very quiet conditions. There were periods of mild activity from the 2nd to 12th, mainly from coronal hole winds, with minor CME effects on the 9th. The coronal hole is the same one that produced the stronger disturbance on the 30th and 31st on its next appearance.

Magnetic observations received from Roger Blackwell, Colin Clements, Stuart Green, Callum Potter, Nick Quinn and John Cook.

MUONS

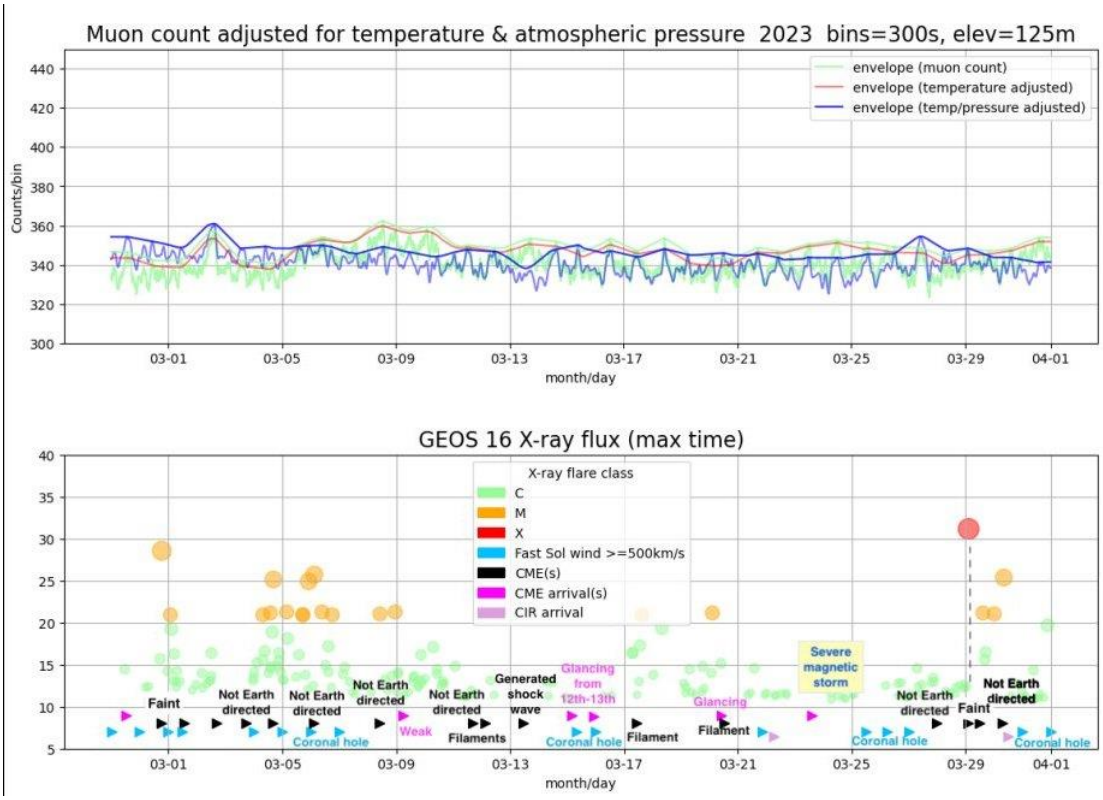

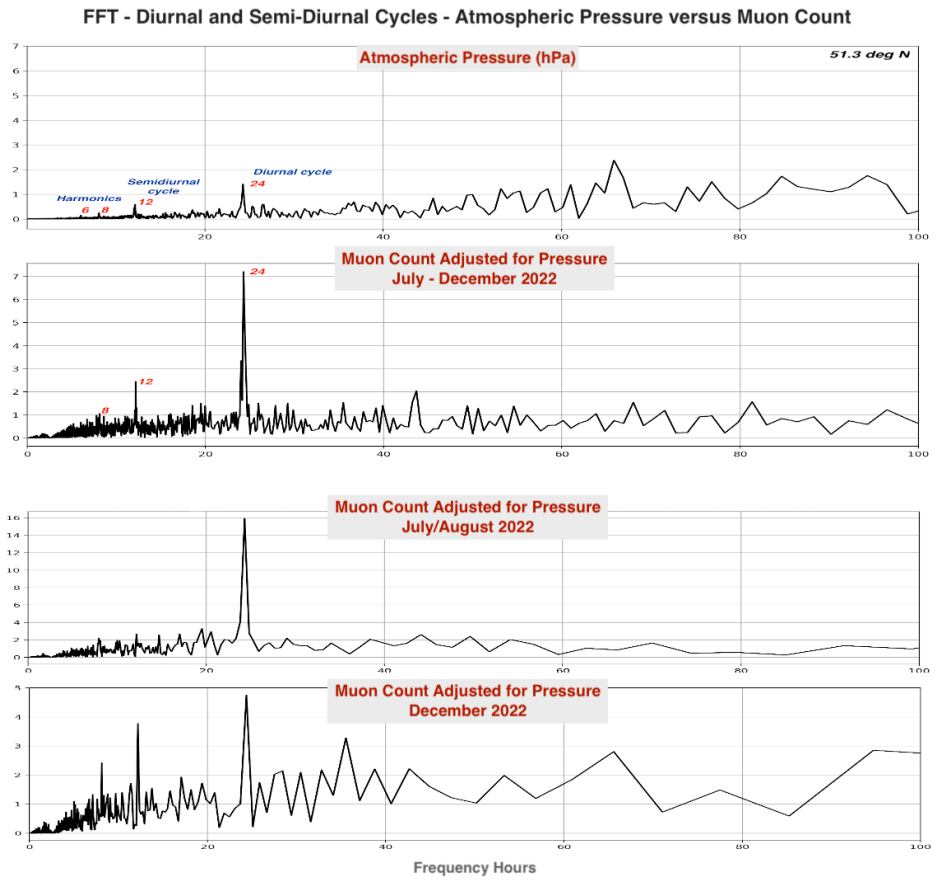

The upper panel shows the muon counts for March, recorded by Mark Prescott, corrected for temperature and pressure as in previous reports. No notable events were recorded, and the counts are generally slightly lower than those recorded in February.

The lower panel shows a series of Fast Fourier Transforms (FFT) of the data. First is the atmospheric pressure recorded in 2022 July to December. The 24-hour diurnal cycle shows up, along with 12-, 8- and 6-hour periods. Next is the adjusted muon counts over the same period. The diurnal period again shows up strongly, with weak harmonics. The same analysis but just for the summer months of July and August eliminates the harmonics. Repeating with December's data amplifies the harmonics relative to the 24-hour diurnal period. Tides are produced in the atmosphere as the sun warms it up and moves through the sky. This effect will be much stronger during the local summer months with the sun higher in the sky, compared with the winter. Mark's analysis of the data matches this effect very well, showing how the expanded, warmer, atmosphere generates more muons from the incoming cosmic radiation. A very interesting analysis.

I was very lucky to get a last-minute place at the BAA Winchester weekend meeting over 14th-16th April. Our section director Paul Hearn gave a very good introductory talk on "An intergalactic hop through the electromagnetic spectrum" on Saturday morning. He also had a display table with Andrew Thomas showing some of the UKRAA equipment available for amateur radio astronomy. The display was very busy through the coffee break periods, with great interest being shown in the muon detection equipment. I hope to be able to include a display of our activities and observations again next year, as I have done at previous meetings. Winchester is always well attended, and a good opportunity to meet up with other members.

VLF SID OBSERVATIONS

Solar flaring activity in April was at a similar level to last month, with 65 C-class and 7 M-class flares. There were no X-class flares, the strongest recorded being M3.0 peaking at 05:44UT on the 6th. This was quite early for most of our signals. 23.4kHz has again been unreliable, with many breaks in the signal.

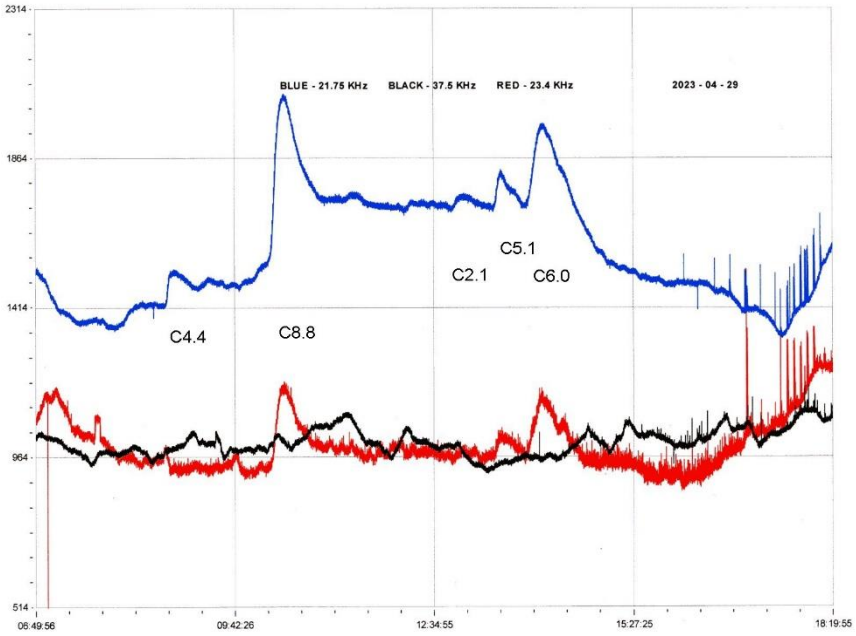

This recording by Colin Clements shows activity on the 29th, with a rather unusual response at 21.75kHz (blue). The C8.8 flare was the largest of the day, but the signal seems to have remained at a high level until the C6.0 flare faded away, a period of over four hours. 37.5kHz (black) has remained very unstable throughout the day.

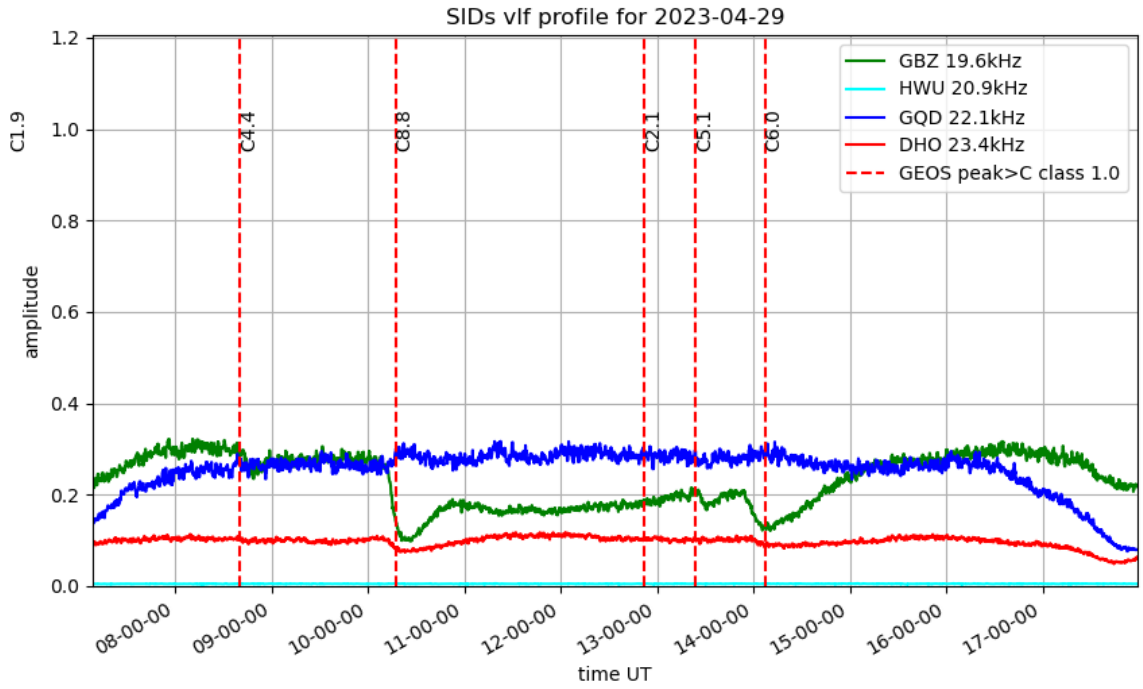

This recording by Mark Prescott does not include these signals but does show the very weak response at 23.4kHz. 19.6kHz shows clear SIDs for the two larger flares, while 22.1kHz barely shows any effects at all.

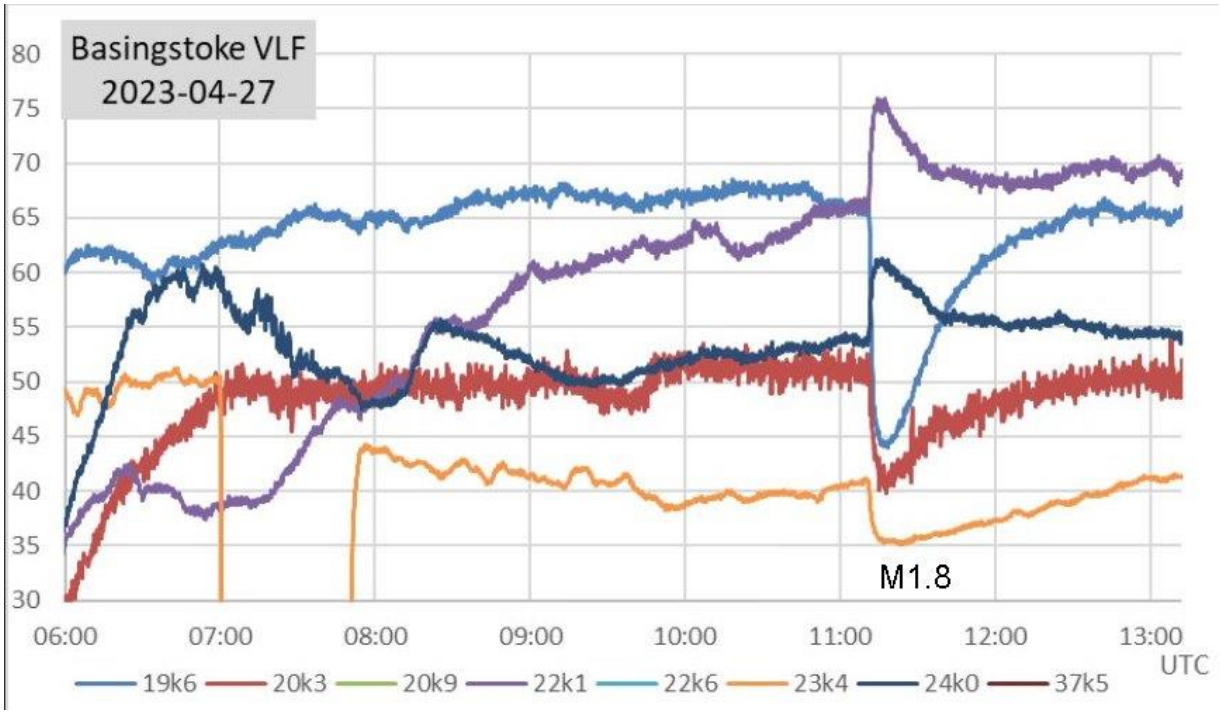

The M1.8 flare peaking at about 11:17UT on the 27th shows well in this recording by Paul Hyde, with a combination of normal and inverted SIDs. The path lengths at 19.6kHz and 22.1kHz only differ by about 27km on a very similar bearing, but enough to produce inverted responses.

There was just a single C2.5 SID recorded on the 26th, peaking at 14:23UT. This was the only classified flare shown in the GOES satellite data. We did however record some strange effects during the morning, shown in the recording by Mark Edwards:

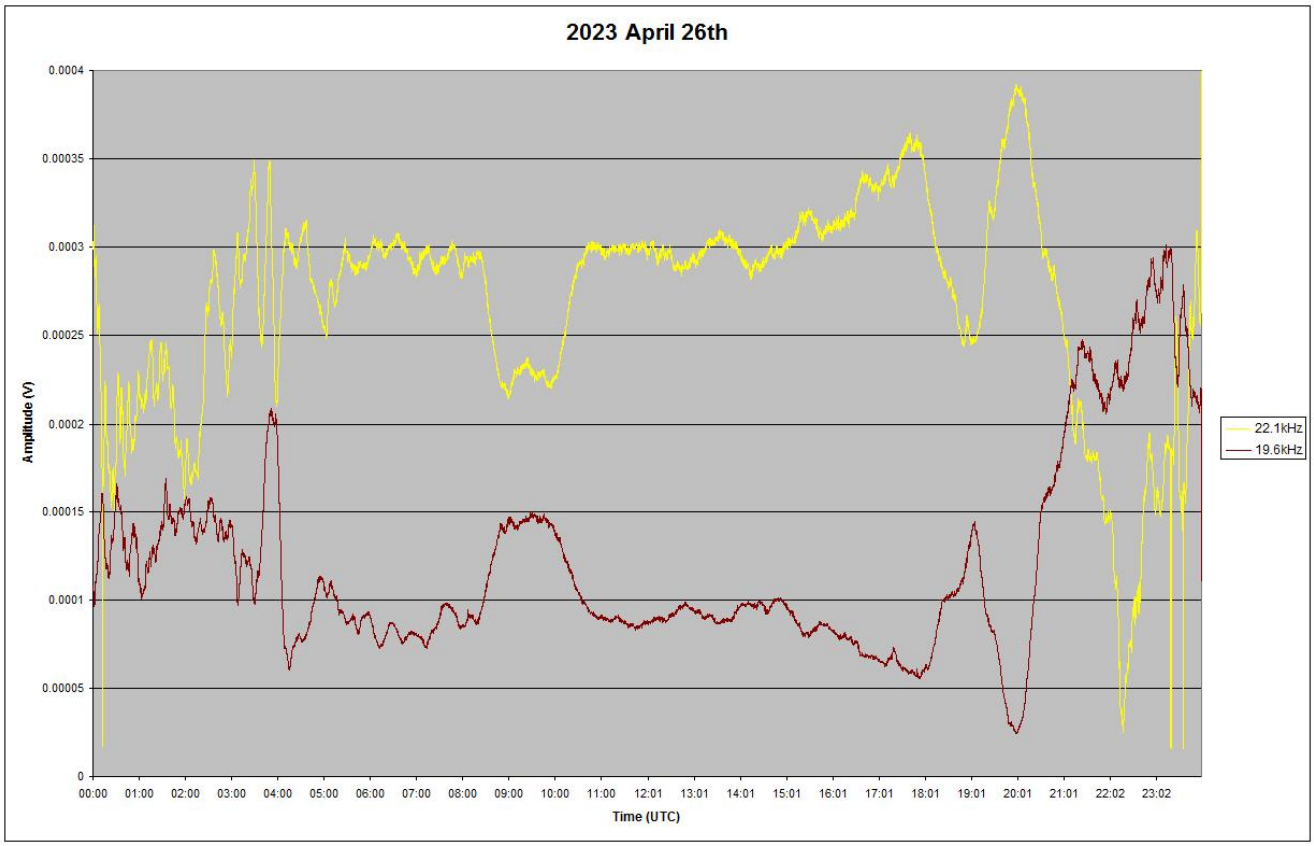

The C2.5 flare is hardly visible in the recording, but the matching pair of 'bumps' from 08:30 to 10:30 are very clear. The matching symmetrical nature suggests that it was not a transmitter effect. The sunrise period also looks rather unusual.

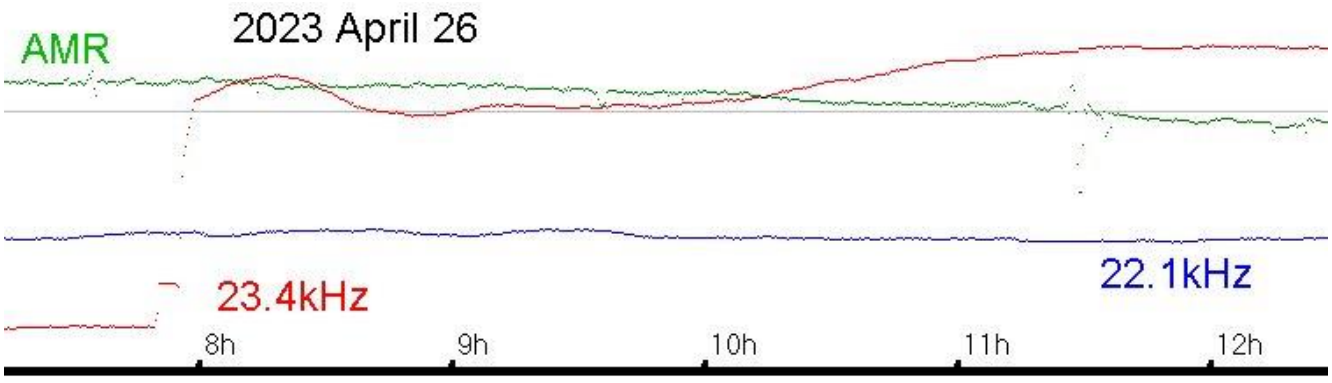

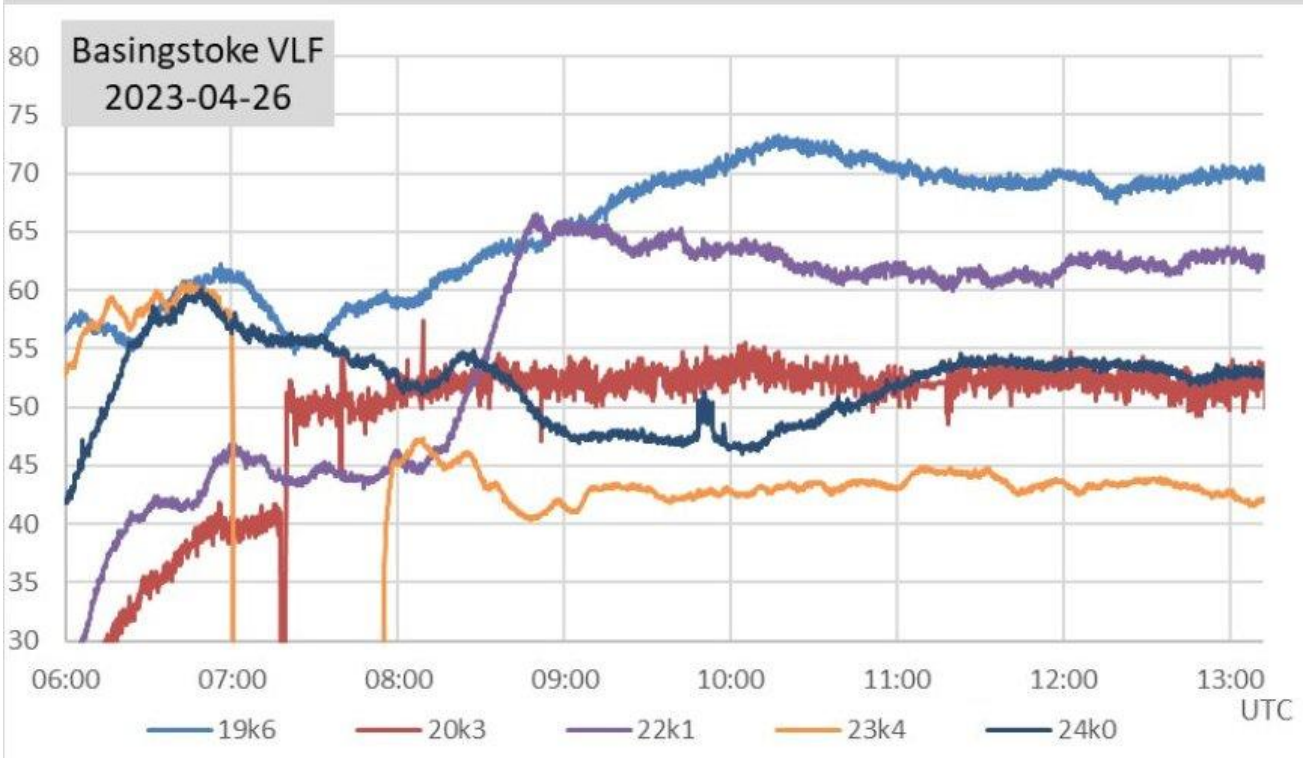

My own recording includes the magnetic signal (AMR), with no disturbance. The pulse at 11:30 is local traffic interference. The chart from Paul Hyde includes other signals, with a similar response at 24kHz. The other signals being much less clear. The 23.4kHz signal in my own recording has a small downwards bump matching in time, with a much smaller response at 22.1kHz. The source of this effect remains unknown but was presumably some weather-related effect on the lower ionosphere.

MAGNETIC OBSERVATIONS

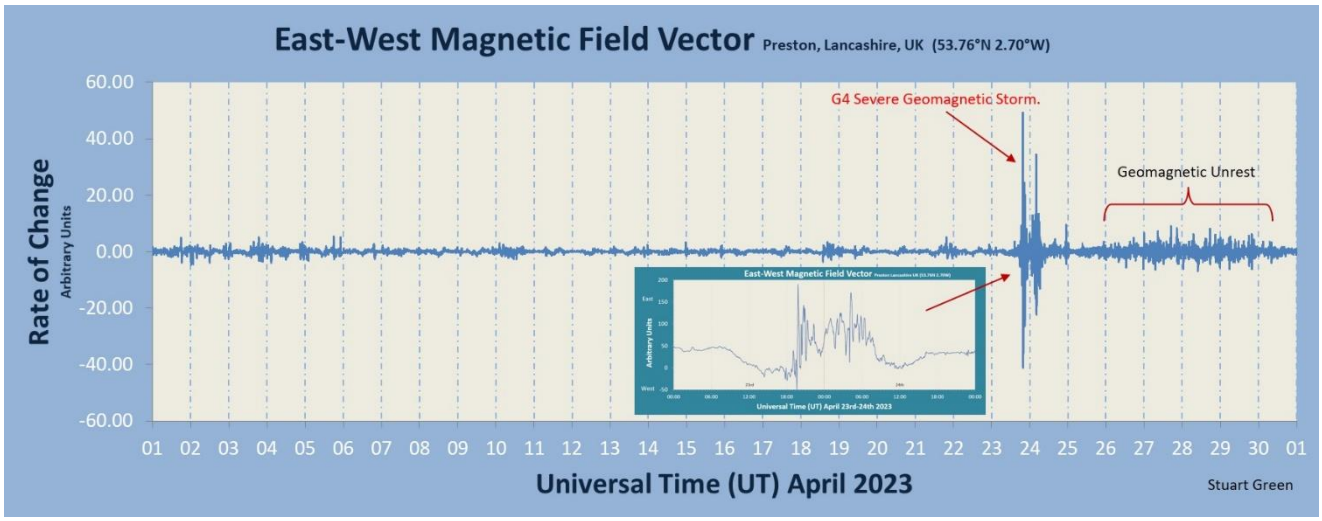

Stuart Green's monthly summary chart shows just a single major disturbance on the 23rd / 24th, following a very calm start to April. The STCE bulletin links this to a CME arrival from the M1.7 flare on the 21st. The SWPC

list AR13283 as generating the flare, located near the central meridian of the sun at the time. Paul Hyde's recording gives a peak time of 18:10UT for the SID.

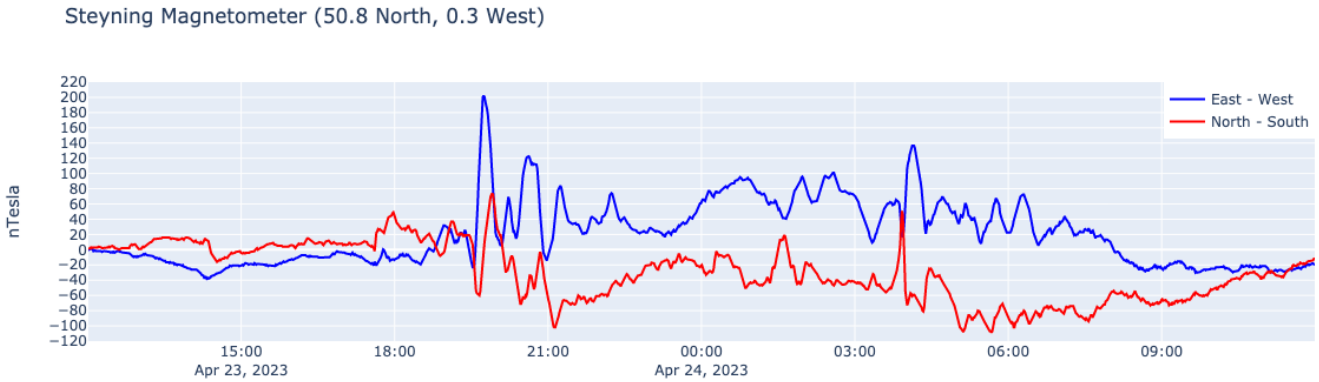

Nick Quinn's magnetic recording shows the very strong disturbance through the evening of the 23rd and into the 24th. The exact impact arrival time is not entirely clear, possibly being at 17:45, other recordings also showing this timing. That gives a CME transit time of about 48 hours, making it the 6th fastest that we have recorded. The fastest was 34h 41m in 2012 March. The peak magnitude of the disturbance is also the highest that I can remember, Roger Blackwell's Mull magnetometer showing +300/-200nT through the night. Aurora were widely reported, even on the local weather forecasts, but sadly nothing visible here. No doubt the Aurora section will have more on that later.

Mild magnetic disturbances continued through to the end of the month, with a number of minor CMEs combining. Roger Blackwell's recording from the 27th is a good sample:

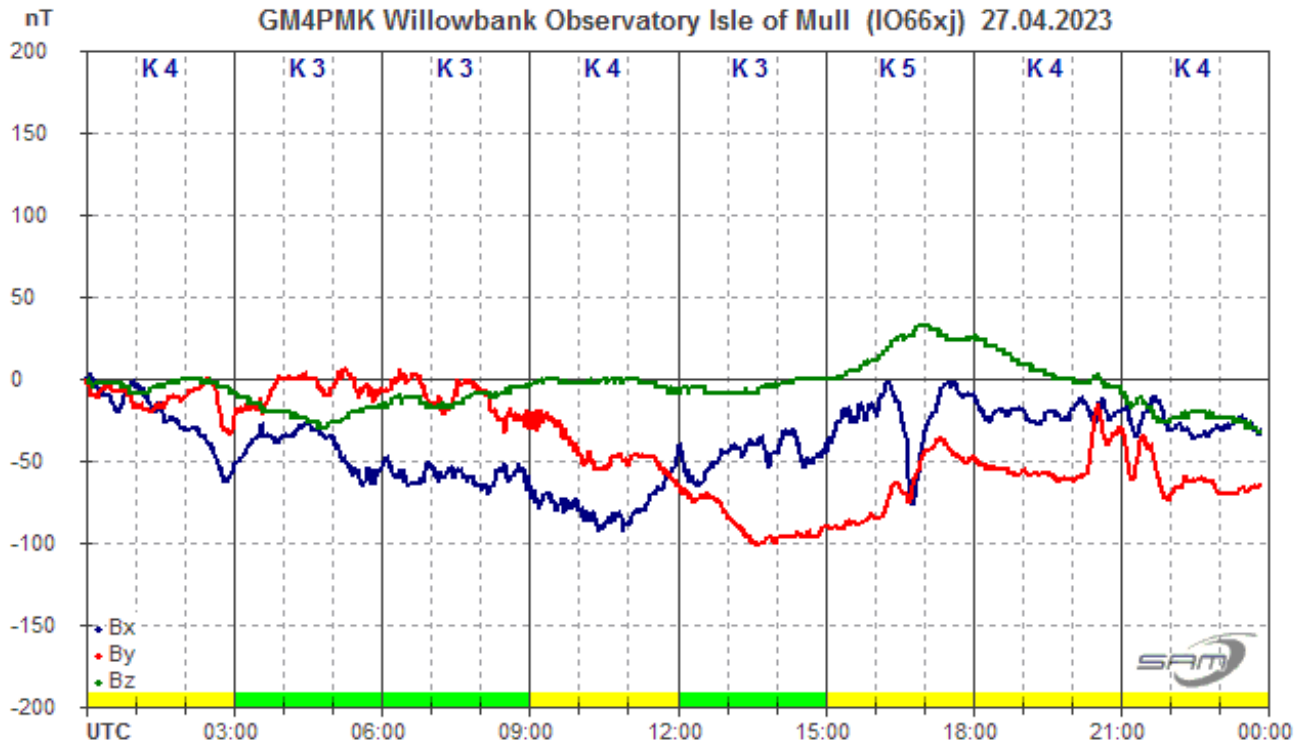

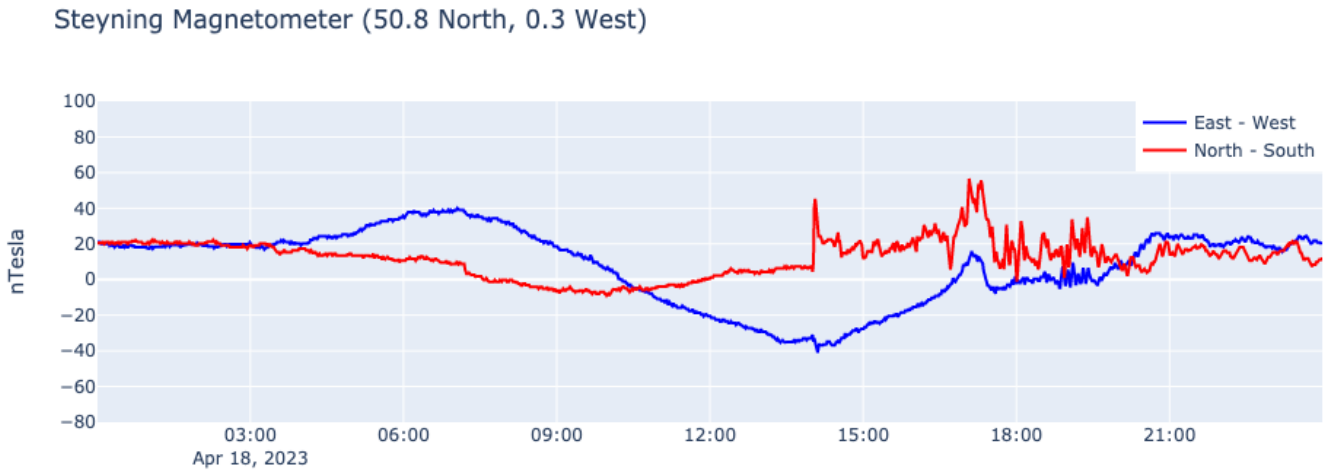

Nick Quinn's recording from the 18th appears to show a shock at about 14:00UT, followed by some rapid turbulence. The source of this is not known, but it does look real and not some local interference.

Magnetic observations received from Roger Blackwell, Colin Clements, Stuart Green, Nick Quinn and John Cook.

SOLAR EMISSIONS

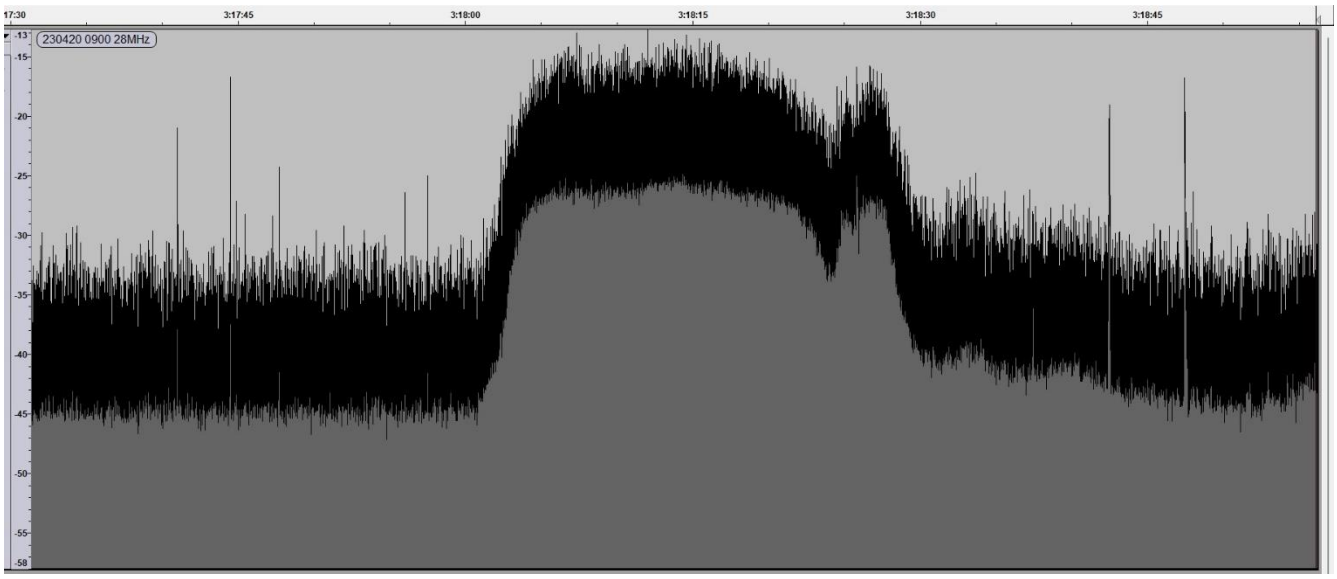

This recording by Colin Briden shows a 28MHz type III noise burst starting at 12:18 on the 20th. It appears to match the timing of the C2.3 flare that we recorded as a SID. It lasted about 18 seconds, with an average amplitude of about 20dB. Colin notes that it has taken some time to find a clear spot in the radio spectrum to make these observations, the usual 30MHz band having interference. 28MHz seems to be clear at the moment.

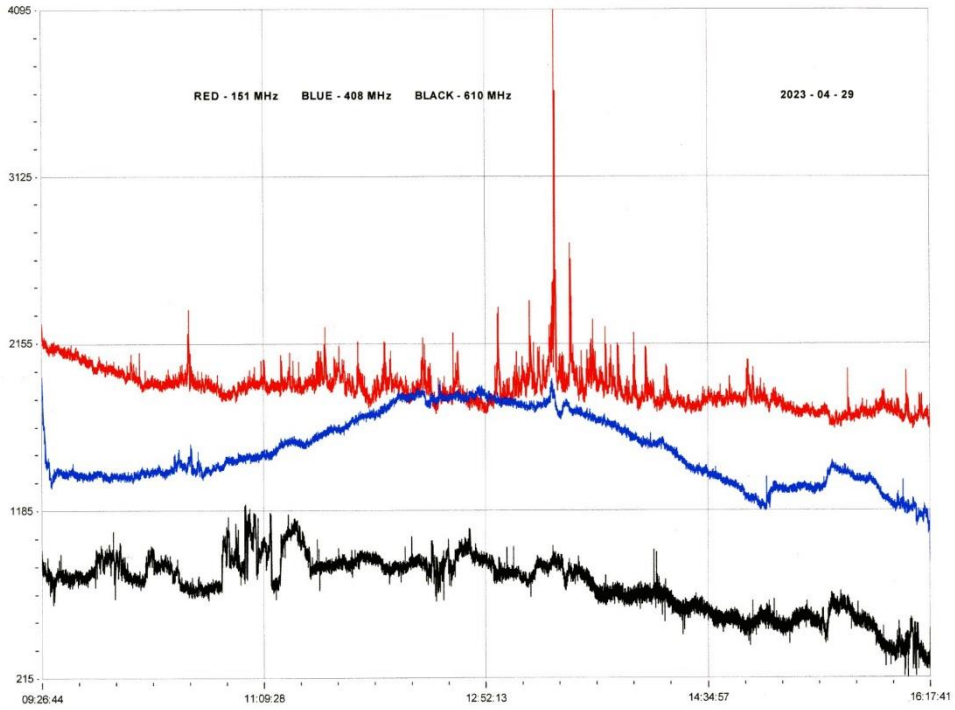

Colin Clements recorded this noise burst on the 29th, with a strong 151MHz (red) signal and much smaller 408MHz (blue) signal. 610MHz (black) is generally noisy and shows no matching increase in noise. This appears to match the C5.1 flare, with maybe some contribution from the C2.1 and C6.0 flares. The matching SID recording is shown on the first page.

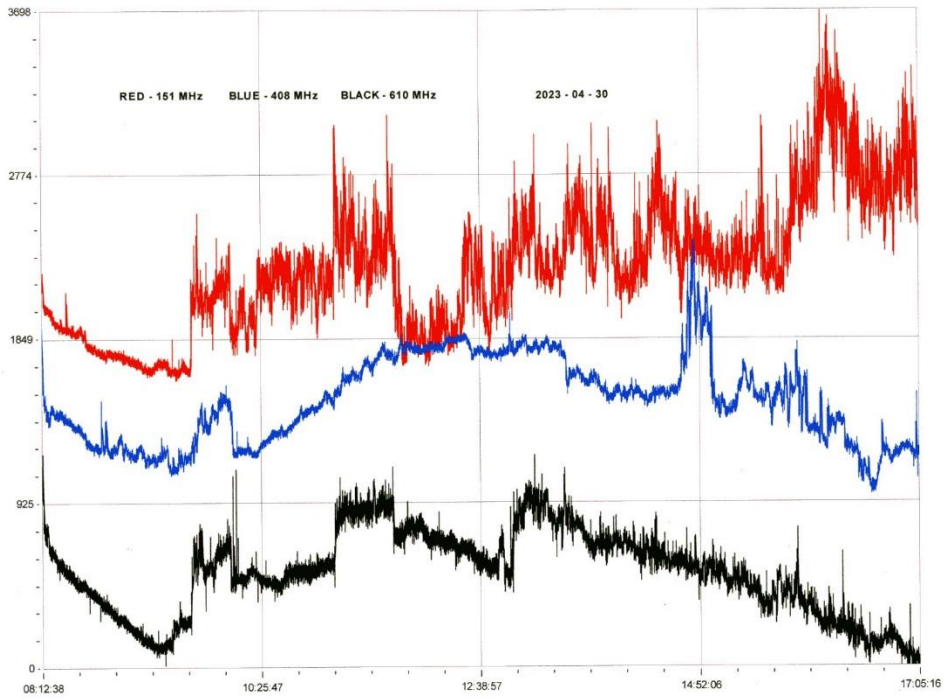

Colin's recording on the 30th shows 151MHz noise lasting all day, with some clearer peaks on the other frequencies. The 408MHz peak starting at 14:40 matches well with the C3.6 flare, but the source of the other peaks is less clear.

MUONS

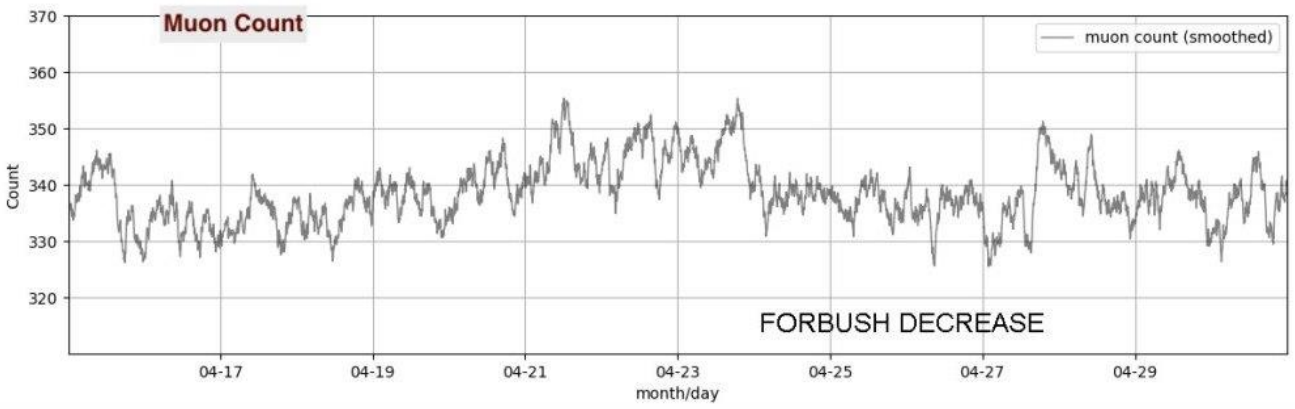

The very strong magnetic disturbance on the 23rd and 24th caused a significant drop in the Muon count recorded by Mark Prescott, as shown in his recording. This effect is called a Forbush Decrease and is caused by compression of the upper ionosphere / atmosphere increasing its density, and therefore reducing the cosmic ray intensity reaching the lower layers. We see this as a reduction in Muon counts. It also reduces the neutron count and was recorded by the Oulu cosmic ray monitor in Finland.

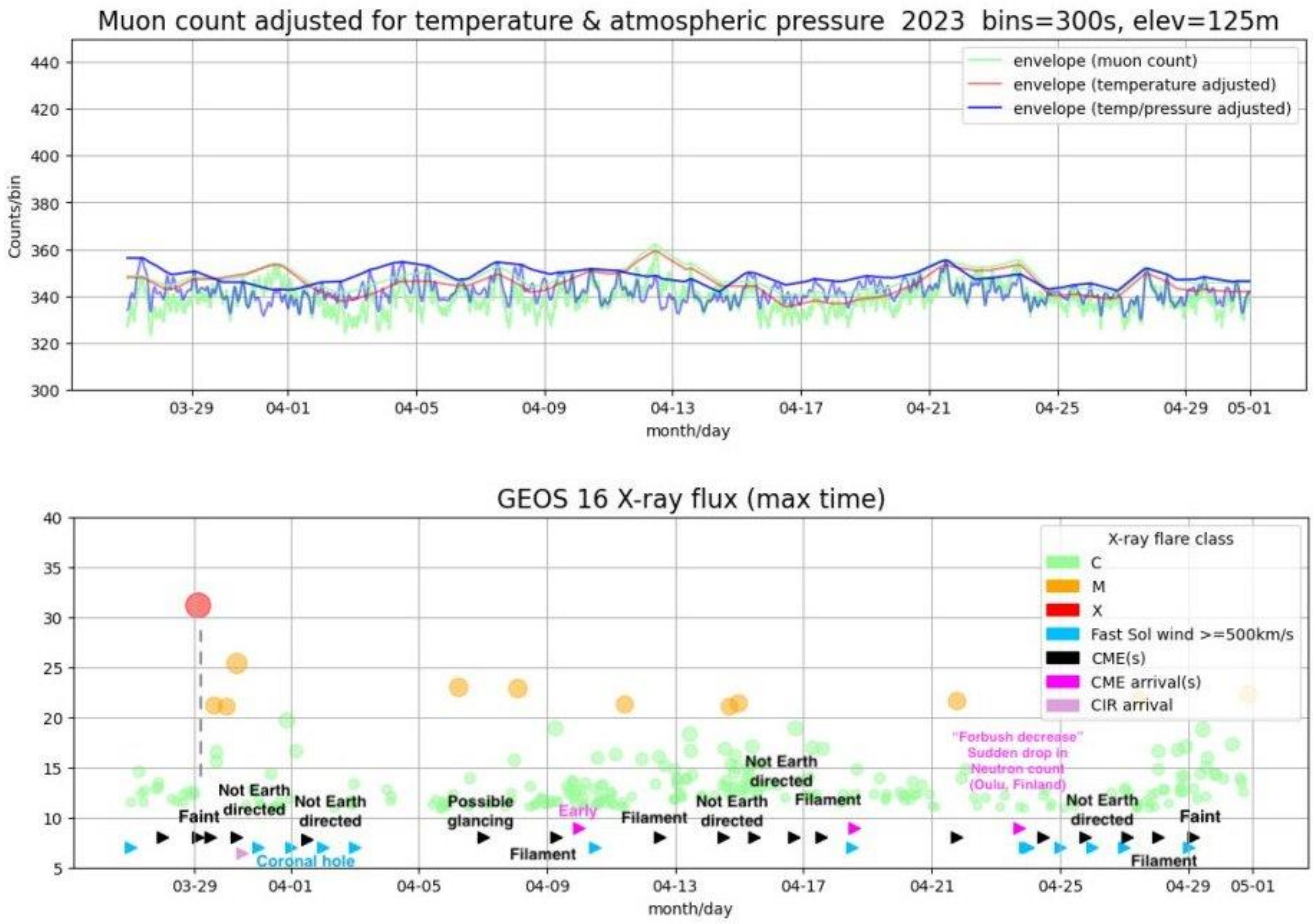

This effect is reduced slightly when the data is temperature / pressure corrected, shown above. The drop in count was very rapid at the time of the CME impact, but slower and smaller drops in counts are also present during periods of a faster solar wind.

BARTELS CHART

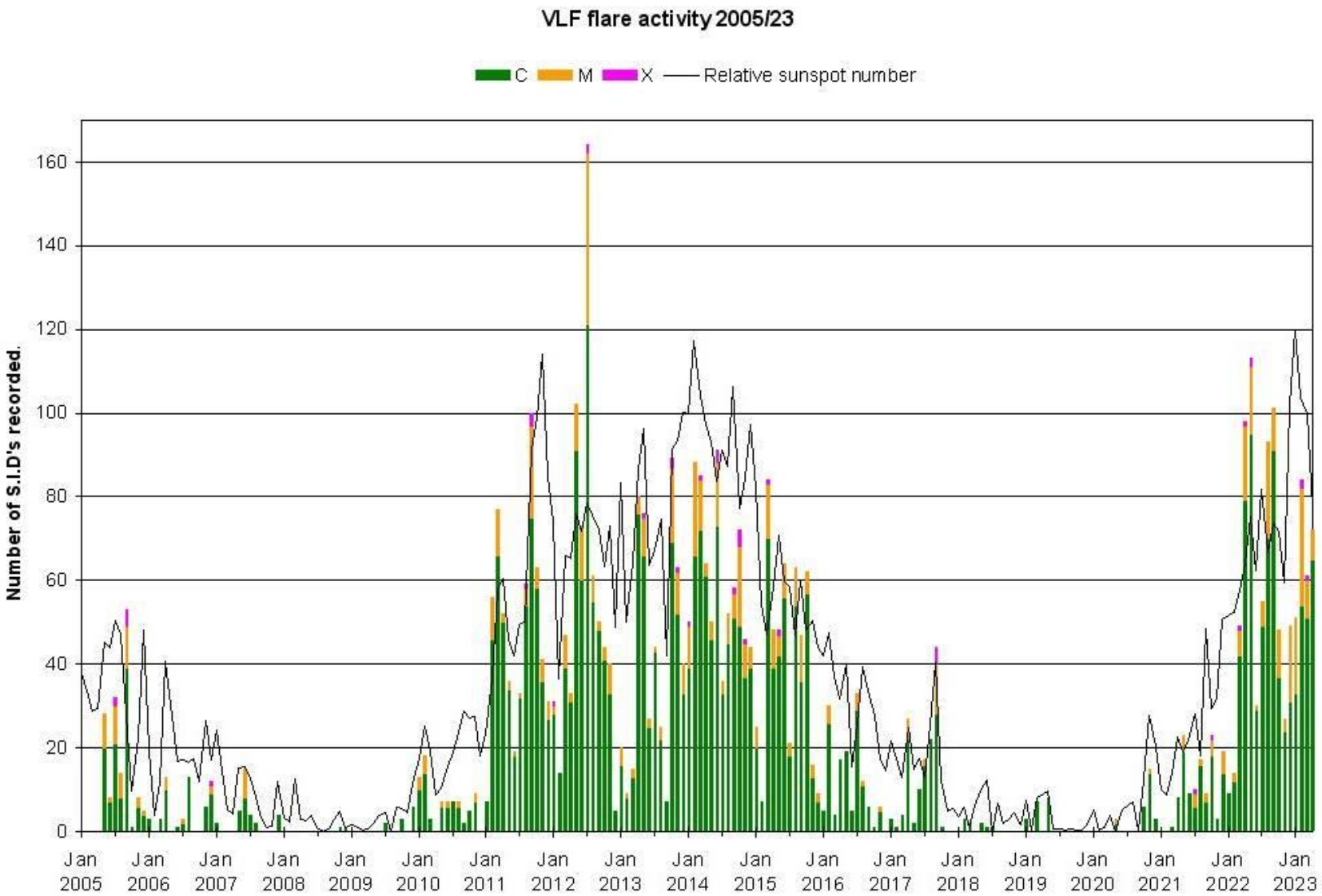
VLF flare activity 2005/23
C
M
X
Relative sunspot number
Number of S.I.D's recorded.
0
20
40
60
80
100
120
140
160
Jan 2005
Jan 2006
Jan 2007
Jan 2008
Jan 2009
Jan 2010
Jan 2011
Jan 2012
Jan 2013
Jan 2014
Jan 2015
Jan 2016
Jan 2017
Jan 2018
Jan 2019
Jan 2020
Jan 2021
Jan 2022
Jan 2023

British Astronomical Association
Supporting amateur astronomers since 1890
Radio Astronomy Section

BAA RA Section Autumn programme 2023

Friday **Sept. 1st** 19:30 BST 18:30 UTC	**Dr. Asayama Shinichiro** SKA System Scientist at SKA Organisation National Astronomical Observatory of Japan	**Square Kilometre Array update.** **+** **An innovative and fun solution for hydrogen line reception**

Fri. Oct. 6th 19:30 BST (18:30 UTC)	**Marcus Leech** President. Canadian Centre for Experimental ***Radio Astronomy***	Amateur SDR based interferometry, hardware and software. (Getting started)

VINTAGE SARA

CHARLES OSBORNE, SARA HISTORIAN

Hard Work Pays Off

A name caught my eye while looking thru some of Sandy Weinreb's articles. The name was familiar and unusual enough that I suspected it was the same person I'd talked to twenty years ago, Hamdi Mani. I did a search on the name and sure enough the connection to radio astronomy and the time frame was about right. I decided to find out more.

In 2003 we started getting a few posted questions on the SARA email list from Hamdi Mani about how to do radio astronomy. At the time he was a student in Tunisia having all the usual problems of living in a place where everything seemed a bit more difficult and twice removed from what seemed like the much more active areas in the US, Europe, and Australia where large observatories are slightly more numerous.

About that time another SARA member commented: "If I lived back east I'd mow the lawn at Green Bank for free just to be around some of that stuff." I thought that sort of sums up the wishes of many SARA members. We're also sort of trapped in day jobs typically doing things that are less than our dream jobs. So, I decided to ask Hamdi how he had managed to escape the deserts of Tunisia and end up working for Sandy Weinreb. There's gotta be a story there.

Hamdi had even been elected Director at large in SARA around 2004.

By 2005 Hamdi managed to work his way into a cultural exchange student position at Caltech. He sent an email to the list server to tell us of his success. Here's an excerpt from that email:

----insert 2005 email---

I am right now on Pasadena , California , USA .
I am having a training on building low noise amplifiers for radio
astronomy at the California Institute of technology .
I am trying to learn the RF/Microwave building techniques like
soldering of small SMT components under a microscope , wire bonding
...
I always wanted to learn that , and now I am getting this Great
opportunity to acquire theses skills .

If everything goes fine for me on the training , I maybe able to get a
temporary job here at Caltech as technician .
---end insert---

And indeed everything worked out so well that Hamdi went on to work for Sandy Weinreb on many projects even today. He has worked on :

SUPERCAM: 64 Pixel heterodyne focal plane array at 350 GHz

GAVRT: Goldstone Apple Valley Radio telescope, an educational 34meter telescope that was once part of the Deep Space Network

NGVLA: Next Generation VLA receiver prototype

GUSTO Telescope: Galactic/Extragalactic ULDB Spectroscopic Terahertz Observatory

He has done a number of IEEE papers on low noise semiconductors.

He went on to work 5 years at Caltech before moving to the Arizona State University THz/Radio Astronomy Lab in 2010 and still works there today. He has his BSEE degree now and owns a cryogenics design company on the side called CryoElec. Looks like high vacuum, low noise amplifiers, and low temperature semiconductors became his passion.

That certainly looks like hard work and enthusiasm pays off. And I'm glad we encouraged and answered his questions in 2003 ~ 2005. Maybe he should be answering questions now.

Vela Pulsar Observations at HawkRAO

Steve Olney

Introduction

Hawkesbury Radio Astronomy Observatory (HawkRAO) is a radio astronomy observatory located at the foothills of the Blue Mountains in the Hawkesbury District - some 60 km N-W of Sydney in Australia. It currently operates an array of circularly polarized Yagi antennas in drift-scan mode and is maintained and run by a single individual (the author). The observatory is located on a domestic residential block of size 3000 m^2. At the time of this report, over 6 years of daily observations have been made of the Vela pulsar. During that time two glitches have been recorded.

This article is a summary of the Vela pulsar observing setup and shows some typical results.

Pulsar Characteristics

My personal interest in radio astronomy lies in measuring some aspect of a particular cosmic object over time and mapping any changes or features in the data. Mind you - having limited space and a severely restricted view of the sky already has decided for me that trying to observe large numbers of objects over a wide range of positions on the sky is not practical. Pulsars are the perfect object for actual observing activities as they have a measurable - but changing - characteristic (the gradual increase in spin period as energy is lost via radiation) that can be observed (See Figure 1). The spin period of a pulsar is so stable that it can be relied upon to provide a consistent

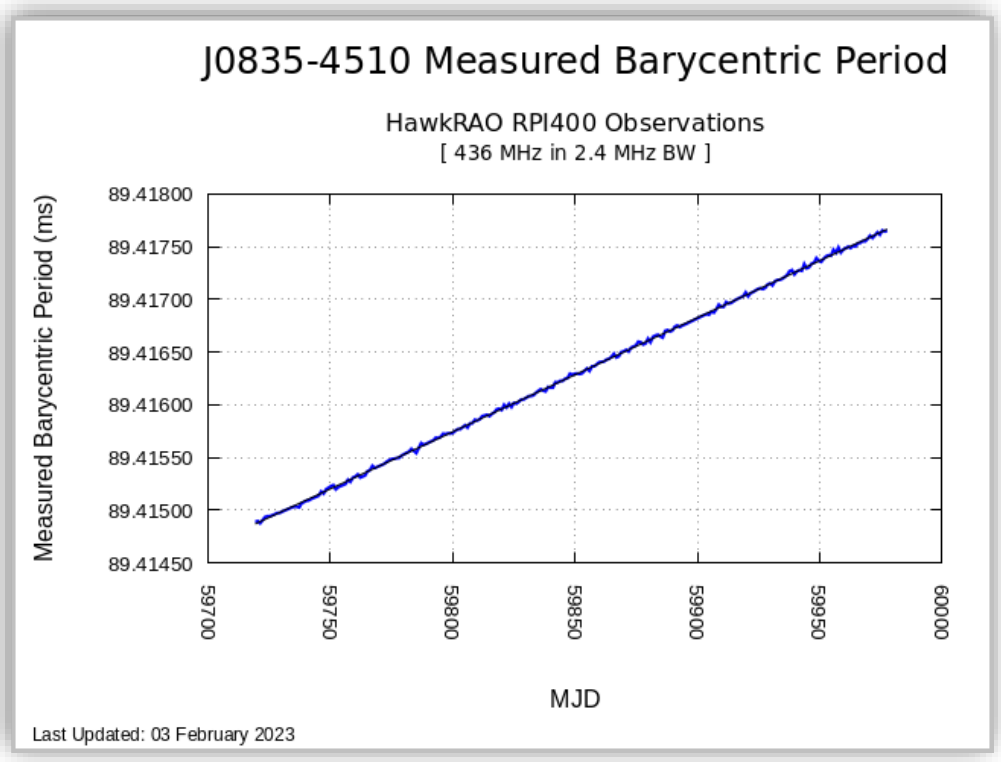

Figure 1: Vela Pulsar Spin period vs MJD

target. This consistency is a key factor in verifying that the signal you see in your results is really a pulsar and not radio frequency interference (RFI) masquerading as one.

Vela Pulsar and Glitches

The reasons for selecting the Vela pulsar as the target for observations are straightforward. Vela is the strongest pulsar at most frequencies and passes almost directly overhead at the southern latitude of HawkRAO. In addition, it is a frequent 'glitcher'. A 'glitch' is a sudden departure from the normal increase in spin period of a pulsar as it loses energy to radiation. For reasons still unknown (although several theories exist) some pulsars show a sudden jump up in spin frequency. The Vela pulsar was the first to be discovered to glitch. Not only is it a frequent 'glitcher', the magnitude of the glitches can reach 3 parts-per-million (ppm). As it is possible, even with a small aperture antenna returning a signal-to-noise ratio (SNR) of around x10, to measure the spin period with a standard deviation (σ) of around 0.2 ppm, many of the Vela glitches are observable. In fact, two such glitches have been observed in HawkRAO data as reported in ATels #12466 and #14808 as shown in Figures 2 and 4.

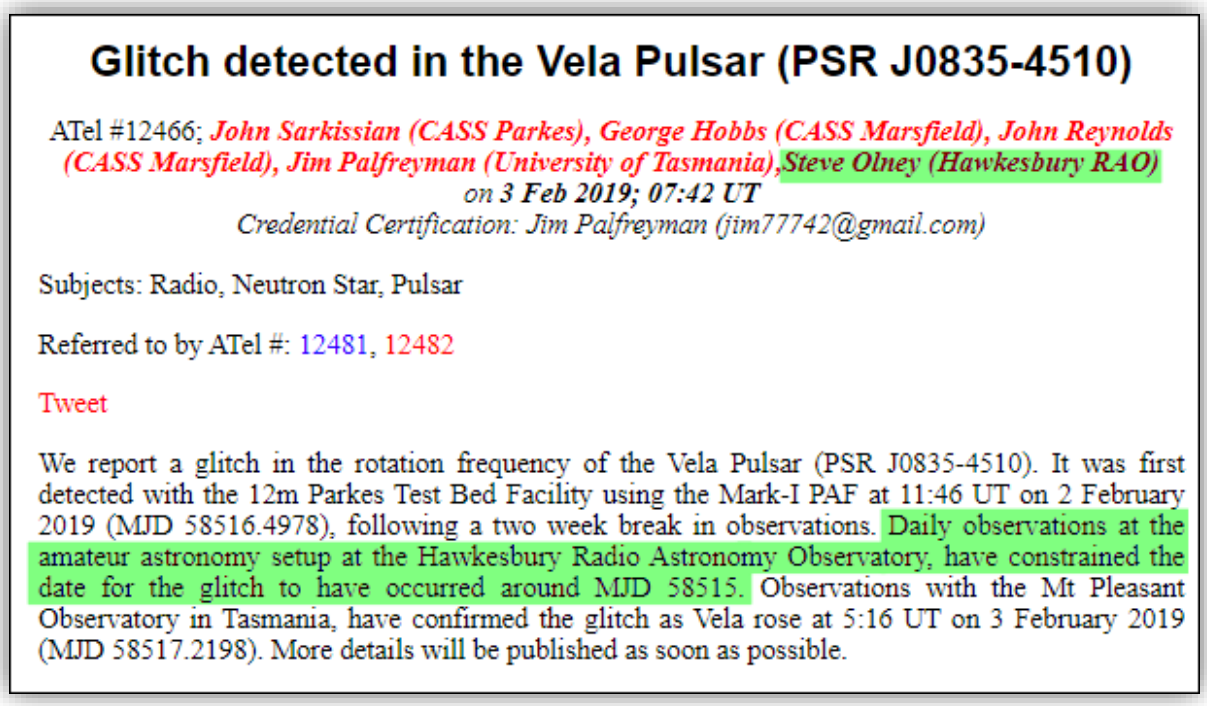

Glitch detected in the Vela Pulsar (PSR J0835-4510)

ATel #12466; *John Sarkissian (CASS Parkes), George Hobbs (CASS Marsfield), John Reynolds (CASS Marsfield), Jim Palfreyman (University of Tasmania), Steve Olney (Hawkesbury RAO)*
on 3 Feb 2019; 07:42 UT
Credential Certification: Jim Palfreyman (jim77742@gmail.com)

Subjects: Radio, Neutron Star, Pulsar

Referred to by ATel #: 12481, 12482

Tweet

We report a glitch in the rotation frequency of the Vela Pulsar (PSR J0835-4510). It was first detected with the 12m Parkes Test Bed Facility using the Mark-I PAF at 11:46 UT on 2 February 2019 (MJD 58516.4978), following a two week break in observations. Daily observations at the amateur astronomy setup at the Hawkesbury Radio Astronomy Observatory, have constrained the date for the glitch to have occurred around MJD 58515. Observations with the Mt Pleasant Observatory in Tasmania, have confirmed the glitch as Vela rose at 5:16 UT on 3 February 2019 (MJD 58517.2198). More details will be published as soon as possible.

Figure 2: February 2019 Vela Pulsar Glitch ATel #12466

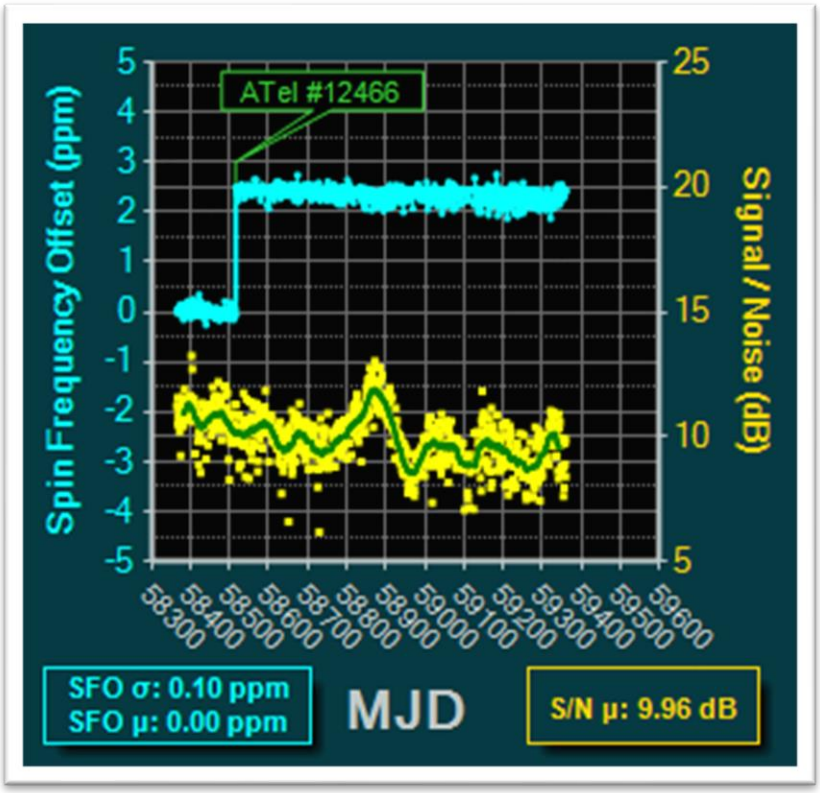

Figure 3: HawkRAO Vela 2019 Glitch Plot

This glitch showed up in HawkRAO data as shown in Figure 3. The magnitude of the jump in spin frequency was around 2.5 ppm and so was clearly seen in the data.

As best as can be determined this was the first ever detection of a glitch in any pulsar by an amateur radio astronomer.

After the recovery phase - where the spin period *partially* returns to the previous period and rate of period increase – the pulsar resumed 'normal operation' until July 2021, where another glitch occurred.

This was the second glitch recorded at HawkRAO and was reported in ATel #14808 (See Figure 4).

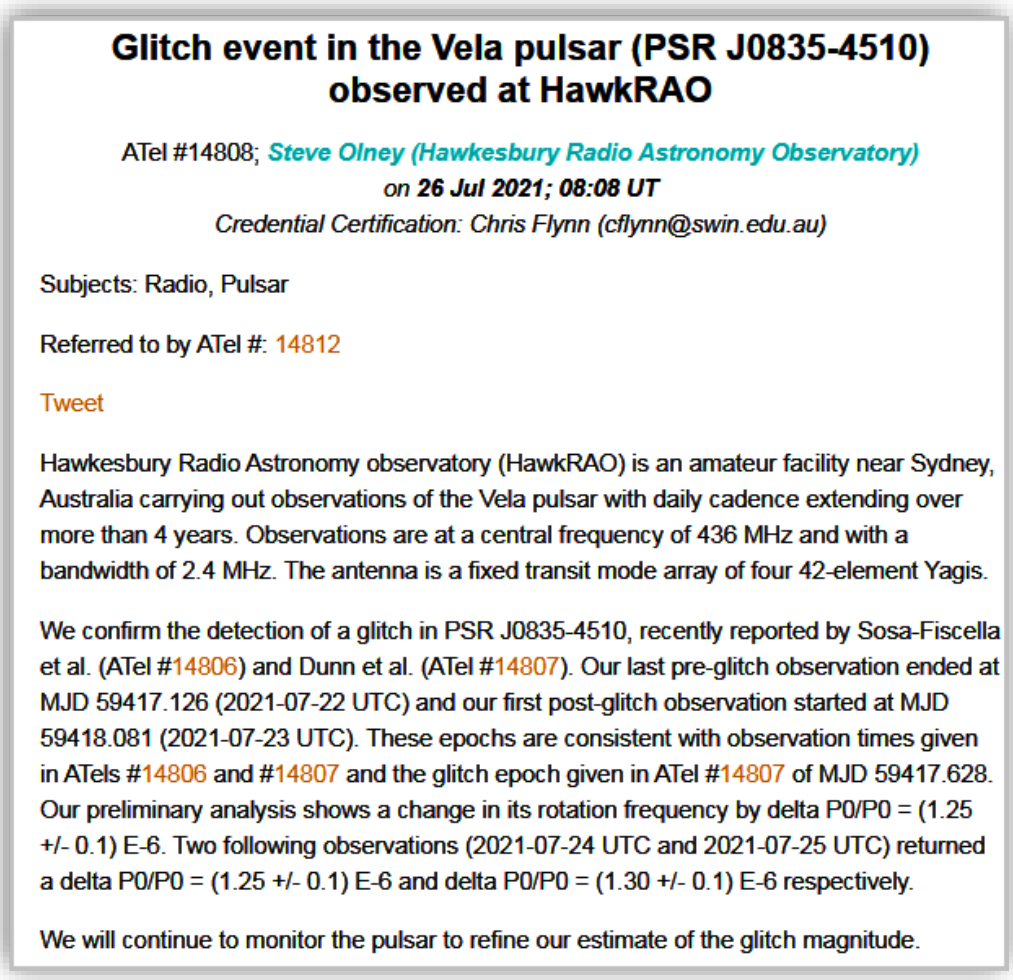

Glitch event in the Vela pulsar (PSR J0835-4510) observed at HawkRAO

ATel #14808; *Steve Olney (Hawkesbury Radio Astronomy Observatory)*
*on **26 Jul 2021; 08:08 UT***
Credential Certification: Chris Flynn (cflynn@swin.edu.au)

Subjects: Radio, Pulsar

Referred to by ATel #: 14812

Tweet

Hawkesbury Radio Astronomy observatory (HawkRAO) is an amateur facility near Sydney, Australia carrying out observations of the Vela pulsar with daily cadence extending over more than 4 years. Observations are at a central frequency of 436 MHz and with a bandwidth of 2.4 MHz. The antenna is a fixed transit mode array of four 42-element Yagis.

We confirm the detection of a glitch in PSR J0835-4510, recently reported by Sosa-Fiscella et al. (ATel #14806) and Dunn et al. (ATel #14807). Our last pre-glitch observation ended at MJD 59417.126 (2021-07-22 UTC) and our first post-glitch observation started at MJD 59418.081 (2021-07-23 UTC). These epochs are consistent with observation times given in ATels #14806 and #14807 and the glitch epoch given in ATel #14807 of MJD 59417.628. Our preliminary analysis shows a change in its rotation frequency by delta P0/P0 = (1.25 +/- 0.1) E-6. Two following observations (2021-07-24 UTC and 2021-07-25 UTC) returned a delta P0/P0 = (1.25 +/- 0.1) E-6 and delta P0/P0 = (1.30 +/- 0.1) E-6 respectively.

We will continue to monitor the pulsar to refine our estimate of the glitch magnitude.

Figure 4: July 2021 Vela Pulsar Glitch ATel #14808

The corresponding HawkRAO data is shown in Figure 5. This time the glitch was about half the magnitude of the 2019 glitch at 1.26 ppm – but still clearly seen in HawkRAO data.

NOTE: For this glitch another amateur radio astronomy observatory in South Australia (Woodchester Observatory) observed the jump as recorded in ATel #14807.

Observation Setup

The setup has undergone a number of changes over the 6-odd years of operation. On the antenna side, the configuration has changed from just a single Yagi to an array of 4 Yagis, and then back down to 2 Yagis. The reason for those changes was to increase the aperture to get a better SNR. The change from one Yagi to four Yagis increased the SNR – but not by the factor of four expected. Apart from the fact that stacking four Yagis into a 2-by-2 array doesn't necessarily give four times the SNR due to increased cabling losses and overlapping apertures, the decreased beamwidth by a factor of two means for a fixed transit mode antenna the observation time is reduced by a factor of two – which gives a reduction of about 1.5 dB in SNR. This can be remedied by arranging the antennas in a 4-by-1 configuration with the long dimension aligned N-S, which gives a narrower beamwidth in

Declination while still retaining the wider beamwidth of one Yagi in Right ascension. This may be a future change. The change back to the current 2-by-1 configuration (with the long dimension aligned N-S) was in response to the 2019 glitch happening in the last few minutes of the 1-hour observation duration enforced by the narrower beamwidth of the 2-by-2 array configuration. The 2-by-1 configuration allowed the return to 2-hour duration observations. I try and not be too saddened by the thought that if 2-hour duration observations were being done in February 2019, the glitch would have occurred about 30 minutes before the end of the observation and the change in spin frequency would have been more clearly seen.

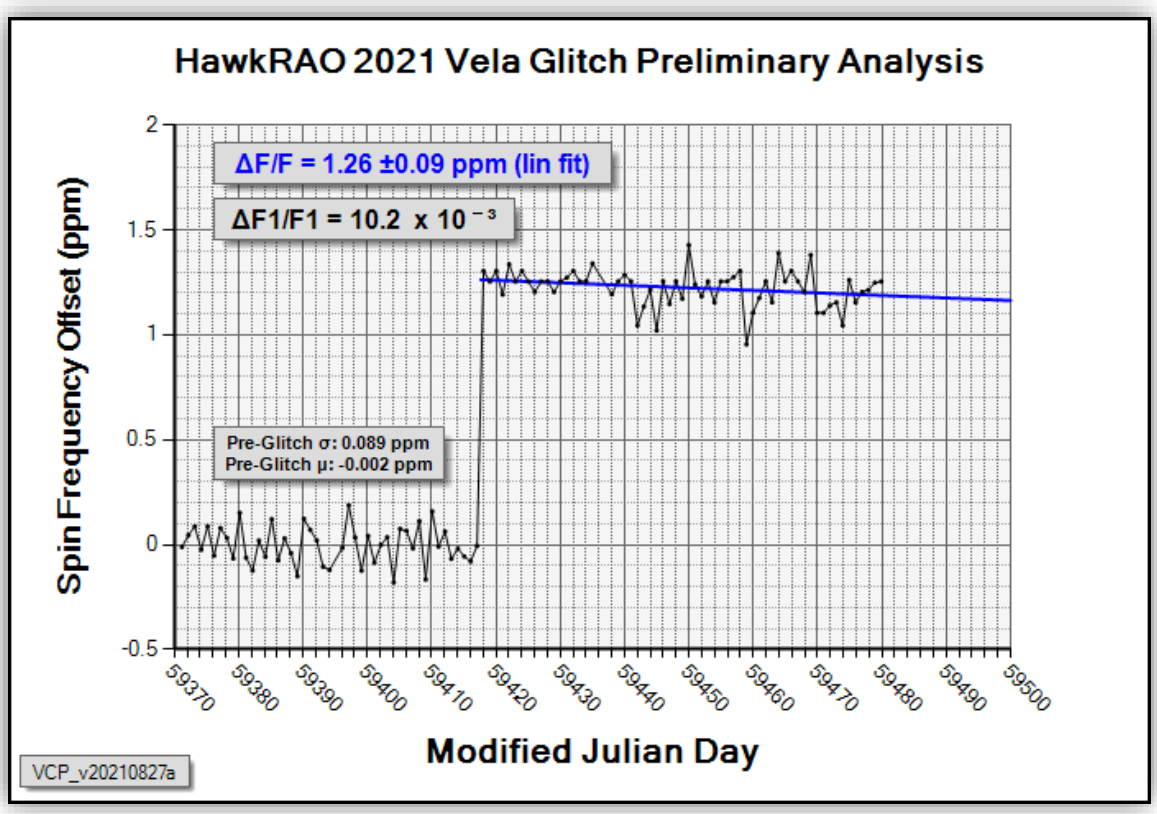

Figure 5: July 2021 Vela Glitch in HawkRAO Data

The antenna array is based on a 42-element circularly-polarized 432 MHz amateur radio Yagi with a quoted gain of 18 dBic. The boom length is about 5.8 m long, but the footprint is small as the antennas are pointing almost straight up as Vela passes almost directly overhead during transit due to its declination being 45° S and the HawkRAO latitude being 34° S.

Coaxial combiners are used to join the antennas in the array. At the antenna the signal is first amplified by a low noise amplifier (LNA), followed by a 436 MHz SAW filter, then further amplified by an amplifier to drive a 20 m cable run into the observatory desk inside. There the signal is further amplified and filtered by a combination of SAW filters and modified cavity filters.

Backend

The signal is then applied to an RTL-SDR dongle receiver which has cooling fins soldered to heatsink the integrated circuits (IC) aided by a small fan. The onboard clock crystal has been supplanted by an outboard temperature compensated crystal oscillator (TCXO) of 0.5 ppm specification. The sampling clock frequency is set to 2.4 MHz as this is the maximum sampling frequency that produces data *without* dropped samples when assisted by the

cooling methods just described. The receiving bandwidth is the same as the sampling clock courtesy of the IQ complex sampling – where each sample consists of two quadrature channels.

Original Data Processing

Originally the data was processed solely with in-house developed software - except for the RTL-SDR dongle drivers and acquisition console application. The original Windows C# GUI software processing involved converting the raw IQ 8-bit unsigned data into the filterbank format – which is essentially a digital version of a bunch of adjacent narrowband filters.

Splitting the bandwidth into separate channels is required because pulsar signals display a characteristic known as 'dispersion'. This is an effect on the signal imposed by the interstellar medium (ISM) as the signal makes its way from the pulsar to an observer, where the higher frequencies in the bandwidth arrive earlier than the lower frequencies. If not compensated for, the pulse profile existing in the higher frequencies will not line up with the pulse profile at the lower frequencies – smearing the pulse shape and thereby reducing the SNR.

By breaking up the bandwidth into channels – such that the channel bandwidth is small enough so that the intra-channel dispersion delay is small enough to not smear the pulse significantly – the data in each channel can be shifted digitally such that all the pulse profiles in all the channels line up and add up to a minimally smeared pulse profile.

After de-dispersion (introducing delays to each channel so they line up in time) the channel data is summed into a single channel format called a 'time series'. This data can be further processed to reduce radio interference (RFI) effects to improve the SNR. Then it is processed by 'epoch-folding' – a process where successive blocks of data are 'stacked' such that the pulse in the data is also lined up over the whole data set. To do this it is necessary to know the period of the target pulsar so that the pulses can be lined up. This process is essentially a one-dimensional version of image stacking in optical astronomy. The SNR improves proportional to the square-root of the number of pulses stacked.

As the purpose of the observations is to actually measure the period in the hope of detecting a glitch, it is not sufficient to just epoch-fold at the predicted period of the pulsar. Instead, the predicted period should be the center of a *range* of epoch-fold operations. At each fold period the SNR is recorded and after scanning the range of periods, the fold period which returns the best SNR is taken to be the current measured period.

The *two* Vela glitches (2019 and 2021) previously mentioned as being recorded at HawkRAO were observed using this original in-house Windows C# GUI software described above.

Hunting For Glitches

The main aim of the HawkRAO Vela pulsar observing setup is to detect Vela pulsar glitches. The method adopted to achieve that aim is to make daily spin period measurements (via a search for best SNR vs fold period) in the hope of detecting the glitches. The *measured* spin period value is compared to a *predicted* spin period calculated from an ephemeris. This ephemeris usually consists of three parts expressed in terms of spin *frequency* referenced to a point in time called the *epoch*.

- F0: the spin frequency at exactly the reference time epoch.
- F1: the first derivative of the spin frequency – which is the rate of frequency change vs time.
- F2: the second derivative of the spin frequency – which is the rate of change of the first derivative.

The predicted spin frequency at some time after the reference epoch can be calculated by the following equation.

$$F_{spin} = F0 + F1.t + F2.t^2 \qquad (1)$$

where *t* is the number of seconds elapsed from the reference epoch.

NOTE: this spin frequency is the *barycentric* spin frequency, which is the spin frequency which would have been observed if the observer was near the center of the Sun. From the more comfortable observing location on Earth, the observed spin frequency will be modified by the Doppler effect of the velocity of the Earth as it moves around the Sun. At any point in time that orbital observer velocity has a component in the direction of the pulsar which depends on the phase of the yearly orbit and both the declination of the pulsar and latitude of the observer. These factors have to be applied to the *observed* or *topocentric* spin frequency to arrive at the *barycentric* spin frequency. This is done so that there is a common spin frequency reference for observatories at different locations on Earth.

Vela glitches so often (on average every 2 ½ years) that an ephemeris found in application packages or on the internet are usually well out of date and if used to do epoch folding searches can cause such a search to be way off the current spin period.

Obtaining a Current Ephemeris

At HawkRAO finding a current vela ephemeris in the early days was a matter of asking professional radio astronomers for their latest values. The answer to this request was not as straightforward as I presumed as such information is often buried in their processing chain somewhere. Another reason is that professional pulsar timing operations do not use the method used at HawkRAO – where an observation of a number of hours is folded to bring the pulse profile up out of the noise sufficiently to be able to get a measure of SNR and is essentially a period/frequency measurement. Professional timing uses 'time-of-arrival' – where pulses are assigned arrival times (corrected to a common time standard) or TOAs. Professionals are able to predict the actual time each pulse will arrive and, except when there is a glitch, link observations and identify individual pulse identities days apart. By contrast the HawkRAO method measures a spin frequency separately for each day and successive observations on different days are not linked. The advantage of the professional way of timing is that the spin period can be measured very accurately for a given SNR. The disadvantage is that when a glitch occurs there is ambiguity as it is unknown how many 'extra' pulses have occurred between a pre-glitch observation and a post-glitch observation and so a number of observations are needed to remove the ambiguity. In contrast the HawkRAO method gives an answer – albeit with much lower accuracy – as soon as the glitch has occurred. Because the spin frequency is measured the day before the glitch and the next day after the glitch, the deviation from the predicted spin frequency is available straightaway. This has enabled HawkRAO observations to give an estimate - within the error band of the spin frequency - some time before the professionals arrive at their very much more accurate value.

Conveniently, after accumulating many days of spin frequency measurement at HawkRAO it is possible to generate an ephemeris from that data by doing a second-order least squares fit. This returns values for F0, F1 and F2 derived from the observed data. The current HawkRAO values are:

- F0: 11.1838223320897
- F1: -1.57544558632375 x 10^{-11}
- F2: 5.74361029675338 x 10^{-21}

The ephemeris is referenced to an epoch of **59719.279304 MJD (Modified Julian Day). It should be noted that these values are empirical values, i.e., they include errors in both the clock frequency (28.8 MHz) as well as the resolution of the clock divider circuits in the RTL-SDR dongle.**

Current Vela Observation System

At the beginning of 2022 a new processing chain was developed which largely abandoned the HawkRAO bespoke Windows C# GUI software platform in favor of a console-based C# pair of programs (developed at HawkRAO) which acted as coding 'glue' for a number of professional applications. The code runs under Ubuntu on a Raspberry Pi 400 (See Figure 6) and consists of a 'Scheduler' – which reads an observation schedule in an external file and – when the time is right – launches another 'Observation' application to acquire, process and display the data. The 'Observation' application itself pipelines a number of separate applications into a processing chain. The chain starts with the RTL-SDR data acquisition application (modified to be able to record data files in excess of 4 GB) followed by successive processing (and data being passed between applications at each stage via temporary files). The chain sequence is as follows.

RTL-SDR → DSPSR → PAZ → PDMP

DSPSR – modified to accept the RTL-SDR as a valid frontend, this application takes the raw IQ 8-bit unsigned data from the recorded RTL-SDR observation file (of the order of 34 GB in size for a two-hour observation) and converts it into a PSRFITS format file (commonly called an 'archive' file) – which is like a compressed version of the filterbank format. In order to do the compression DSPSR needs the dispersion measure (DM) and nominal spin period of the target pulsar.

PAZ – 'zaps' RFI to improve the SNR.

PDMP – takes the processed archive file and performs a search over a range of dispersion measures around the DM value supplied to DSPSR and over a range of spin periods around the value of spin period also supplied to DSPSR. These values are included in the PSRFITS file that DSPSR produces and so is accessible to PDMP.

Figure 6: RPI400-Based Vela Pulsar Observation System

The data from the results of the PDMP search is plotted using **GNUPLOT** and a collection of plots is automatically uploaded to the HawkRAO website. Figure 1 at the beginning of this article is an example of one of the plots.

More Result Plots

Further plots are made using GNUPLOT. The next plot (Figure 8) is of the offset in ppm of the *measured* spin period versus the *predicted* spin period as calculated from the current ephemeris. On this plot the vertical scale is ppm offset in the measured period. The horizontal scale is MJD. Note that the MJD start has been increased from the start of observations some 6 years ago to a more recent beginning about 260 days ago. This was done for two reasons – the first being that previous data contains glitches and so the spin period at those earlier observations would not follow the current post-glitch ephemeris, the second being the plot would be too cramped if it included all 6 years - ~2000 days' worth of data.

Note also that in Figure 7 the largest recorded Vela glitch of 3.159 ppm is shown as a horizontal green line. This glitch occurred at MJD 51559 (February 2000). It can be also seen that the vertical offset scale is asymmetrical with positive values limited to 1 ppm. This is because Vela is not expected to have a 'reverse glitch' of any great magnitude – although small magnitude ones have been observed in some pulsars.

It can be seen from the plot in Figure 7 that there is some deviation from the HawkRAO ephemeris prediction derived from previous observation data. This could be that the post-glitch recovery phase was still settling down – or simply an error in the second-order least squares fit used to generate the ephemeris. In any case the deviation is small – of the order of 0.2 ppm – and so not of much concern at this stage.

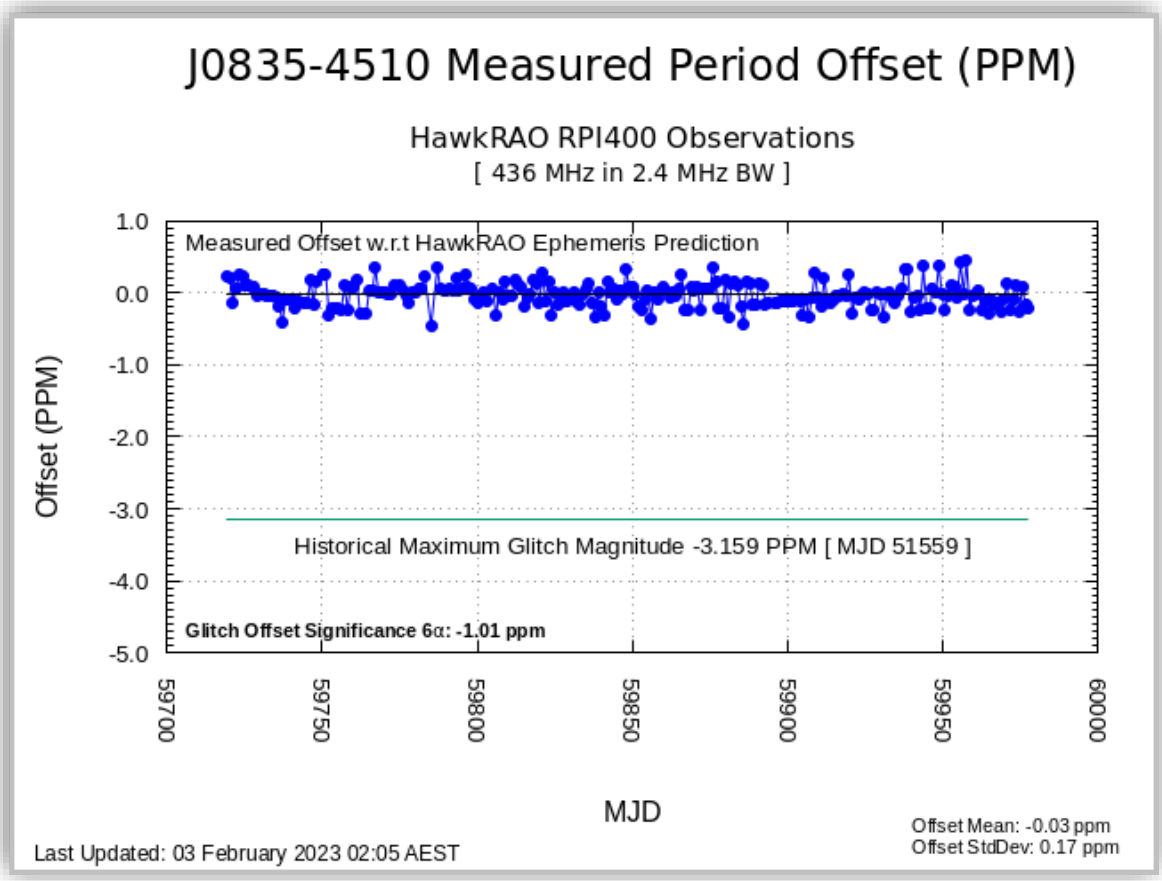

Figure 7: Measured Spin Period from Ephemeris Prediction in PPM

After the spin period offset plot, a plot of SNR versus MJD is done. This is shown in Figure 8. There are some cyclic characteristics in the plot which could be a mix of flux density variations due to the ISM (Vela itself is assumed to be fairly constant in terms of flux density) from refractive scintillation and varying levels of RFI at HawkRAO. The slow downward trend could also be the result of plant growth next to the antenna – like the next-door neighbor's Illawarra Flame Tree.

PDMP Period Search Result

In addition to the GNUPLOT plots generated separately, the PDMP image itself is also uploaded to the website. The image in Figure 9 is the output of a PDMP period search. The top 5 lines contain information about the observation. The four plots are:

- Top-left: a bulls-eye plot of the search matrix results of steps through a DM range against fold period. A nice compact spot in the middle is a sign of a successful period search.
- Middle-left: Phase-vs-Time - shows the pulse strength over the time of the observation. For a pulsar with strong scintillation the pulse trace might come and go over the observation - but Vela shows little variation between the ~100 second sub-integrations. A perfectly vertical blue line indicates that the ephemeris used is accurate. A glitch - where the period decreases abruptly - would cause the blue line to tilt to the left as the pulses would arrive earlier than predicted by the current ephemeris.

- Middle-right: Phase-vs-Frequency - shows the strength over the observation bandwidth. The narrow bandwidth (2.4 MHz) means that any variation across the observation bandwidth would be due to front-end filter responses. A perfectly vertical blue line indicates the signal has been de-dispersed at the correct DM.
- Bottom-left: Pulse Profile. This plot is the pulse signal integrated over the whole observation time and bandwidth. A signal-to-noise ratio (S/N) is derived from the profile - although for a S/N less than about 15 this is likely inaccurate.

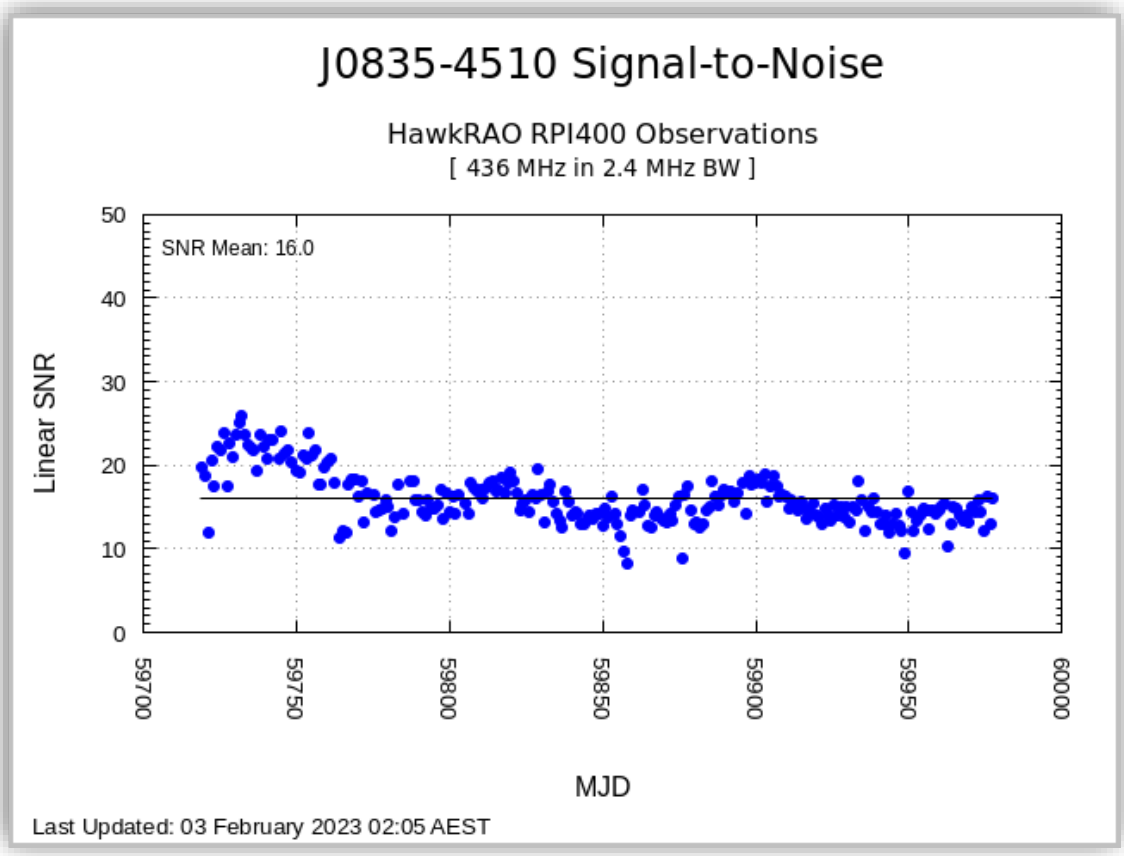

Figure 8: Signal-to-Noise versus MJD

The PDMP plot shown in Figure 9 is of a good observation run with a returned SNR of x16. The plot code has been modified to include observatory identification (i.e., [Site: HawkRAO]) and also the pulse profile has been altered to line up with the 'Phase vs Time' plot and the resolution has been altered to improve the text readability.

The PDMP plot is a powerful verification method as it rules out broadband transients – whose presence would be seen during the observation (2 hours in this example) in the 'Phase vs Time' plot. The 'Phase vs Frequency' plot rules out narrowband RFI as these would appear as horizontal lines.

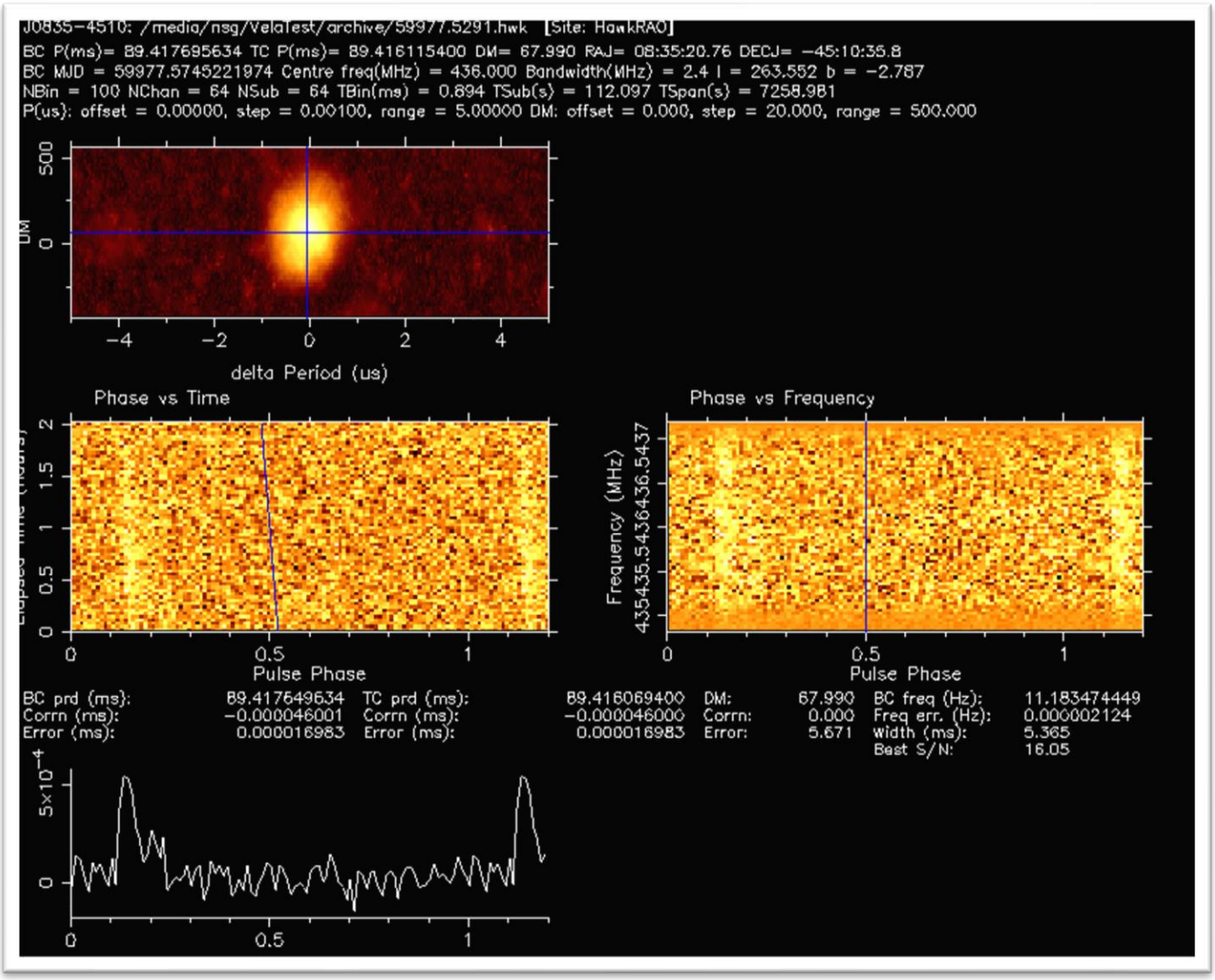

Figure 9: PDMP Output Plot Image

Continuing the Observations

The daily observations are entirely automated and no intervention is required except for moving the build-up of the raw IQ RTL-SDR data files (~34 GB each) off the working 1 TB Solid State Drive (SSD) to avoid it running out of space. About a month's worth of data can be stored before space needs to be freed up.

The other 'maintenance' to be done every couple of days is checking that the separate Windows 10 mini-PC used to upload the results to the HawkRAO website hasn't been restarted by a Window update. There doesn't seem to be a way of blocking those updates reliably. That separate mini-PC is needed because there is no cloud interface software available for the ARM64 of the Raspberry PI. There are ways to work around this but they were found to be both too complex and also somewhat unreliable.

Observations will continue in the above-described manner for the foreseeable future – except perhaps for changing the Yagi antenna array configuration from 2-by-2 to 4-by-1. I am wary of doing that because of the concern that a Vela glitch could occur during the several days' downtime needed to make the change. Looking at

past glitch events I think the next reasonably large one will most likely come between July and September this year (2023). However, trying to predict when the next Vela glitch will occur is a bit of a mug's game, as Vela glitches come according to their own timetable driven by – as yet – unknown causes.

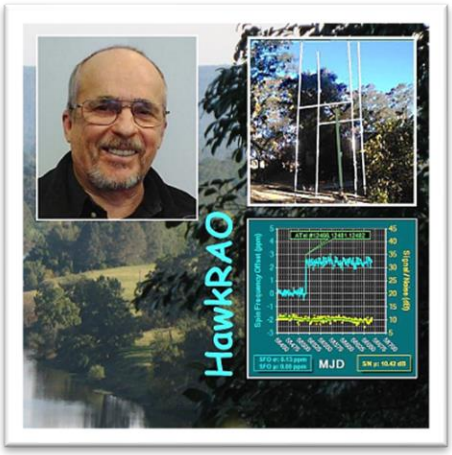

About the author: Steve Olney is the owner and operator of the Hawkesbury Radio Astronomy Observatory (HawkRAO) located some 60 km North-West of Sydney, Australia. Whilst completing a Diploma in Electronics, and later a Degree in Electrical Engineering, he was employed by AWA in the Engineering Products Division where he was trained in all aspects of Engineering including the Test Room, Production Line (two years production line soldering experience), Crystal Manufacture, Transformers, Plating Shop, Lathe Shop, Drawing Office - not to mention Design Engineering. He found that that training was invaluable as it had a good reputation in the industry - useful for when applying for subsequent employment. After some 10 years at AWA the rest of his employment was in the field of medical electronics with several sojourns into technical teaching. Now retired he has the opportunity to address his interest in radio astronomy and to learn as much about the subject as possible - applying that knowledge to the numerous fascinating projects that radio astronomy provides.

Website: https://sites.google.com/view/hawkrao/home

Radio Blackouts!

Whitham D. Reeve

Absorption in Earth's ionosphere affects both terrestrial and celestial radio waves by impeding or blocking radio propagation in all or parts of the high frequency radio band. A complete blockage is called an *HF radio blackout* or simply *radio blackout*; the synonymous phrases *shortwave fade* and *shortwave fadeout* also are often used. Another phrase that may be encountered is *sudden ionospheric disturbance* (SID), but it usually is used to refer to the effect of a solar flare on VLF radio propagation and not HF propagation. Unfortunately, there is a lot of jargon and no *standard* terminology in radio science.

The causes of absorption that lead to a radio blackout are different at lower latitudes than at higher latitudes and are the subject of this article. The first section below discusses the basic mechanisms that cause radio blackouts followed by sections on how solar phenomena controls these mechanisms at different latitudes. Included are three examples in terms of worldwide absorption plots for specific solar events in March and May 2023. The explanations that follow are simplifications, and many technical details are left out to make this article more accessible. Readers wishing to further explore ionospheric radio propagation and the physics involved are referred to [Davies] and references therein.

---

1. Earth's Ionosphere

The ionosphere consists of free electrons and positive ions in equal numbers – a plasma – that coexist with neutral particles consisting of atoms and molecules, mostly nitrogen and oxygen. The plasma, by definition, is electrically neutral overall. As a radio wave in the high frequency band propagates through the ionosphere, the radio wave's oscillating electric field causes the free electrons along its path to oscillate at the same frequency. The positive ions in the ionosphere are too massive to be affected by the electric field and as a practical matter are immobile. The electric field does not affect the neutral particles.

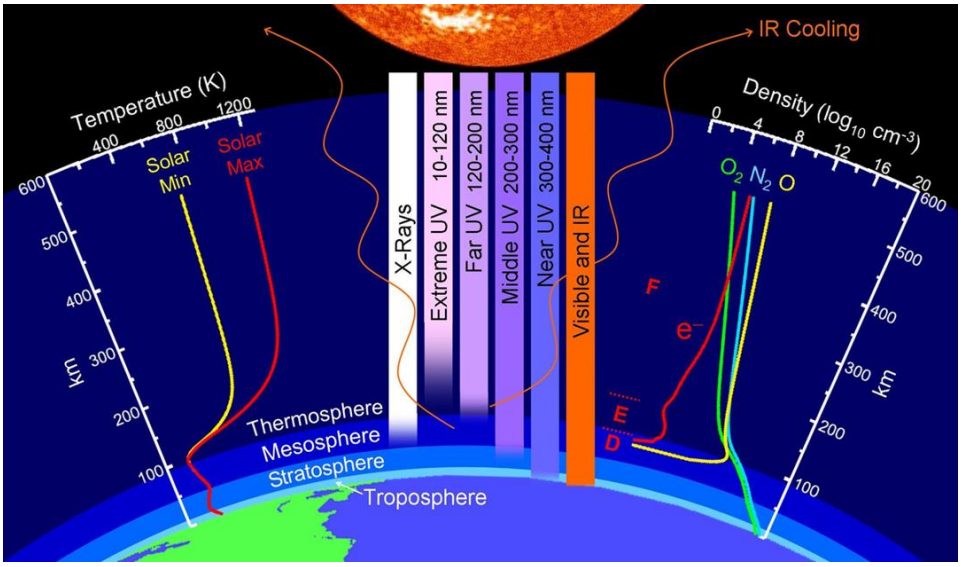

Figure 1 ~ Characteristics of Earth's atmosphere up to 600 km altitude. The chart on the right side shows particle densities. Also shown are the ionosphere regions D, E and F. The red line represents the free electron density (e). Below about 500 km, the densities of the neutral particles, molecular nitrogen N_2 and atomic oxygen O, dominate and in the D-region they, along with molecular oxygen O_2, dominate by a large margin. Image source: NASA

Although the neutral particles in the ionosphere outnumber the charged particles (figure 1), the charged particles determine the medium's electrical properties. Earth's magnetic field also influences these properties by affecting

the movement of the free electrons. The electrons are *trapped* by the forces exerted on them as they move in the magnetic field.

If the oscillating electrons do not collide with ions or neutral particles, they reradiate the energy from the radio wave. The only effect on the propagating radio wave (in this simplified discussion) is refraction and reflection due to the differing electron densities along the radio propagation path. However, where the density of neutral particles is high enough, the electrons can collide with them. The collisions cause the oscillating electrons to lose energy as heat and electromagnetic noise, thereby reducing the energy available for reradiation. Thus, the radio wave experiences *absorption* and is attenuated.

The atmosphere's density and collision rate vary with altitude, so absorption and the efficiency of radio wave propagation also varies with altitude. Most of the absorption occurs in the lower ionosphere where the collision rate of the electrons with neutral particles is highest. This is the ionosphere's D-region at approximately 50 to 90 km altitude. A skywave from a terrestrial transmitter passes through the D-region at least twice, once on its way up from the transmitter to the higher reflective and refractive regions of the ionosphere and once again on its way back down to a receiver (figure 2). If the propagation involves multiple hops, then each hop passes through the D-region twice and experiences absorption on each pass. On the other hand, celestial radio waves pass through the D-region only once on their way down to a terrestrial receiver, so absorption is on the order of one-half of that experienced by a 1-hop skywave.

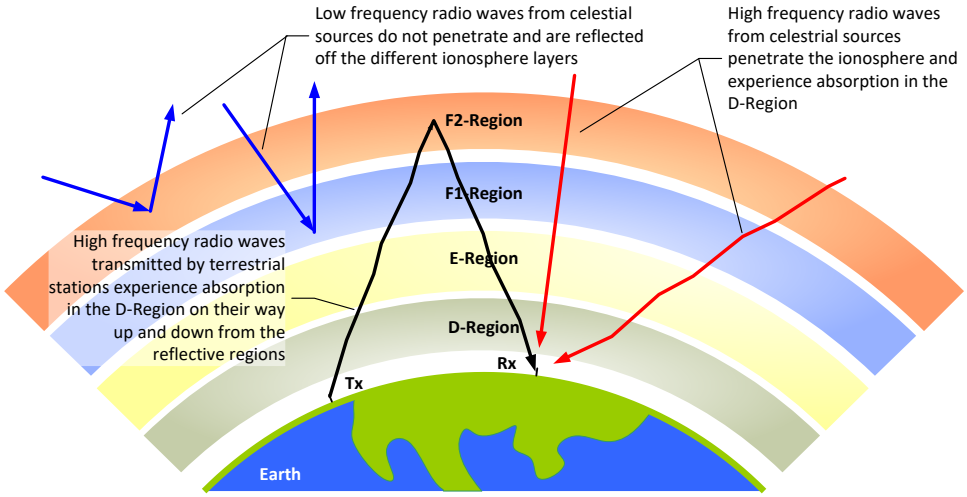

Figure 2 ~ Reflection and refraction take place in the upper regions of the ionosphere, E and F, from approximately 90 to 500 km altitude, while absorption primarily is in the lower region, D, from approximately 50 to 90 km. The ionosphere's properties are highly dependent on the frequency and level of solar activity. Drawing not to scale. Image © 2023 W. Reeve

2. Solar Effects

When the Sun is quiet, the density of the neutral particles in the ionosphere's D-region is relatively constant over time, so local variations in the electron density determine the amount of absorption. The electron density is a function of many parameters and normally varies with the position of the Sun in the sky, latitude, season, and progress of the solar cycle. The broad characteristics of these variations are predictable when the Sun is quiet. The lower HF frequencies are only moderately affected, and higher frequencies are affected very little.

When the Sun is active and a solar x-ray flare occurs on the side of the Sun facing Earth (figure 3), the flare radiation travels at light speed toward Earth, arriving in a little more than 8 min. Some of the radiation penetrates the upper ionosphere and is able to reach the D-region, causing a sudden increase in electron density and leading to a much

more significant and rapid change in the amount of absorption. The absorption can increase so much that the D-region becomes opaque to HF radio waves. Generally, radio waves at lower frequencies in the HF band are most affected. The degree of absorption at any frequency depends on the angle at which the radio wave enters the D-region.

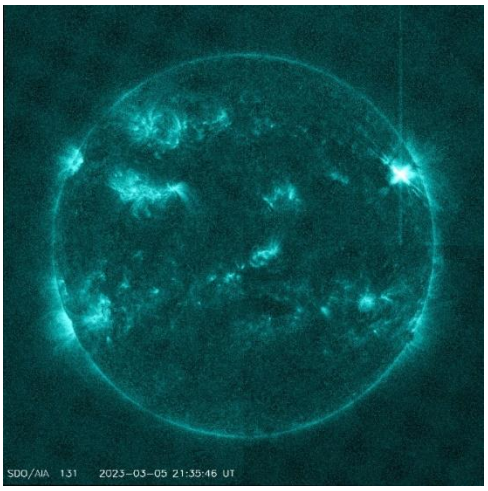

Figure 3 ~ Snapshot of the Sun and a solar flare at 131 Å (13.1 nm) wavelength as recorded by the Solar Dynamics Observatory (SDO) on 5 March 2023 at 2135 UTC. This wavelength shows the hottest material in a flare. The flare intensity was M5.0 and is the bright area near the northwest (upper-right) limb. The flare produced a radio blackout at Anchorage on 15 MHz (see text). Image source: NASA

Solar X-ray flares radiate over a very wide range of wavelengths, but it is the 0.1 – 0.8 nm wavelength range (often called *soft x-ray band*) that is significant to ionospheric radio propagation. Radiation at these wavelengths is able to penetrate the upper ionosphere and reach the D-region. The D-region ionization by solar x-rays is greatest above the *sub-solar point* (the point on Earth's surface where the Sun is directly overhead). The amount of ionization and absorption decreases with distance from the sub-solar point, reaching zero at the day and night solar terminators (gray lines). The night-side of the Earth's ionosphere is not directly affected by solar flares, but flares have been observed on the night-side in the HF radio band under very rare circumstances {Typinski}.

Flares are rated C, M, or X according to the flux radiated at 0.1 – 0.8 nm wavelengths. Spacecraft (for example, GOES) are used to measure these wavelengths because they cannot be measured from the ground. The C, M, and X classification is based on the full-disk x-ray emission from the sun. C-class flares are the most common but least intense and X-class are the least common but most intense, and M-class are in-between. During periods of high solar activity, such as around solar maximum, the background flux may increase to C-class levels for days at a time even without flare activity. The ionosphere's D-region electron density is determined by the total x-ray flux regardless of the source, so these periods of high background flux can significantly affect radio propagation.

The depths of absorption are predicted by Space Weather Prediction Center by estimating the effects of the flare x-ray radiation and energetic protons on the ionosphere [Sauer]. These are plotted as D-Region Absorption Predictions (D-RAP) (figure 4) and are available on the SWPC Radio Dashboard {SWPC}. The absorption predicted in the D-RAP plot resulted in a 15 MHz radio blackout as recorded at Anchorage, Alaska (figure 5).

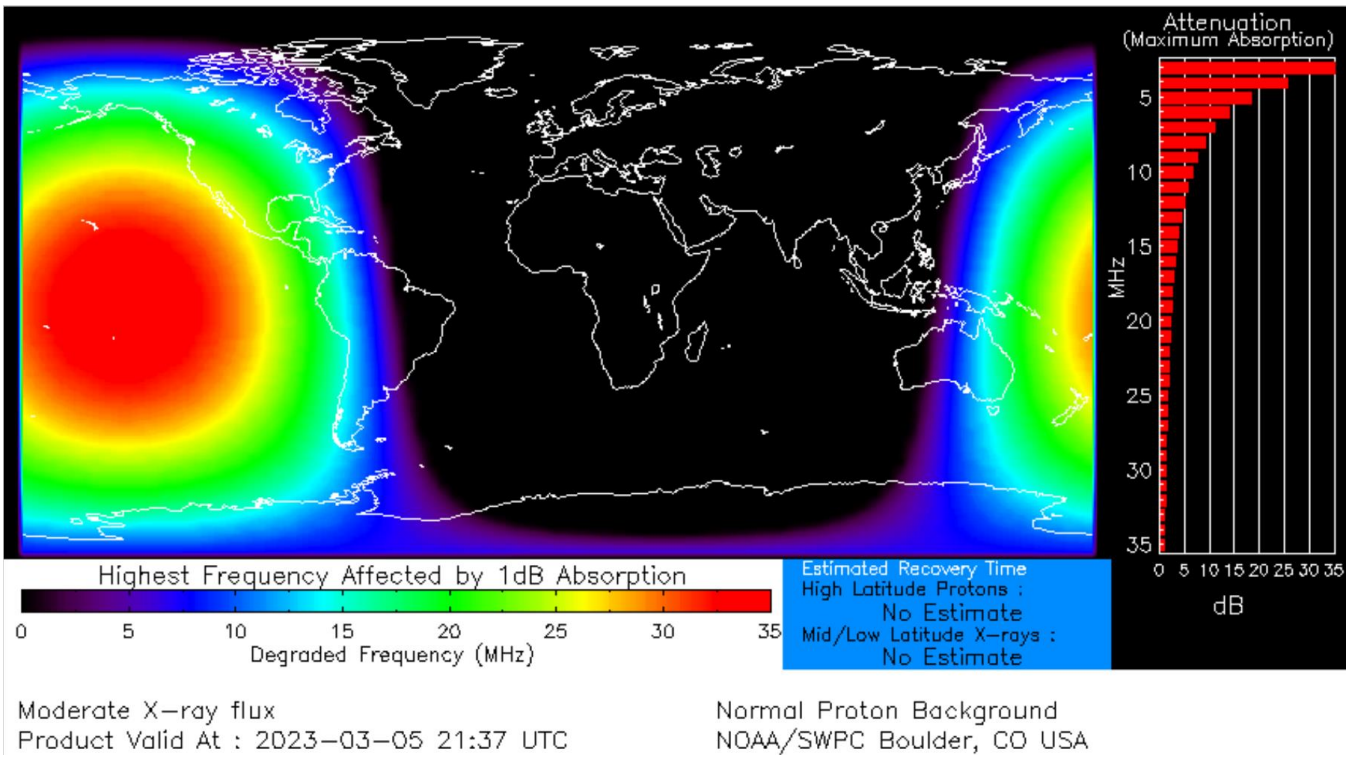

Figure 4 ~ The D-RAP image from 5 March 2023, shows the result of an M5.0 x-ray flare that affected trans-Pacific radio paths. The colors show the highest frequency that experiences 1 dB of absorption but they also indicate the amount of absorption at lower frequencies (the absorption usually affects lower frequencies more than higher frequencies). The histogram on the right shows the predicted absorption in frequency increments of 1 MHz. For example, the absorption at 20 MHz was about 2.5 dB while at 5 MHz the absorption was about 18 dB. Image source: Space Weather Prediction Center

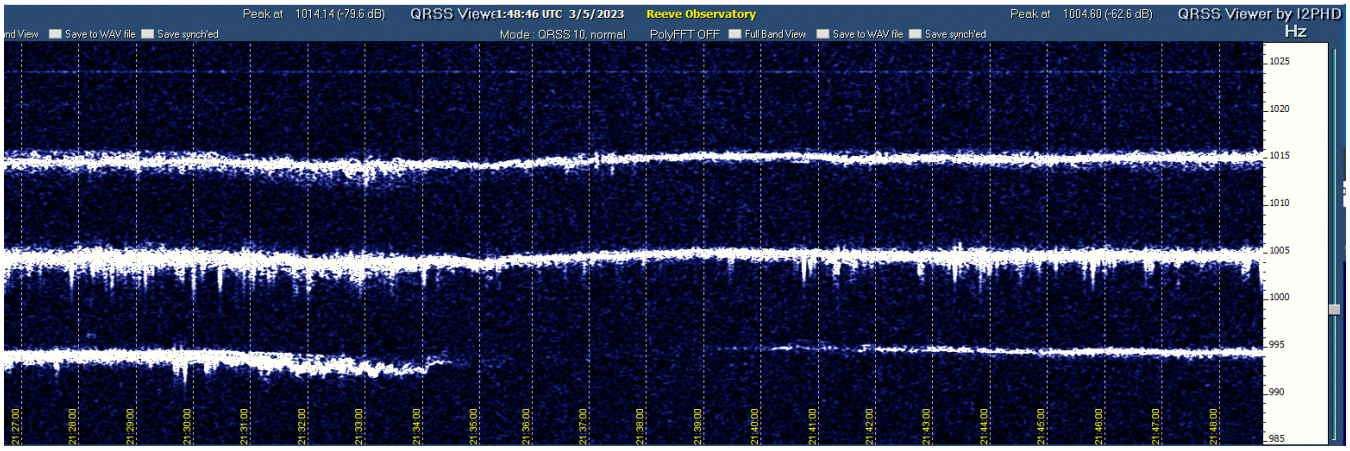

Figure 5 ~ Argo plot for the same time period as the previous figure. Three traces are shown. The lower trace at 995 Hz is the demodulated signal from WWV or WWVH at 15 MHz, and it is seen to blackout at 2134 with partial recovery around 2142 UTC. The middle trace at 1005 Hz is the demodulated signal from WWV or WWVH at 20 MHz. It does not blackout but the signal characteristics do change during the same time period. The upper trace at 1015 Hz is the demodulated signal from WWV at 25 MHz. As with 20 MHz, it does not blackout but there is a slight change in the received signal characteristics. The three receivers that produced the signals for this plot were set to LSB mode and tuned 995, 1005 and 1015 Hz above the carrier frequencies of 15, 20 and 25 MHz, respectively.

3. High Latitudes

Solar flares typically do not affect higher latitudes in the same way as lower latitudes. It is interesting that during winter months at higher latitudes, the absorption is 2x or 3x higher than found under similar conditions during the summer months at those latitudes, and the absorption is much more variable from day to day during winter. At higher latitudes, the absorption from flare radiation is lower because the radiation obliquely penetrates the atmosphere and passes through more of it, and the radiation loses considerable energy before it reaches the D-region (figure 6).

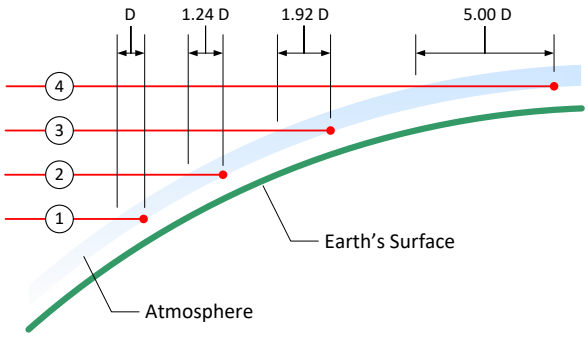

Figure 6 ~Exaggerated effect of incidence angle on radiation intensity received by the D-region. These examples show the Sun's radiation (red lines) hitting the upper atmosphere at arbitrary lower and higher latitudes. At lower latitudes ①, the distance traveled by the radiation through the atmosphere is D, but at higher latitudes ④, the distance traveled is 5 D and much more of the radiation is absorbed before reaching the D-region. Drawing not to scale. Image © 2023 W. Reeve

The relative absorption varies with the solar zenith angle X according to $(\cos X)^n$ where n has been found to vary from 0.7 to 1.0. For example, in the simple case where n = 1, if the Sun's zenith angle is 38° (elevation angle of 52°, which it reaches on the summer solstice at Anchorage, Alaska), the relative absorption is about 79%. If the zenith angle is 75° (15° elevation), the value is much lower at 26%, indicating that the D-region is not nearly as absorptive at the lower elevation angle because the flare's radiation energy is reduced by more atmosphere. It is for this reason that radio blackouts at high latitudes usually are not caused by the x-ray radiation from a flare.

Instead of flare radiation, radio blackouts at high latitudes usually are caused by *Solar Energetic Particle* (SEP) events, also called *Solar Particle Event*, SPE, and *Solar Radiation Storm*. Solar energetic particles consist of protons, mostly from hydrogen and some other atomic nuclei, and electrons ejected by the Sun and accelerated to near light speed. These particles usually reach Earth in less than an hour.

The geomagnetosphere normally shields the Earth from these protons. However, during geomagnetic disturbances, the interaction between the interplanetary magnetic field (IMF) and Earth's magnetic field allows the protons to easily enter the high latitude region around the geomagnetic pole called the *auroral zone*. The SEPs that are involved have energies ranging from 1 to 200 MeV. By assuming the energy is entirely kinetic, the particle velocities can be calculated with a relativistic kinetic energy calculator. If the protons in question are hydrogen nuclei with a rest mass of 1.66×10^{-27} kg, the corresponding velocities range from about 14×10^6 m s^{-1} for 1 MeV particles to 170×10^6 m s^{-1} for 200 MeV particles, or approximately 5% to 57% of the speed of light.

When the protons collide with the atmospheric particles, they release their energy by stripping electrons from the atoms and molecules, thus increasing the electron density and radio wave absorption at high latitudes. This is called *Polar Cap Absorption*, PCA (figure 7). PCA usually leads to a complete blackout of transpolar radio propagation. The duration of a PCA event can range from several hours to days and depends on the proton flux levels. Studies have shown a close correlation between PCAs and Type IV solar radio noise storms.

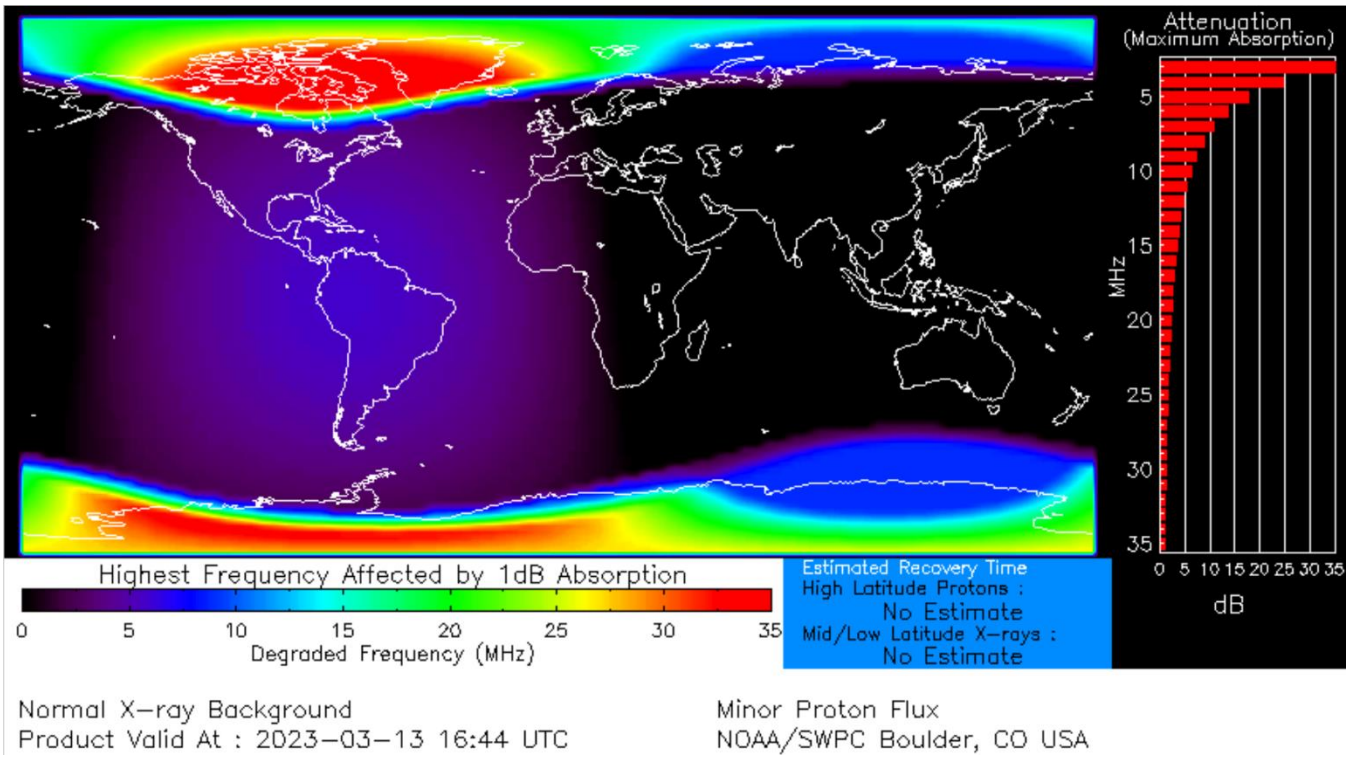

Figure 7 ~ D-RAP image from 13 March 2023 shows the strong absorption at high latitudes caused by an SEP event, which led to a Polar Cap Absorption event. The SEP event was associated with a full-halo CME that erupted on the far-side of the Sun and was first visible in LASCO C2 imagery at 0336 UTC. The SEP required about 1 h to propagate from the Sun to Earth's vicinity. The highest frequencies for 1 dB absorption are shown by the colors in the main panel (absorption at lower frequencies is higher). The histogram on the right shows the absorption in 1 MHz increments at the time of the snapshot. This snapshot at 1644 UTC is representative of the absorption that varied throughout the UTC day. This event had no obvious effect on propagation from WWV or WWVH to Anchorage (Anchorage is below the edge of the absorption region at upper-left) but likely affected transpolar radio paths. Image source: Space Weather Prediction Center

The electron density enhancement from an SEP event depends on several complex factors including the incident proton flux at the top of the atmosphere, the rate at which electrons are produced through ionization and the rate at which the free electrons are subsequently lost by recombination with ions and attachments to other atoms and molecules. All of these depend on the neutral particle and electron densities prior to the event.

The level of geomagnetic disturbance usually determines the extent and duration of a PCA. The 3-hour K-Index, which is determined from ground magnetometers, generally provides a reliable indication of geomagnetic activity. However, in the case of the 13 March 2023 event discussed above, the geomagnetic activity was relatively low throughout the day, possibly because the flare and associated CME that produced the SEP event were on the far side of the Sun and did not directly affect the IMF and its interaction with Earth's magnetic field. This illustrates that solar events and their effects on Earth fall into a statistically *wide* range.

Another example of a PCA event caused by solar energetic particles, or radiation storm, occurred on 8 May 2023 (figure 8). Although the two plots in this figure were taken at 2026 UTC, the event lasted most of that day and for three days afterwards. The upper image shows both the predicted PCA and the coincidental global D-region absorption caused by an M2.3 x-ray flare. The lower image shows the North Pole effects for the same time period.

Compare the 8 May plot, which predicted at least 5 dB absorption as high as 31 MHz, with the previous plot for 13 March, which predicted 5 dB of absorption at only 11 MHz.

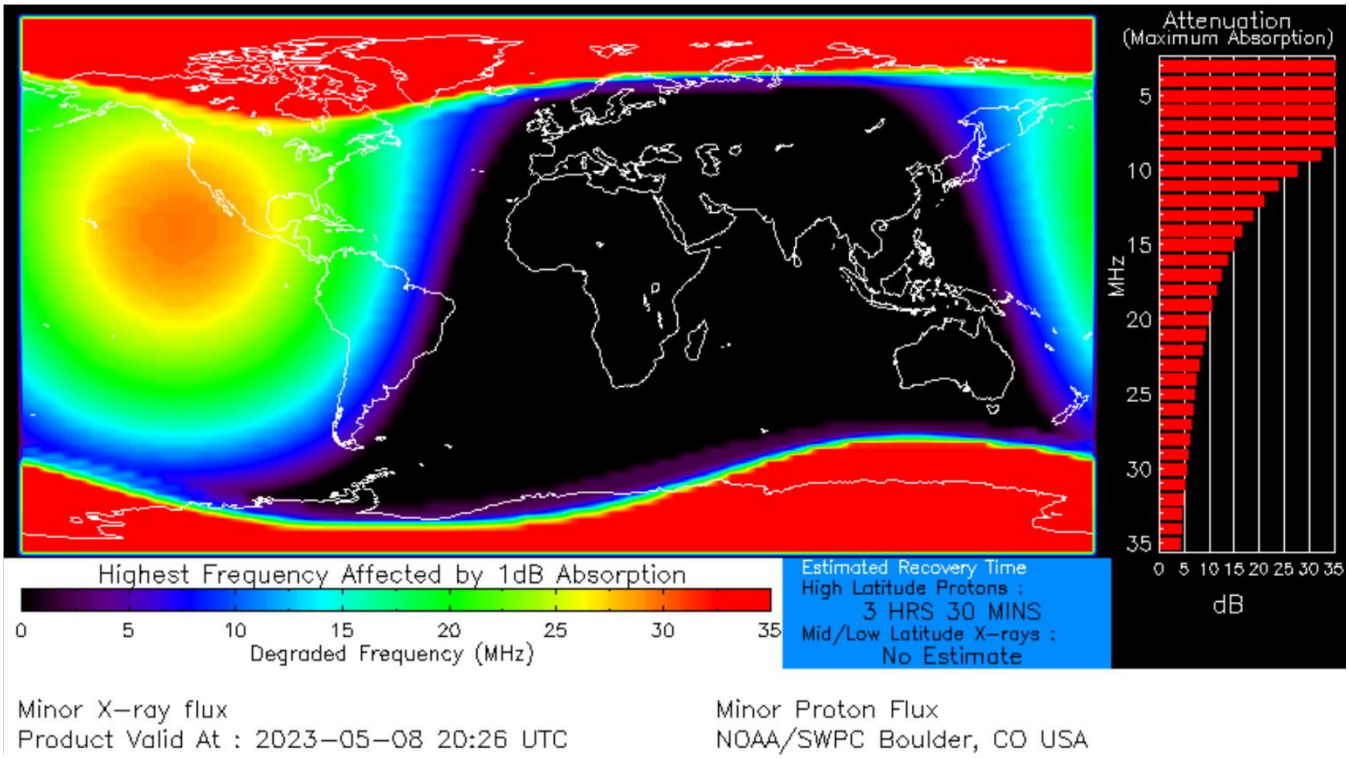

Figure 8.a ~ D-RAP image from 8 May 2023 shows the strong absorption at high latitudes caused by an SEP event, which led to a Polar Cap Absorption event. This snapshot at 2026 UTC is representative of the PCA that persisted until mid-UTC day on 11 May. This event had no obvious effect on propagation from WWV or WWVH to Anchorage. Image source: Space Weather Prediction Center

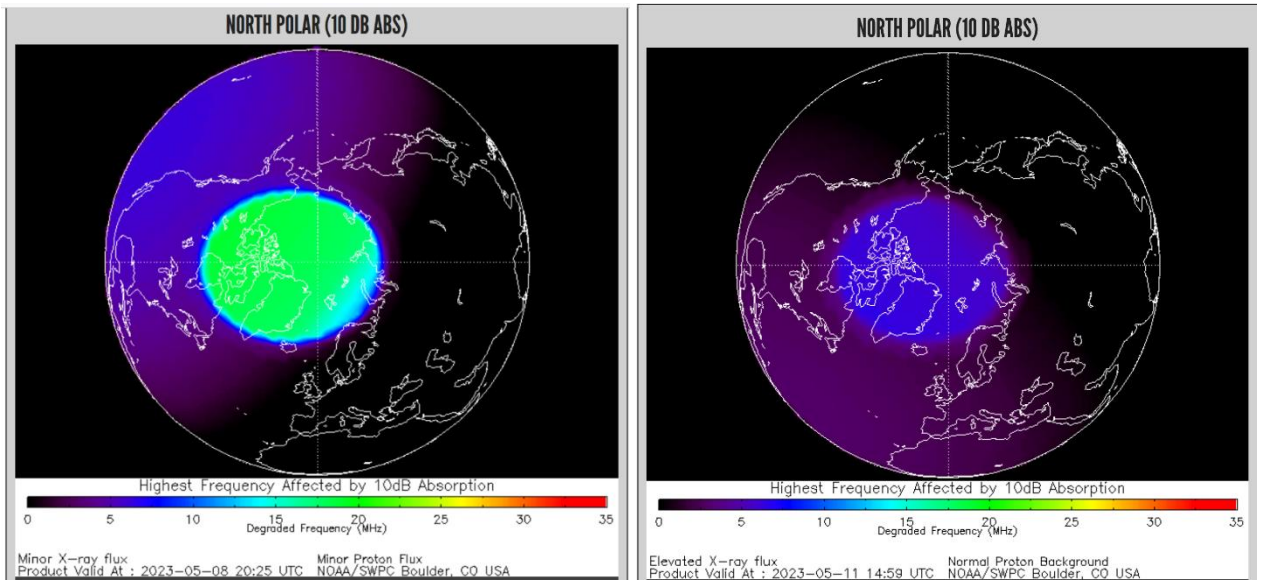

Figure 8.b ~ Left: DRAP plot of absorption at the north polar region resulting from the SEP event of 8 May 2023 and predicted at the same time as the global plot. Note that the polar plot differs from the global DRAP plots in that the basic absorption level is 10 dB for the polar plot and 1 dB for the global plot. In the event shown here, 10 dB of absorption was predicted for approximately 22 MHz. Lower frequencies would incur higher absorption. Right: DRAP plot just after mid-UTC day on 11 May as the radiation storm's effects were subsiding. Image source: Space Weather Prediction Center

The 8 May flare coincidentally produced sudden frequency deviations starting just after 2019 UTC and lasting for several minutes (figure 9). SFDs occur when the radio propagation path length is abruptly changed as the electron density in the ionosphere is enhanced by a strong flare and the reflection region is rapidly moved upward or downward. Although a radio blackout was predicted by the D-RAP program for the date shown, the only effects observed at 15 and 20 MHz at Anchorage were the SFDs.

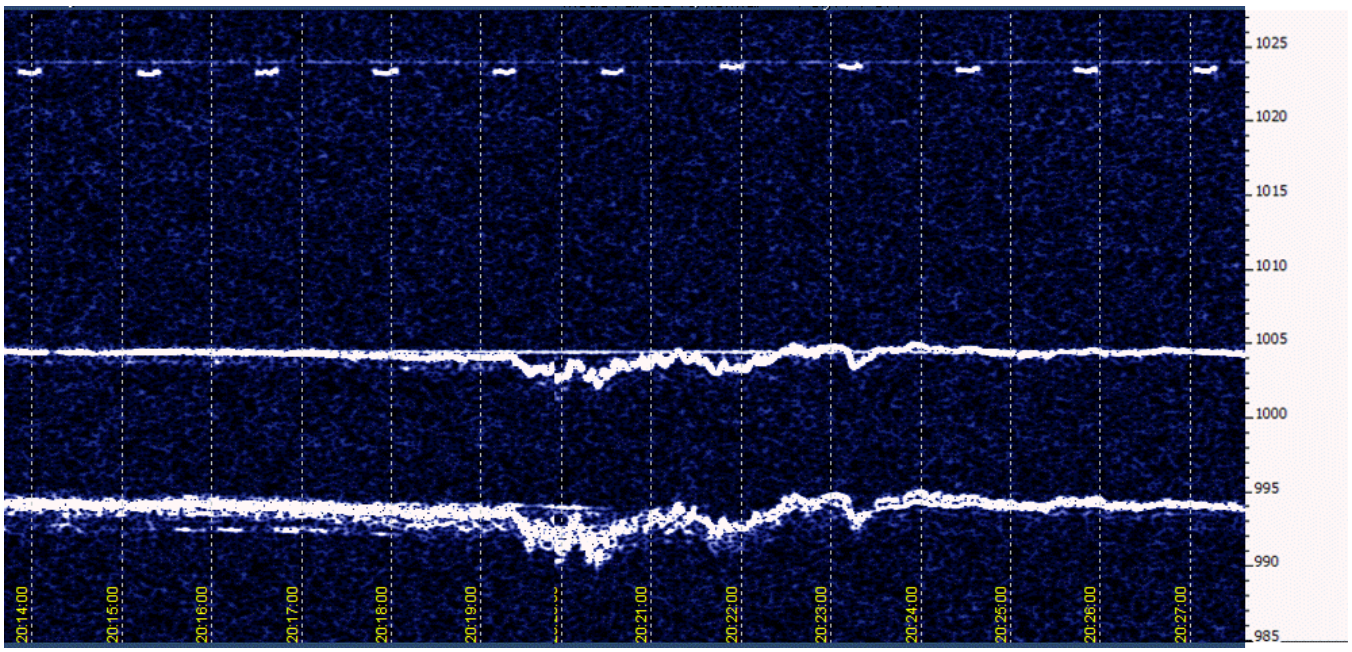

Figure 9 ~ Argo plot showing the demodulated signals at 15 MHz (lower trace at 995 Hz) and 20 MHz (middle trace at 1005 Hz). If signals had been received at 25 MHz, there would be an upper trace at 1015 Hz but 25 MHz propagation to Anchorage was unsupported by the ionosphere at the time. The dashed traces near the top are spurious signals. The sudden frequency deviations resulting from the M2.3 x-ray flare, which began at 2011 UTC and peaked at 22025, are not particularly severe (about 4 Hz at 15 MHz) but are long-lasting.

---

4. References

[Davies] Davies, K., Ionospheric Radio, Institution of Engineering and Technology, United Kingdom, 1990 (earlier versions are less expensive)

[Sauer] Sauer, H., Wilkinson, D., Global Mapping of Ionospheric HF/VHF Radio Wave Absorption Due to Solar Energetic Protons, 2008, https://doi.org/10.1029/2008SW000399

{SWPC} Space Weather Prediction Center, Radio Dashboard: https://www.swpc.noaa.gov/communities/radio-communications

{Typinski} A Solar Radio Burst at Night, observed by Dave Typinski in Florida and reported in the 23 March 2023 issue of Spaceweather.com: https://spaceweather.com/archive.php?view=1&day=23&month=03&year=2023

Investigation of SAT-Finders for Small Radio Telescopes in X- and Ku-band

Christian Monstein and Whitham D. Reeve

1. Introduction

In a previous Radio Astronomy article [Monstein] we discussed the use of a so-called *SAT-Finder* between the LNB (low noise block converter) on a dish antenna and the receiver/spectrometer. A SAT-Finder aids the installation and configuration of the radio telescope by providing a tool with a visual and acoustical indicator (beeper). It is very useful for finding the Sun or a satellite with a radio telescope antenna that do not have azimuth or elevation angle indicators. It is quite easy to position the antenna while using the beeper by listening for maximum received signal strength.

To avoid interference from satellites during radio astronomical observations, we plan to use frequencies below 10.8 GHz, close to the radio amateur X-band and below the Ku-band. To support this plan, we decided to investigate four different setups, three of which use SAT-Finder units. As discussed in the next section, we found they have quite different performance in terms of attenuation at the lower end of frequencies of interest and when standing waves are present. Our investigation used an RF input frequency range of 10.455 to 11.280 GHz with a down-conversion by the LNB to the 45 to 870 MHz native frequency range of the CALLISTO solar radio spectrometer instrument.

---

2. SAT-Finder observations

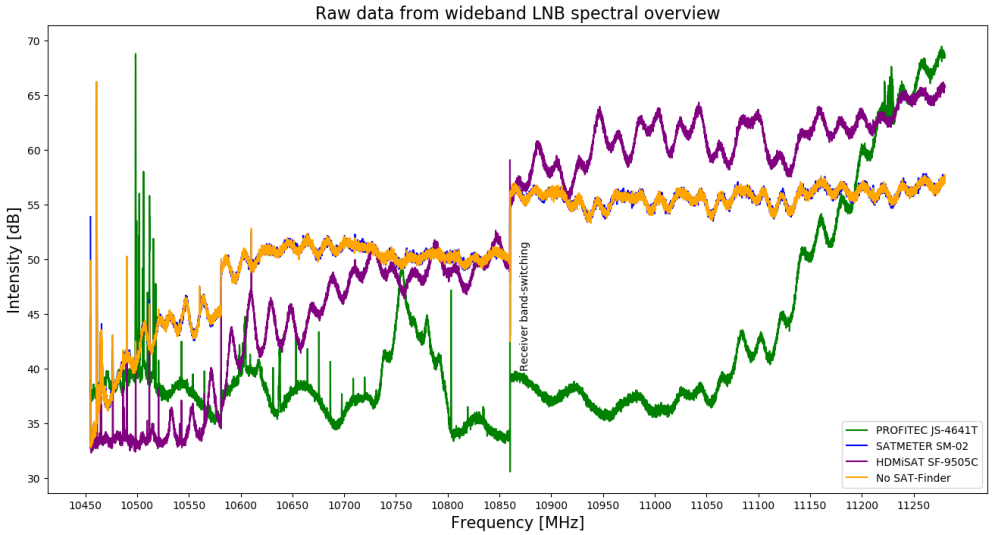

Figure 1 ~ Spectral response of four different setups as observed by using the 'Save spectral overview' function on the CALLISTO frequency agile spectrometer. Note that the SATMETER SM-02 plot (blue trace) is overlaid by the No SAT-Finder plot (orange trace). The quality of the four setups in terms of attenuation and standing waves, the latter seen as ripples in

the plots, are quite different. The discontinuity in the intensity at 10860 MHz is caused by the CALLISTO tuner changing internal frequency bands from its mid-band to high-band. Another, less obvious, discontinuity is seen at 10585 MHz when the tuner switches from its low-band to mid-band.

We investigated four setups, the results of which are shown in figure 1:

- ✓ Profitec JS-4641T, procured from Amazon.com
- ✓ Dagatron SATMETER SM-02, procured from local supplier Conrad in Switzerland
- ✓ HDMISAT SF-9509C, also procured from Amazon.com
- ✓ No SAT-Finder at all

The PROFITEC JS-4641T (figure 2) showed strange behavior below 10.8 GHz (green trace in figure 1). For one thing, it indicated a lot of unwanted signals probably due to inadequate shielding. However, even more disturbing was the large attenuation of at least 20 dB below 10.8 GHz. Admittedly, the unit's specified intermediate frequency (IF) range is 950 to 2150 MHz, corresponding to the wideband LNB's radio frequency (RF) of input 11.36 to 12.56 GHz. We conclude that this SAT-Finder is useless at frequencies below 10.8 GHz where severe problems arise.

Figure 2 ~ *Satellite Finder* JS-4641T from Profitec with an analogue display meter and beeper. This unit works fine for frequencies above about 11.15 GHz but it is not usable at lower frequencies due to high attenuation and spurious signals. The knob at lower-right marked dB is used to adjust the sensitivity of the display and beeper.

The Dagatron SATMETER SM-02 (figure 3 and blue plot in figure 1) is an older unit. It showed a relatively flat spectrum and minor standing waves. This unit proved to be very useful for observations, but it was quite expensive at about $200. As a result, it was found to be unacceptable for use with a low-cost radio telescope.

Figure 3 ~ Dagatron SATMETER SM-02 has an analogue display and works fine down to about 10.6 GHz. The unit is expensive because it contains a battery and allows control of the LNB polarization and measurement of the LNB voltage and current.

The third unit was a *Digital Satellite Finder* HDMISAT SF-9509C (figure 4 and violet plot in figure 1). The IF specification is 950 to 2150 MHz, corresponding to a wideband LNB RF input of 11.36 to 12.56 GHz. This unit has

an internal attenuator and an internal amplifier with a gain of about 10 dB. It can be used below 10.8 GHz, but it produces terrible standing waves, making it inadequate for spectral observations. In addition, its attenuation below 10.7 GHz is in the order of 15 dB, which is too high for certain receivers.

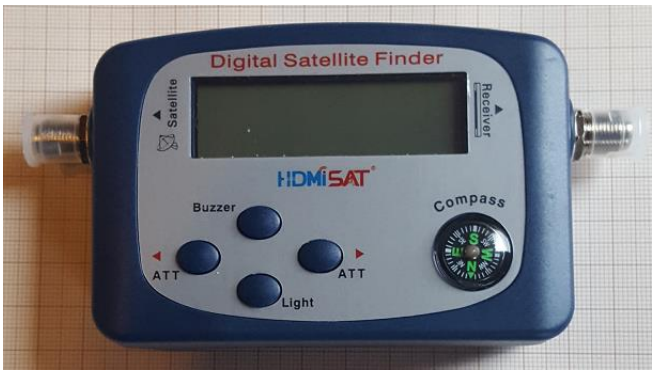

Figure 4 ~ Digital Satellite Finder HDMiSAT SF-9509C contains a digital display, an internal amplifier and an attenuator. The compass at bottom-right can be used to roughly set the azimuth of the telescope antenna.

The last unit investigated turned out to be the best and cheapest, namely no SAT-Finder at all. The spectral response of this setup (orange plot in figure 1), which consists of the LNB, cables, bias-tee and radio spectrometer, is good. Attenuation in the low end of the band is only about 5 dB and standing waves are relatively low and acceptable. The disadvantages are there is no display or beeper; therefore, antenna positioning has to be performed by observing a receiver level meter (if equipped) or the light-curve or spectrum level produced by the receiver/spectrometer.

---

3. Conclusion

Before using any SAT-Finder as a visual and acoustic indicator for a small radio telescope, it is necessary to check its attenuation and standing waves. Cheap units may be acceptable, but it is worth trying several to avoid using one that produces strange or unusable results. An inexpensive NanoVNA vector network analyzer may be used to examine system attenuation as well as standing waves in the spectral response. It is only necessary to have F-male to SMA-male coaxial adapters to perform these tests.

---

4. References

[Monstein] Monstein, C. and Reeve, W., Planning for the 2023 and 2024 Solar Eclipses at VHF, UHF and Ku-band, Radio Astronomy, March-April 2023

Estimation of spectrometer integration time based on noise figure measurements

Christian Monstein, Freienbach, Switzerland, *Monstein Radio Astronomy Support*
Whitham D. Reeve, Anchorage, Alaska USA

Abstract
For instrument qualification of CALLISTO spectrometers, a Python script was generated to derive integration time based on noise figure measurements with a calibrated noise source. Measurement of noise figure and Y-factor allows us to make use of the radiometer-equation to derive integration time Tint, assuming we know the radiometric bandwidth RBW of the spectrometer. A demonstration shows that the result is in the order of ±10 percent. This test is essential to prove that the correct SMD-components are soldered on the CALLISTO PCB during manufacturing.

Index: Noise figure, Y-factor, ENR, noise source, integration time, bandwidth, CALLISTO

Introduction

The aim of this document is to describe how to measure integration time on a CALLISTO spectrometer to ensure that the right components are installed and that they are working as expected. The main idea is to make use of the well-known basic radiometer-equation, the measured Y-factor and the measured signal-to-noise ratio SNR. It is assumed that we know the radiometric bandwidth of the spectrometer which usually is determined by a dedicated bandpass filter, such as the ceramic filter used in the CALLISTO. Other spectrometers may use an FFT-channel or a filter-bank.

Description of equipment, requirements

The equipment used to perform such measurements are the spectrometer connected to a computer, a calibrated noise source with sufficient excess noise ratio and corresponding power supplies. In the present document all units were supplied by *Monstein Radio Astronomy Support*. Besides excess noise of the noise source we also need to note the ambient temperature, which is used in the equations as Tcold or Tref for the reference temperature. In the present case, Tcold = Tref = 273.15 K + 22.7 ˚C = 295.85 K. We also need to know the radiometric bandwidth denoted as RBW. For the CALLISTO, RBW = 300 kHz.

Radiometrics

The basic equation is the so-called *radiometer-equation*, given in equation (1), which indicates the relationship between the receiver or spectrometer noise temperature *Tsys* and the temperature resolution *Trms*. The temperature resolution Trms defines the residual uncertainty in a noise temperature measurement.

$$Trms = \frac{Tsys}{\sqrt{RBW \cdot \tau \mathrm{int}}} \mathrm{K} \qquad (1)$$

The unknowns are temperature resolution Trms, system temperature Tsys and integration time τint. All temperatures are in kelvin. To get to the missing information we perform a hot/cold-measurement by applying a calibrated noise source to the input of the receiver or spectrometer. For sensitive instruments, typically analog instruments, a noise source with +15 dB ENR is sufficient, while for digital instruments such as sampling spectrometers we need a stronger source of at least +33 dB ENR (figure 1). In the case of additional low noise

amplifiers (LNA) in front of the receiver or spectrometer, a much weaker noise source is required, typically in the order of +5 dB ENR. The lower ENR prevents saturation of the system by the noise source.

Figure 1: Calibrated semiconductor noise source to perform Y-factor and noise figure measurements. This type provides +33 dB ENR while another one used for CALLISTO measurements provides +15 dB ENR. The voltage source is +28 Vdc.

After connecting the noise source, we first apply Tcold to the system for a few seconds or even minutes. Tcold, in our case 295.85 K, is produced by the unpowered noise source. The time of observation should not exceed the Allan-time to avoid any systematic errors in the measurement. In the case of CALLISTO, the Allan-time is in the order of 100 seconds. Therefore, applying Tcold for 30 s ... 1 min is fine. Then, we power the noise source, which applies Thot, for about the same time as Tcold. As a result, we get a dynamic spectrum as shown in figure 2-left. The color-table indicates blueish for 'cold' and reddish for 'hot. In the plot for the CALLISTO, we can see the three internal receiver bands, which have different background levels or offsets. In the case of an FFT-spectrometer, we would only see one band with more or less the same background across the whole spectrum.

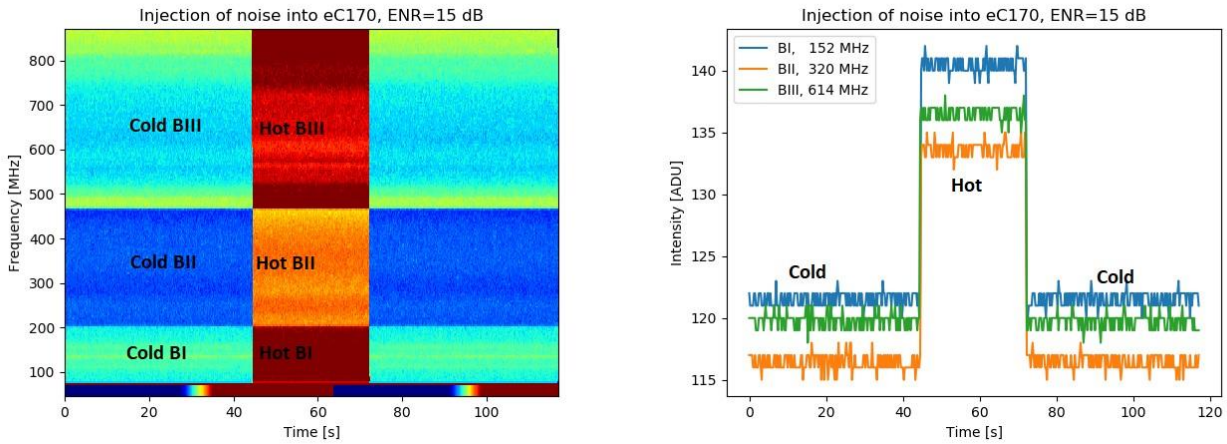

Figure 2: Left image: Dynamic spectrum of cold/hot/cold measurements. Frequency is on the left vertical scale and time on the bottom horizontal scale. We clearly can see three receiver internal tuner bands, 45 – 175 MHz, 175 – 450 MHz and 450 – 870 MHz, and their individual backgrounds. Right image: Three light curves for pre-selected frequencies out of the radio astronomy bands. Here, they are 152 MHz in band I, 320 MHz in band II and 614 MHz in band III.

From the dynamic spectrum we take out one or more light curves for further analysis. Here there were three frequencies selected. These fall into specific frequency bands that are protected by ITU (International

Telecommunications Union) for radio astronomy, hoping that they are free from interference (RFI). Frequencies that suffer from RFI cannot be used for analysis! The result of this selection is shown in figure 2-right.

Now we have sufficient data to start analysis. First, we derive average level of the applied Tcold condition, which we call ycold (cold intensity in arbitrary units such as digits or analog-digital converter units (ADU). Then, we derive the average level of the applied Thot, which we call yhot (hot intensity, again in arbitrary units such as digits or ADU). The third analysis step is to determine the rms (root mean square) value of the cold part, which represents instrument resolution. In the Python script it is simply called 's', which stands for standard deviation or rms. Now, we have sufficient information to perform the calculation of the signal-to-noise ratio SNR shown in equation (2).

$$SNR = \frac{yhot - ycold}{s} \tag{2}$$

In case of the CALLISTO, the SNR varies in the range of 60 ... 95, depending on receiver band and serial number.

For further investigation we need to know the receiver noise figure NF. This can be achieved by determining the so-called Y-factor shown in equation (3).

$$Y = \frac{yhot}{ycold} \tag{3}$$

Then, we need to know the hot temperature Thot which is provided by the powered noise source. See equation (4).

$$Thot = Tref \cdot \left(10^{\left[ENR(dB)/10\right]} - 1\right) \text{K} \tag{4}$$

Based on our knowledge of the noise source ENR and Y, we get the noise figure of the spectrometer expressed in dB shown in equation (5).

$$NF = ENR - 10 \cdot \log_{10}\left(Y - 1\right) \text{dB} \tag{5}$$

In the case of CALLISTO, we get values in the range of 8 dB ... 10 dB, depending on receiver band and serial number. In the case of an SDR, we get values in the order of 30 dB ... 50 dB, depending on the sampling rate, channel width, amplification gain and noise figure.

Now we have sufficient information to derive the system or receiver temperature Tsys, expressed in kelvin. See equation (6).

$$Tsys = Tref \cdot \left(10^{\left[NF(dB)/10\right]} - 1\right) \text{K} \tag{6}$$

For the CALLISTO, we get values for Tsys in the range of 1600 ... 2700 K, depending on the receiver band and serial number. The next step is to apply all intermediate results to derive the product [RBW x Tint] as shown in equation (7). In the case of the CALLISTO, the product [RBW x Tint] is in the order of 280 ... 400, depending on the receiver

band and serial number. In other words, the temperature resolution Trms is on the order of a factor of 300 below the system or receiver temperature. Alternatively, we can measure a solar radio burst with an antenna temperature factor 300 below system temperature Tsys of 1600 ... 2700 K, which is in the range 5.3 K ... 9 K.

$$RBW \cdot \tau \mathrm{int} = \left[\frac{Tsys}{Tenr} \cdot SNR \right]^2 \tag{7}$$

Finally, we can get the measured integration time Tint as given in equation (8).

$$\tau \mathrm{int} = \frac{\left[RBW \cdot \tau \mathrm{int} \right]}{RBW} \mathrm{s} \tag{8}$$

In the case of CALLISTO, we get values in the order of 0.9 ms ... 1.3 ms, depending on the serial number.

Additional comments

The above equations are easy to put into a Python script. One should take care not to mix linear entities with logarithmic entities, usually expressed in dB. In the case of the CALLISTO, all observational data first needs to be converted into dB and in a 2nd step into linear scale before applying to the above equations. In case of an SDR the output values are usually in units of power which is a linear scale.

Experiments with the HackRF One SDR have not yet shown any useful results. This is due to the fact that for all available noise sources the output noise was always larger than any Y-factor. In such a case, the equations cannot be applied. Channel bandwidth or radiometric bandwidth (RBW) times integration time should be such that the noise (rms) is slightly smaller than any Y-factor. Or, alternatively, the noise source needs to provide more than 60 dB excess noise ENR. Such units generally are only available from illegal sources (as jamming devices).

Example CALLISTO + CLP-5130-1N Antenna

Let us develop an example based on a Creative Design model CLP-5130-1N logarithmic periodic dipole array (LPDA) connected to a CALLISTO and observing at 410 MHz. This example assumes that there is no loss between antenna and CALLISTO and that here is no RFI, everything is taken as ideal. Assuming the flux of the quiet Sun at 410 MHz (λ = 0.73 m) is S = 44 sfu (1 solar flux unit = 1 x 10^{-22} W m^{-2} Hz^{-1}) on Saturday, 2023-04-15, the antenna gain is 6 dBi (linear ratio 3.98), Boltzmann constant k = 1.38 x 10^{-23} J K^{-1}, and the antenna is tracking the Sun, we get an antenna temperature according to equation (9).

$$\mathrm{Tant} = \frac{S \cdot \lambda^2 \cdot G}{8 \cdot k \cdot \pi} = 27 \mathrm{K} \tag{9}$$

The peak-to-peak noise is about 6 times Tint (rms) = 32 ... 54 K (calculated in section 3 above, assuming Gaussian statistics). The calculation shows the signal from the Sun only provides about 27 K. Therefore, we will not be able to detect the quiet Sun unless we install a low noise amplifier (LNA) to reduce the system noise temperature. The LNA should have a gain of at least 10 dB and a noise figure of less than about 4 dB.

Installation and configuration of a small radio telescope

Christian Monstein

1. Introduction

The small radio telescope, observing in X-/Ku-band is meant to demonstrate solar radio radiation during eclipse. It can also by used to observe dynamic solar radio bursts or to measure the average disc temperature of the Moon. Main components are shown below and described in detail in this document.

Figure 1 ~ View of the complete telescope (frontend), pointing to the sun. Main components are:

- Tripod (several versions possible)
- Azimuth rotor mounted to the tripod
- Elevation rotor on top of azimuth rotor
- Elevation axis (not visible in this image)
- Satellite dish with clamping adapter
- Low noise block LNB (wide band!)
- Coaxial cable for LNB
- Coaxial cable for azimuth rotor
- Coaxial cable for elevation rotor

All components will be described later in this document.

Not shown in this image left is the so-called backend which is composed out of:

- Option Sat-Finder to visualize RF-level and eventually hear the beeper sound
- Bias-Tee to feed in DC voltage 12V … 18V including power adapter
- Callisto frequency agile spectrometer including power adapter and USB-interface
- Windows Notebook or computer with power adapter and mouse.

Figure 2 ~ Detail view of the azimuth rotor fixation on top of the tripod pole.

Mechanical components used are:

- One rotor with original axis removed
- 2 x large aluminium plates
- 4 x threaded screw bars M8
- 8 x washers
- 24 x hexagon nuts M8
- 1 x 90° F-adapter (REC)

All 4 black clamping profiles shall be mounted such that the slits are on one and the same side. Do not change position of the slits to guarantee absolute vertical mounting of the rotor package on top of the tripod. Use wrench number 13 to tighten the nuts. Try to install the rotor at lowest possible elevation to keep mechanical stability as good as possible.

Take care that the tripod is either standing on a flat, horizontally aligned platform and/or adjust the tripod legs in a way that the vertical pol is perfectly vertically aligned.

Figure 3 ~ Detailed view of elevation rotor on top of the azimuth rotor.

Mechanical components used are:

- 1 x rotor with original axis removed and replaced by a dedicated aluminium axis which will later hold the satellite dish.
- 2 x aluminium plates to fix the rotor on a flange adapter
- 1 x flange adapter to connect azimuth axis and elevation rotor package.
- 8 x hexagon socket screws M8 to mount plates
- 1 x hexagon socket screw M8 to fix flange adapter on azimuth axis
- Hex wrench (Allen key) type 6

Install elevation package such that the elevation axis is pointing to west, assuming cable of azimuth rotor is connected on the north side.

Take care that the elevation axis is perfectly aligned horizontally, use a balance for testing.

Figures 4a, b ~ Circular slits for antenna mounting need to extended by about 10 mm, such that the offset angle of the antenna can be fully compensated for. Drill a whole and file it wide enough as depicted in figure 4b (red arrows).

Figure 5 ~ Install antenna clamping adapter as close as possible to the elevation rotor to minimize moment on the elevation axis. While the axis is pointing west, mount dish such that feed arm and coaxial cable are also on the west side. Tighten the 4 hex-nuts with a wrench.

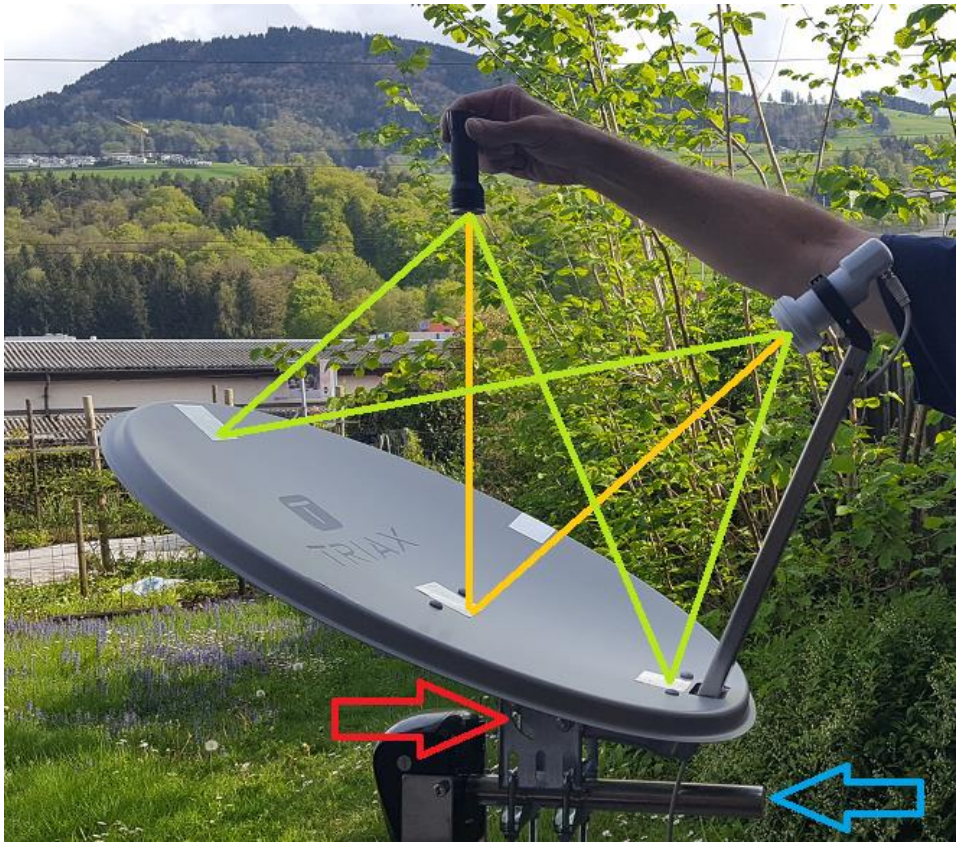

Figure 6 ~ To adjust respective compensate offset angle of the dish you may use a torch and hold it perfectly and vertically above the center of the dish. The light should then be reflected by 4…5 mirrors (glued onto the dish) to the center of the LNB cover. Ideally, this is done during the night or in a dark-room. Once aligned, tighten the screws (red arrow) which fix the dish onto the clamping adapter. Take again care, that the elevation axis (blue arrow) is perfectly horizontal aligned. The main goal is, that the whole setup is aligned such, that the incoming radio radiation is perpendicular onto the elevation axis. Any error in this alignment scheme prevents the control system to track the source (e.g. Sun) for several hours.

Important: This procedure is NOT meant to adjust focus distance but to adjust the offset angle of the dish. Focusing the LNB will be done later with the help of the Sun which is in the far-field.

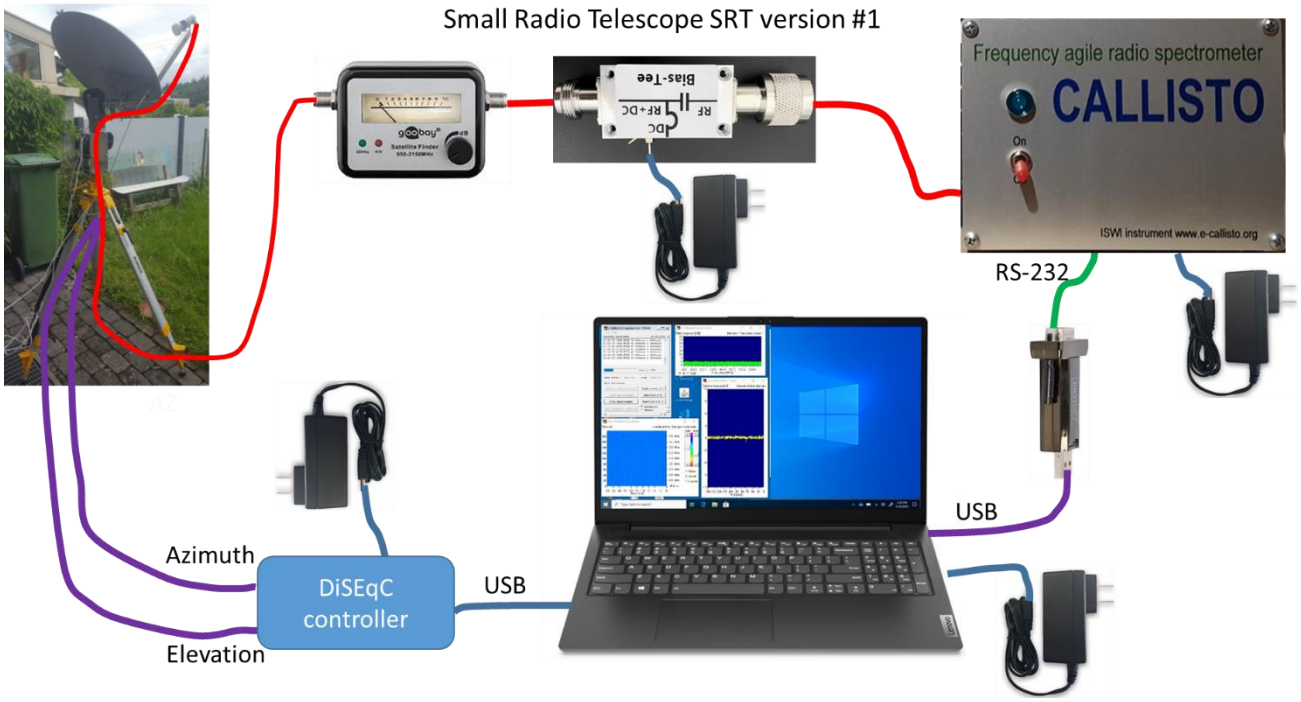

Figure 7 ~ Rough sketch of interconnection of cables and sub-systems. Sat-Finder shall be optional because it attenuates the incoming radio signal by a factor of up to 100. It is fine during configuration or demonstration but, during eclipse observation we recommend to short-cut the sat-finder and to connect LNB directly with the Bas-Tee. Red cables indicate coaxial cables carrying radio signals and are of type F/male both ends. Violet cables are also satellite cables with male F-connectors both ends but do not need to be of high quality in terms of rf-attenuation.

2. Orientation

The orientation of the telescope and the knowledge of all angles of the telescope is essential. The sketches and descriptions are for northern hemisphere, for southern part of the world several angles and directions need to be changed.

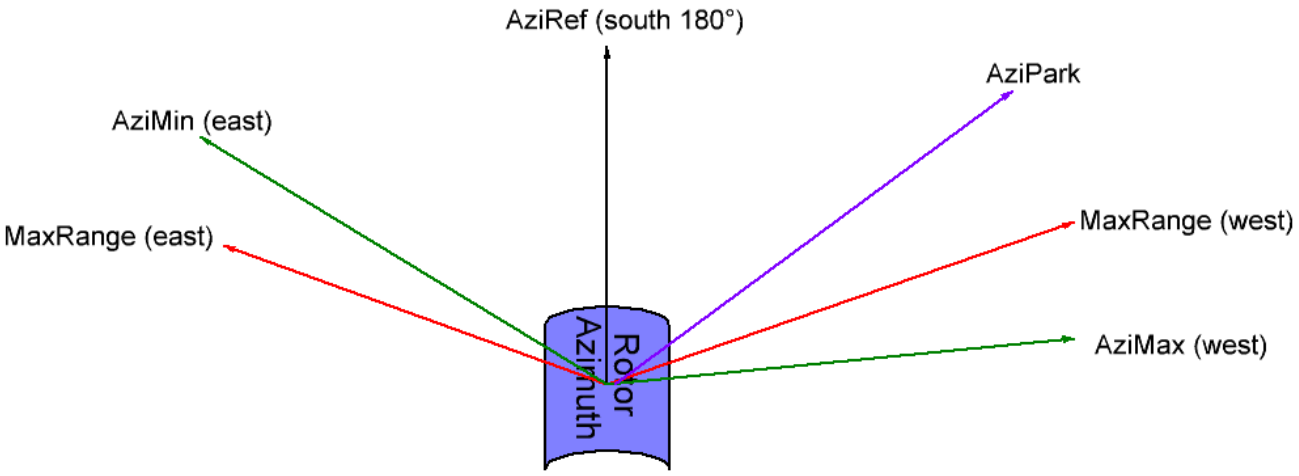

Figure 8 ~ Azimuth rotor, seen from above with east on the left side and west on the right side.

The constant value MaxRange describes the maximum rotation angle of the azimuth rotor. Depending on manufacturer they vary between 67° and 77°. Our current rotors can rotate by +/- 77°. AziRef denotes to azimuth reference, pointing usually to south. We have to distinguish between rotor azimuth and source azimuth. The telescope azimuth is usually chosen such that it fits with meridian transit or with totality of eclipse. Errors in mechanical azimuth alignment can be corrected by editing software reference AziRef. In my case with all the neighboring constrains due to bushes and houses AziRef is selected to 160°. AziMin and AziMax are software limits (green arrows) where we do not want to observe any source due to local constraints such as trees, houses or any other infrastructure. In case shown in figure 8 we cannot even reach the soft-limit due to the fact, that MaxRange is smaller (red arrow). In the east part the soft-limit is within MaxRange due to the house of the neighbor. Violett arrow AziPark denotes to an azimuth position where the telescope is waiting when no observation is performed, e.g. a position of a geostationary satellite. Alle these angles are constant values and part of the configuration, they need to be carefully selected and edited in the Python script sunpos_AZI_ELE.py.

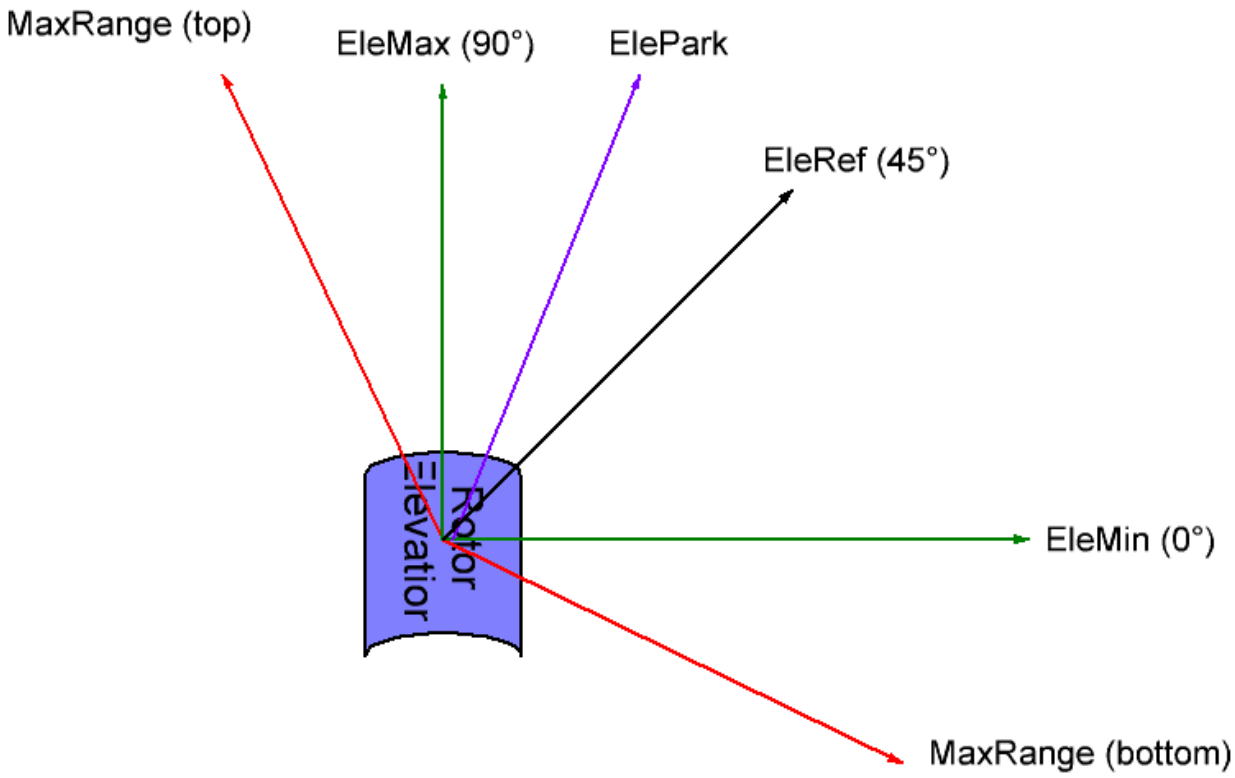

Figure 9 ~ Elevation rotor, seen from west side, south on the right and north on the left. Nadir at the bottom and zenith at the top of the sketch.

The constant value MaxRange describes the maximum rotation angle of the elevation rotor. Depending on manufacturer they vary between 67° and 77°. Our current rotors can rotate by +/- 77°. EleRef denotes to elevation rotor angle 0° and in rotor-reality, with respect to horizon at 45°. We try to adjust the antenna as good as possible to this angle but fine adjust is done by software by changing the value of EleRef in the Python script. EleMin describes the soft-limit of the lowest elevation we want to observe. To avoid ground spill over we select an angle in the order of 10° or so. And the top soft-limit we usually select it to 90° or less in case there is a tree or a roof in the line of sight. Constant ElePark describes the sleep-position of the telescope while no observation is taking place. It could point to the geostationary position of a satellite.

3. Example Eclipse 2023

Before the telescope can be installed and configured, we need to know where we want to perform the observation and at what time we want to concentrate our observations. For that we need any planning tool which allows to derive azimuth and elevation for any location, date, and time.

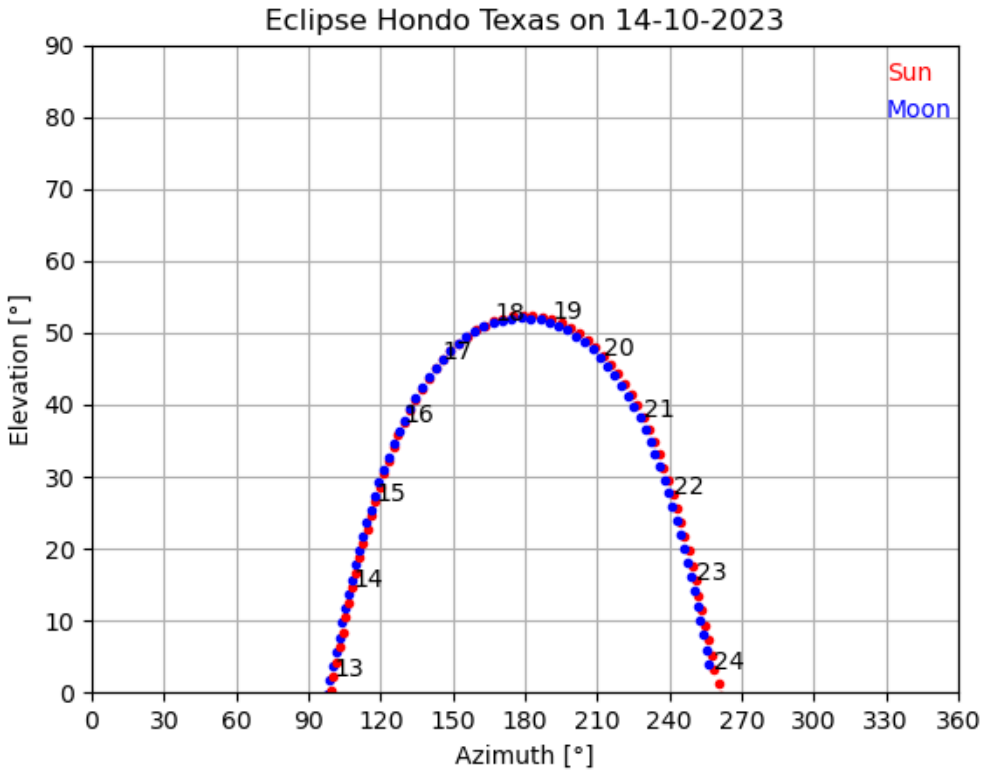

Figure 10 ~ Azimuth and elevation for Hondo in Texas during eclipse on October 14, 2023.

As the totality of the eclipse is at about 16:50 UT, we choose our azimuth reference AziRef to 150°. This is the position with azimuth rotor angle = 0°. Then we can cover +/- 77° from the reference which allows to start observation even before sun-set (150° - 77° = 73°). And after the eclipse we can observe till 150° + 77° = 227° which is about 21 UT. In case we want to observe longer the we need to rotate the telescope by let's say 60° to AziRef = 210°. Then we can observe 210° + 77° = 287° which is later than sun-set.

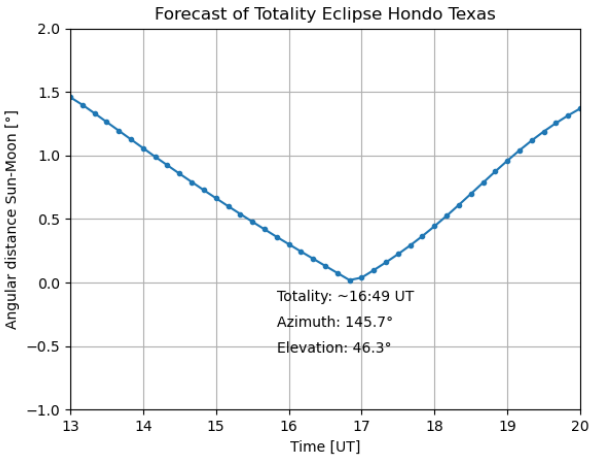

Figure 11 ~ Angular distance between Sun and Moon versus observation time in UT. This plot, generated by a Python script gives us a more detailed indication of reference position AziRef, in this case I'd choose 150° as starting value.

4. Checklist, process of installation & configuration

1. Select location according to weather conditions, accessibility and object of observation
2. Mount tripod on a flat ground, pole vertical by using a balance
3. Install azimuth rotor, then elevation rotor, then dish and finally LNB
4. Install all coaxial cables for LNB and rotor control
5. Connect DiSEqC-interface and CALLISTO to computer and find out COM-port number and enter port-number for telescope control in Python script sunpos_AZI_ELE.py and port number for CALLISTO in file callisto.cfg
6. Check date and time, we need UT to a precision of better than 10 seconds
7. Get precise longitude, latitude, altitude with at least 3 decimals, temperature and air-pressure and edit Python script
8. Define azimuth reference AziRef, set the telescope in this direction as good as you can
9. Use PUTTY (9600 baud, 8 data bits, 1 stop bit, no parity and flow control None) to set azimuth- and elevation-rotors to reference (azi0 ENTER and ele45 ENTER) The antenna should now move from 45° south to zenith. Then you may mechanically fine adjust elevation using a balance. Using commands azi, rotate the system from -77° to 77° and measure if the elevation axis is perfectly horizontal. Use a digital balance with a resolution of 0.1° or better.
10. Run script sunpos_AZI_ELE.py in Spyder and play with AziRef and EleRef until you get maximum signal from the sun. Before that perform mechanical adjustment of the telescope by centering sun light on the cover of the LNB. Use a clean, white paper in front of the LNB to see whether the light is outside of the LNB. For better visibility, use a sheet of white paper centering in front of the LNB
11. Once fine adjust is done within Spyder, enable ssfree.exe script call for telescope control.
12. Check and edit parameter for CALLISTO in file Callisto.cfg, also read the related docs about CALLISTO.
13. Start observation either in manual or in automatic mode.

Mechanical tooling needed:

- Wrench #13
- Hex wrench (Allen key) #6
- Drill 8 mm
- Rasps (flat round, semi-round)
- Torch
- Digital balance

Software required:

- Windows operating system Win 7. 8. 10 or 11
- Python3.x with Anaconda and Spyder installed. Libraries ephem, serial installed
- System Scheduler ssfree.exe installed and configured for tracker
- PUTTY installed and configured for DiSEqC and CALLISTO
- Callisto software installed and configured: https://e-callisto.org/Software/CallistoInstaller_V22.zip
- On desktop: device manager and task manager, Spyder, Anaconda prompt, DiSEqC-control

Lunar radiation observed by a small dish at 80 GHz. Part 2, more about atmosphere, brightness temperatures and results.

by Dimitry Fedorov UA3AVR and Joachim Köppen DF3GJ

In Part 1 (March-April 2023 issue) we have considered the telescope building, the observation procedures, the role of atmosphere in observation and data processing. Here we shall continue with a description of the procedures to extract the lunar brightness temperatures, discuss related issues and compare results with corresponding professional observations.

Method FC (Flux Calibration) and more about the atmospheric attenuation

Since the internal noise described by T_{RX} is the most important contributor to the receiver response (the Moon noise power) we consider a procedure not sensitive to possible errors in T_{RX} or dependent on the previously known NF.

In the Flux Calibration method we compare the lunar noise with the noise from a source of known temperature.

We may define the ratio

$$R = (Y_{moon} - 1) / (Y_{cal} - 1) = (P_{moon} - P_{sky}) / (P_{cal} - P_{sky}). \quad (12)$$

which contains the observed values $Y_{moon} = P_{moon}/P_{sky}$ and $Y_{cal} = P_{cal}/P_{sky}$. On the other hand, we can also express the powers by Eqs. (1), (7), and (10), Part 1 in terms of temperatures. This gives an interpretation of R as:

$$R = (\eta * T_{moon}/L(e)) / (T_{cal} - (\eta * T_{sky}(e) + T_{amb} * (1-\eta) * k)). \quad (13)$$

Since the value R is known from the measurements, we can deduce the value of T_{moon} as:

$$T_{moon} = L(e)/\eta * R * (T_{cal} - \eta * T_{sky}(e) - T_{amb} * (1-\eta) * k), \qquad T_{sky}(e) = T_{sky0} * (1-1/L(e)). \quad (14)$$

The second formula in Eq.(14) presents an explicit form of $T_{sky}(e)$, see Eq.(4), Part 1. The receiver noise T_{RX} is completely gone in Eq.(14): this is because the comparison with the source of known temperature allows us to deduce an effective noise temperature of the receiver (T_{RX} can be computed from Eq.(7) and (11), Part 1, but this is not necessary for getting the lunar temperature). The FC method can further be simplified by making use that T_{cal},T_{amb}, and T_{sky0} are equal or very close to each other. Then we get this expression:

$$T_{moon} = L(e)/\eta * R * T_{amb} * (1 - \eta * (1-1/L(e)) - (1-\eta) * k) \quad (15)$$

Note that Eq.(14) and (15) contain *L(e)* – the atmospheric absorption along the observation path from the Moon *including clouds*. The simplest way to get *L(e)* is to take here the value obtained in NF method, see Part 1. The NF method gives *L(e)* under assumption that the receiver NF is previously known. But since the receiver NF is known with some uncertainty, the *L(e)* could suffer from a corresponding uncertainty. Nevertheless, having such *L(e)* is better than nothing. In order to estimate how this uncertainty affects our results we will calculate the brightness temperatures also without the clouds contribution (i.e. only with ITU gaseous losses) for comparison. With only the two measurements of calibrator Eq.(7) and the empty sky at the Moon's elevation Eq.(11) we have no further

information that allows us to determine the value for *L(e)* which would be consistent with the effective noise temperature of the receiver. Only measures of the sky noise at several elevations could provide this information.

From Beam Temperatures to Brightness Temperatures

We definitely know that temperature is distributed unevenly over the lunar disk at high frequencies including 80 GHz; moreover, the distribution itself depends significantly on the lunation phase. The temperature of the disk center T_{center} is a customary measure for the lunar radio brightness at a given frequency [1].

Two examples for the observed temperature distributions are shown at Fig. 1 as isotherms on the lunar disk. The beam temperature T_{moon}, which we obtain by the measurements, can be expressed via a temperature distribution as

$$T_{moon} = \frac{1}{4\pi} \oiint T_B(\theta, \varphi) \cdot \mathrm{D}(\theta, \varphi) \cdot \sin\theta \, d\theta \, \mathrm{d}\varphi, \qquad (16)$$

where $T_B(\theta, \phi)$ - is the brightness distribution across the disk (=0 outside the Moon), $D(\theta, \phi)$ the directivity pattern of the dish vs angular variables θ,ϕ. The integration over the full sphere in Eq.(16) is limited to the lunar disk only, as outside the Moon we have $T_B(\theta, \phi) = 0$. At the disk center ($\theta = \phi = 0$) the central temperature is $T_{center} = T_B(0,0)$, and the ratio T_{moon}/T_{center} (or the reversed one, T_{center}/T_{moon}) computed from Eq. (16) can be used to deduce the Moon brightness measure T_{center} from the measured data.

A problem lies in a scarcity of observed brightness distributions at various frequencies and lunar phases. However, already a simple modeling of the heating of the lunar soil by the Sun gives a very good match of the observed variation of the phase dependence of the lunar temperature [3]. Therefore, it is reasonable to take a theoretical approach enjoying a freedom to know the distribution for arbitrary frequencies and lunation phases.

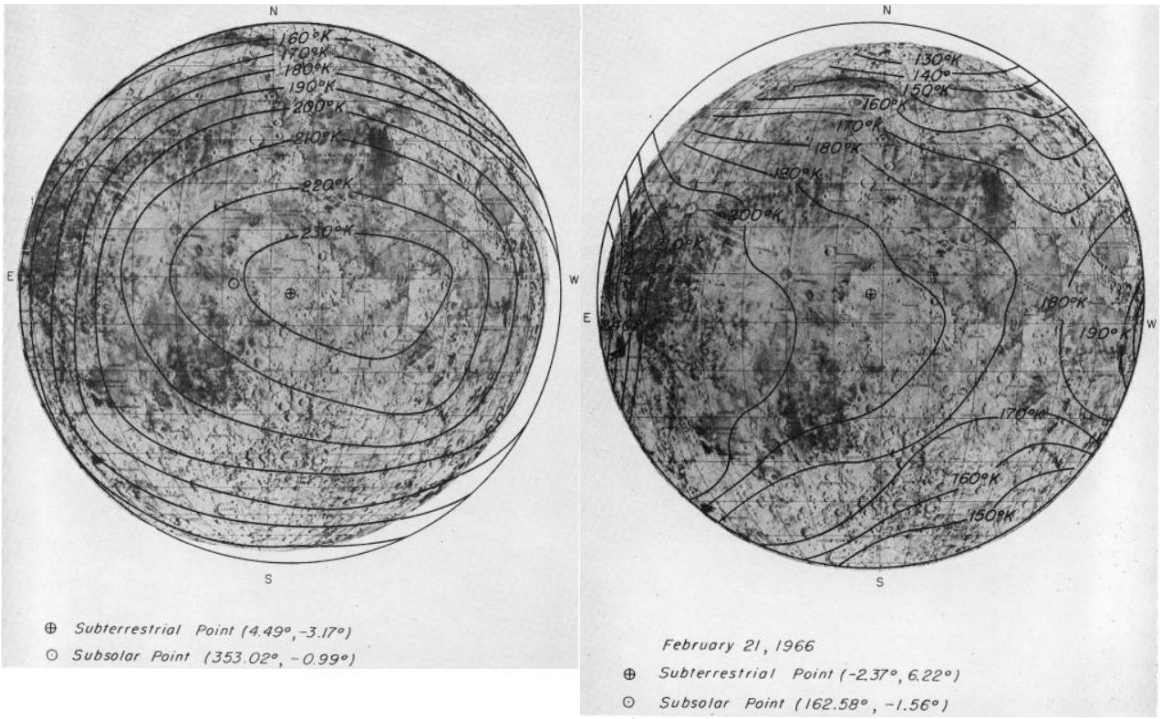

Figure 1: The observed distributions of radiation temperatures across the lunar disk [2]. At left – wavelength 8.6 mm, phase 12° after Full Moon, at right – wavelength 3.2 mm, phase 196° after Full Moon (or 16° after New Moon).

We used a simple model for lunar soil heated by the Sun. It is based on the one-dimensional heat equation [3,4] and allows to produce radio images of the Moon for any phase and frequency. Surface features like maria and highlands are not treated in the model. Brightness distributions derived from the model give sufficiently accurate results for our purposes and conditions. The reader can build own map images (see Fig. 2) using a JavaScript written by Joachim Köppen DF3GJ, https://portia.astrophysik.uni-kiel.de/~koeppen/JS/LunarRadioMaps.html.

The model data allow also calculating the temperature at the disk center as well as the beam temperature with an antenna pointing to a specified spot. The beam has a Gaussian shape. The mouse marker inside the disk displays the brightness temperature at the corresponding spot in the disk. Note that the phase 0° designates the Full Moon. With a version of this program, we computed the ratio to convert the Moon beam temperature T_{moon} from observation data to the brightness temperature at the disk center T_{center}. Fig. 3 shows this ratio as a function of lunation phase for a HPBW=0.3° beam centered on the disk. With this ratio known we can take into account the brightness distribution across the disk; a *nota bene* is that the Filling Factor [5,6] of the Moon in the antenna beam is also treated in this way.

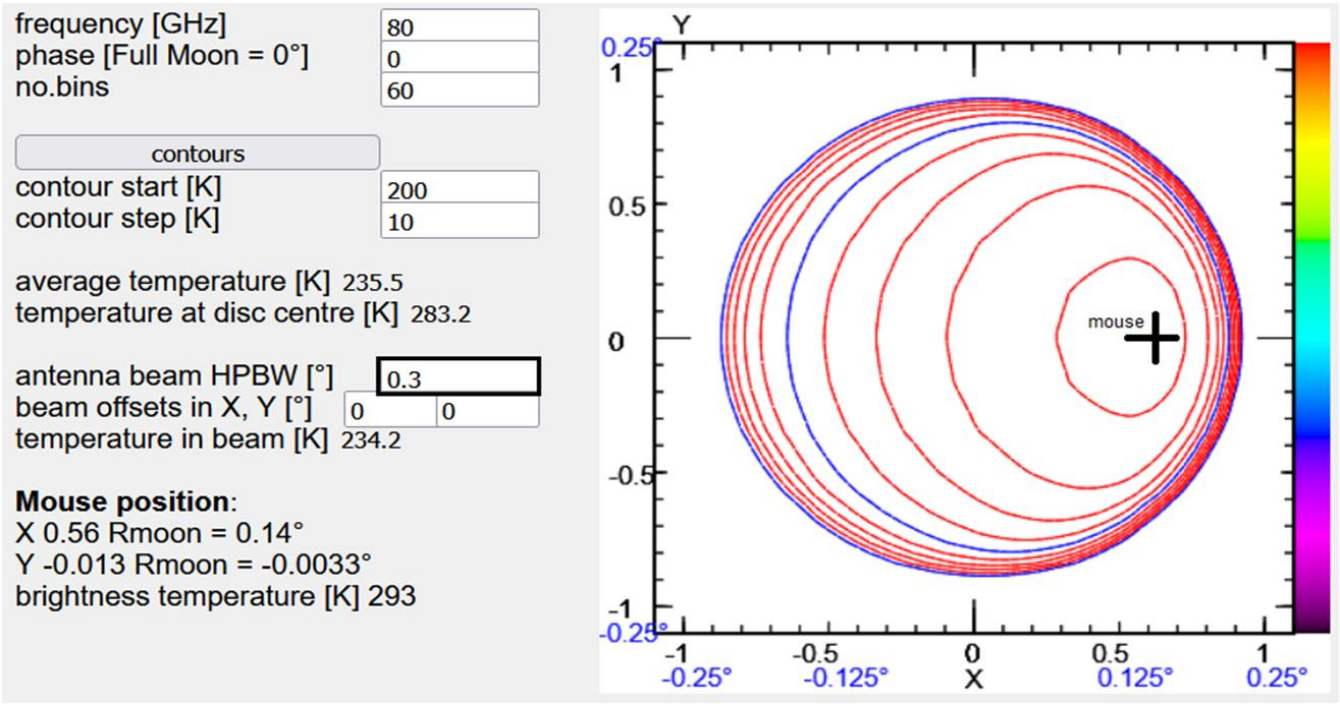

Figure 2: Radio image of the Moon for 80 GHz at Full Moon with the lines of equal brightness temperature (or isotherm map).

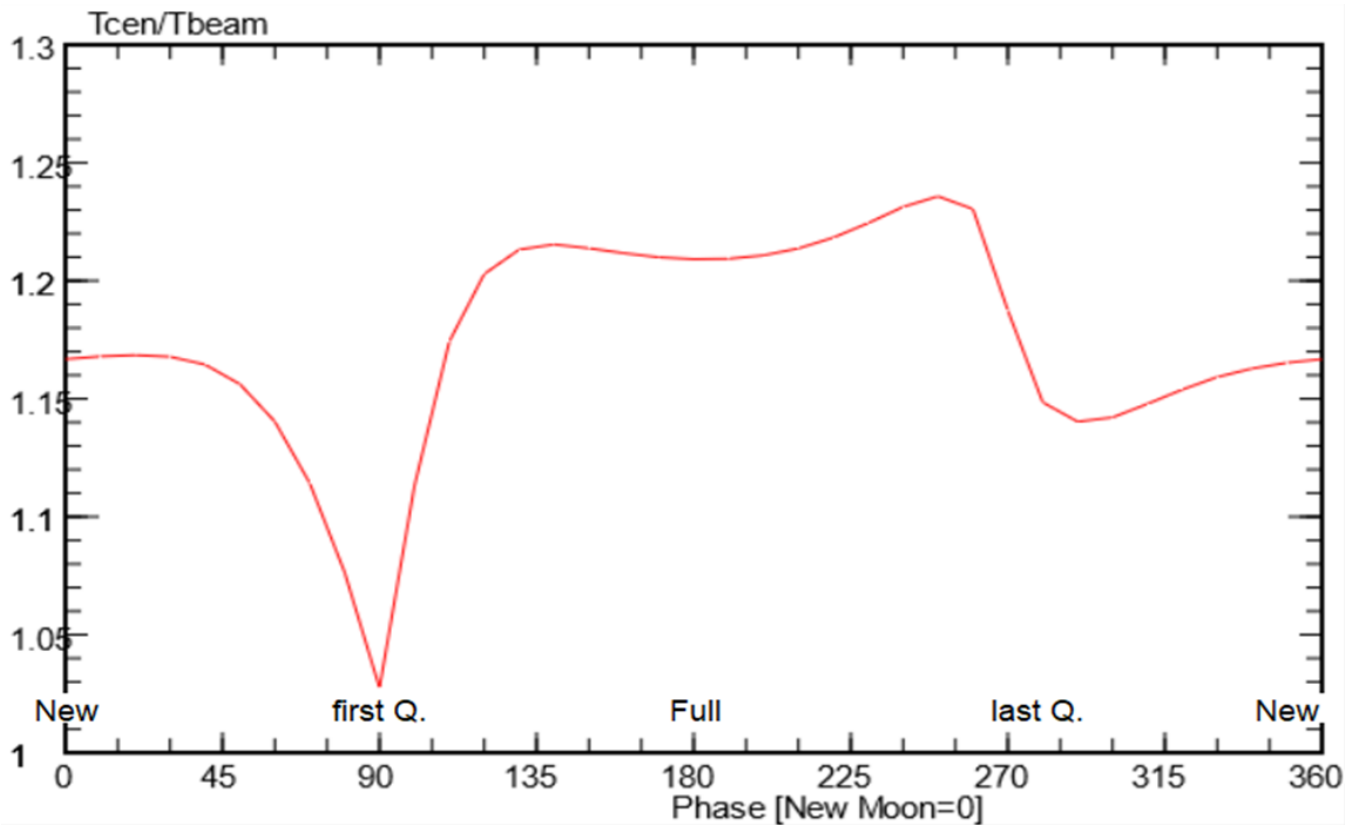

Figure 3: The ratio of the temperatures at the disk center to the Gaussian beam temperature (HPBW=0.3°) at 80 GHz computed with a version of the JavaScipt tool.

Results for lunar Brightness Temperatures

The analysis tools and data processing issues have now been described, and we are ready to present the results for the Moon brightness temperature in Fig. 4, together with fits from radio astronomical investigations of the Moon [7,8] from the early 1960s (Kislyakov in 1962 and Troitsky in 1965).

Both methods we introduced, NF and FC give nearly identical results. As expected, the lunar temperature rises from a minimum near the New Moon, and reaches a maximum a bit after the Full Moon. Our temperatures are about 20 K lower the professional observations; the discrepancy is less 10%, which means a very good agreement with the Kislyakov and Troitsky data. A few data are problematic: for example, when the calibrating load was not well cooled down to the ambient temperature T_{amb} of a very frosty winter day (December 2021, phase 257°) or when excessive atmospheric losses were expected (> 4 dB) for hot and wet summer weather (June 2022, at low Moon elevation <20°, phase 129°).

We may say a few words about why our dots tend to be somewhat lower than the Kislyakov and Troitsky fit curves. It hints that the receiver noise figure NF=5.5 dB may be underestimated. The small black circles indicate that the NF method with NF=6 dB give results about 30 to 50 K higher, which can improve the agreement.

We also explored how much the results are affected by the treatment of the atmospheric absorption in the FC method: the small blue crosses show that neglecting the clouds would lead to slight underestimates in the temperatures, from 10 to 20 K. There are two exceptions: with a 70 K difference at phase 129° (June 2022, wet

summer weather) with high atmospheric losses on the line-of-sight to the Moon (> 4 dB, a low Moon elevation <20°) and at phase 188° with a 40 K difference.

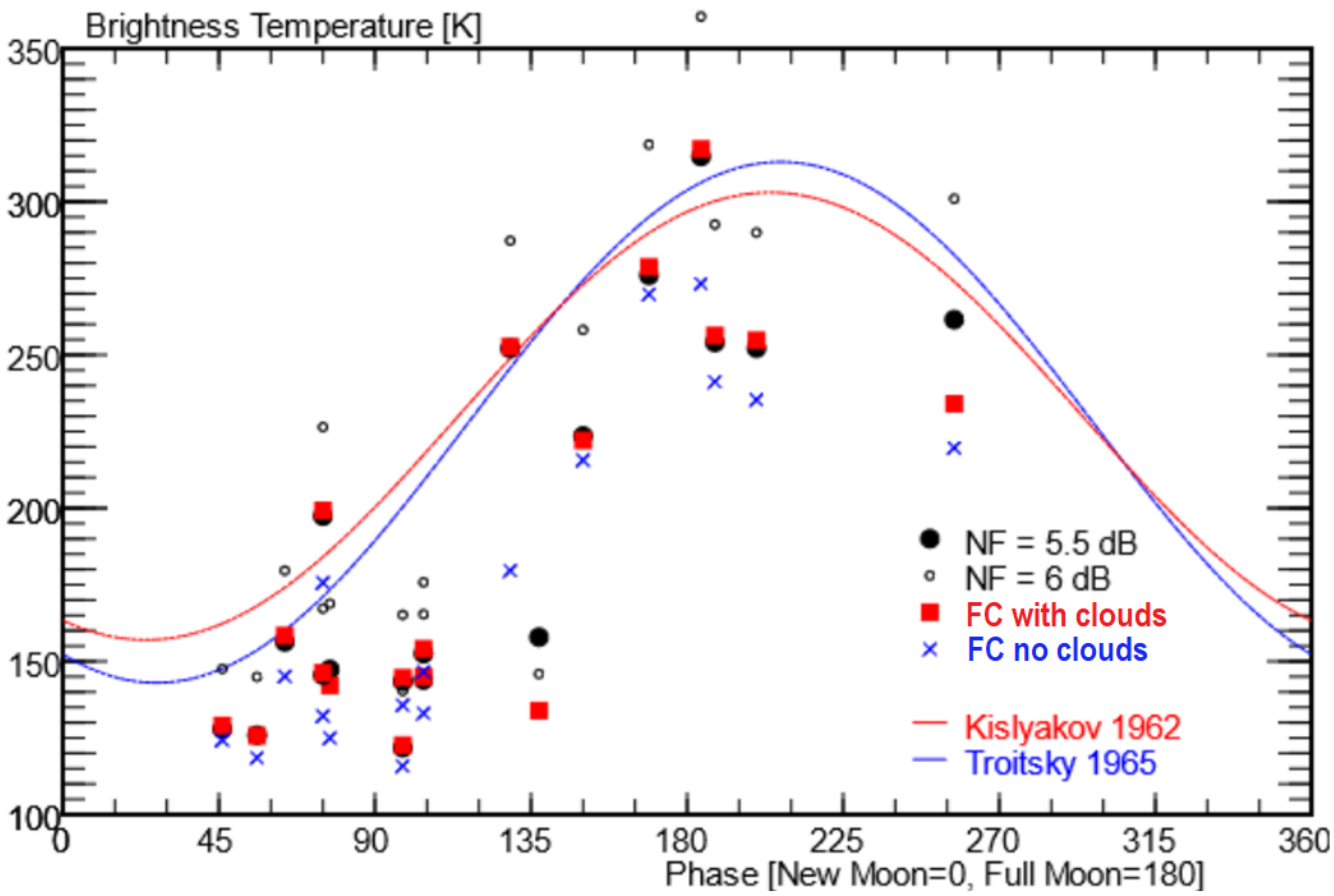

Figure 4: The brightness temperatures of the Moon (the center temperatures) at 80 GHz as a function of the illumination phase received by above described methods. The curves are sinusoidal fits from professional observations [7,8].

More about results, error considerations

We already discussed how the FC method is sensitive to accuracy of the atmospheric attenuation. It is useful to discuss how much the results are affected by other possible errors.

The accuracy of the measured power values is about 0.01 dB (RMS after noise averaging or 0.03 dB taking the noise peaks). With such prescribed accuracy in the noise meter all observations were performed (the noise meter allows to set a needed accuracy in noise averaging [9]). Varying the power data by these values would show that the lunar brightness temperature changes by 4 K. If these power errors occur in measurements of the calibrating load, the temperature change is 3 K.

About uncertainties of the antenna performance parameters, η and k. Results are more sensitive to errors in the Main Beam Efficiency η because of the both methods give $T_{moon} \sim 1/\eta$. If η is decreased from 0.65 to 0.55 (by about 15% in worse direction), the temperatures from the NF and FC methods are raised by about 20 to 30 K, i.e. by 15% too. Reducing k from 0.5 to 0.3 (in better direction) leads again to increasing temperatures in the method FC by 20 to 50 K. If the deviations in η and k would be interpreted as of random origin and independent in corresponding uncertainty ranges a resulting range for total uncertainty touches the Kislyakov and Troitsky fit curves.

In T_{center}/T_{moon} ratio calculations we used an assumption that the antenna beam is centered in the disk. Nevertheless, deviations of the beam from the lunar center are possible in observations. It is practical and convenient to adjust the antenna positioning until a maximum signal is reached; this maximum may not coincide with the disk center. We investigated how the calculated beam temperature changes when the beam is shifted along the X-axis using the JavaScript tool [10]. With HPBW=0.3° the maximum position remains for all phases in a range 0.025° – 0.04° from the disk center. It is not too much in comparison with the beam width of 0.3° and the lunar size 0.5°; the difference in temperatures T_{moon} of centered and shifted to the maximum beams do not exceed 1-2 K. Thus, we conclude the calculations of the brightness temperatures using the ratio from Fig. 3 are trustworthy.

Finally we note that the scatter in our data is about ±25 K; it can be compared with the scatter of about ±20 K in Kislyakov's observations, see [11] for 75 GHz data.

Comments and concluding remarks

A small dish radio telescope (radiometer) at 80 GHz can be built and used for sky observations. Its sensitivity allows to detect thermal radio sources in the sky like Sun or Moon without difficulty. Such an instrument may remind us of Itty-Bitty Telescopes (IBT) at 11-12 GHz, although its building and observation issues are a bit more complicated. We performed systematic observations of the Moon at 80 GHz using this radiometer in 2021-2022. The difference in the Moon radiation for different illumination phases is clearly seen at 80 GHz.

The measured data were interpreted in terms of lunar brightness temperatures at the disk center, T_{center}. The brightness temperatures are distributed across the disk unevenly at 80 GHz; moreover, the distribution itself strongly depends on the Moon illumination phase. A JavaScript tool was created especially for building radio images of the lunar disk for arbitrary phase and to calculate how the center temperature is related to the temperature in the antenna beam, T_{moon}, which is measured in observations.

The beam temperature T_{moon} was obtained by two methods. The first one is based on the knowledge of the receiver noise figure, measured previously by other means. In the second method we measure the noise from a calibrating load with a known temperature and thus are independent of a measurement of the receiver noise temperature. Both methods give nearly identical results. The atmospheric attenuation is relatively high at 80 GHz and plays a significant role in the both methods.

The obtained brightness temperatures well agree with previous Radio Astronomical observations (in the period of intensive radio Moon investigations) and confirm the expected dependence on lunar phase, albeit our values tend to be a bit lower (by about 20 K). As far as we know, this is a first amateur attempt ever to observe the Moon behavior at mm-waves, and we are happy to report that this attempt is quite successful.

References

[1] P.R. Foster, *Radio Observations in the Short Microwave Region*, Quarterly Journal of the Royal Astronomical Society, 10, 206 (1969).
[2] D.E. Clardy, A.W. Straiton, *Radiometric Measurements of the Moon at 8.6- and 3.2-Millimeter Wavelengths*, The Astrophysical Journal, 154, 775 (1968).
[3] J. Köppen DF3GJ, *Noise from the Moon*, DUBUS 3/2021, p. 100;
https://portia.astrophysik.uni-kiel.de/~koeppen/JS/LunarTemps.html
[4] J. Köppen DF3GJ, *The 2015 Lunar Eclipse Observed at Radio Frequencies*, DUBUS 2/2020, p. 78
[5] T.L. Wilson, K. Rohlfs, S. Hüttemeister, *Tools of Radio Astronomy*, 6th ed, Springer, 2013, p. 207.
[6] J. Köppen DF3GJ, *A Closer Look at Filling Factors*, DUBUS 4/2021, p. 15.
[7] A.G. Kislyakov, *The Radio Emission of the Moon on 4 mm*, I.A.U. Symposium 14, 511 (1962).

[8] V.S. Troitsky, *Investigations of the surfaces of the Moon and Planets by the thermal radiation*, NIST, IV Session: Passive radio observations of the Moon, 1585 (1965), see page 1596.
[9] D. Fedorov UA3AVR, *Notes from the noise test lab, part 2*, DUBUS 1/2020, p. 30.
[10] J. Köppen DF3GJ, *Lunar Radio Images* (2021), https://portia.astrophysik.uni-kiel.de/~koeppen/JS/LunarRadioMaps.html
[11] J. Köppen DF3GJ, *Lunar Radio Temperatures* (2020), https://portia.astrophysik.uni-kiel.de/~koeppen/JS/LunarTemps.html.

About the authors

Dimitry Fedorov was first licensed as radio amateur since 1982, as UA3AVR since 1983. In 1990 graduated as MS in electronics in Moscow Power Engineering University. Now works as research and development engineer in wireless industry, LTE/5G NR, RF and microwave modules development. Previous scientific experience in nuclear and particle physics, worked in Moscow State University, Institute of Nuclear Physics and Universität Tübingen, Institut für Theoretische Physik, see profile blog at https://www.researchgate.net/profile/Dimitry-Fedorov-2. Radio Astronomy hobby since 2012, mainly in applications for weak signals reception. You can contact the author at ua3avr@yandex.ru.

Joachim Köppen (DF3GJ) is a retired astrophysicist having worked in theory and observations of planetary nebulae and in evolution of galaxies in Heidelberg, Kiel, and Strasbourg. Having been infected by the radio and electronics virus as a small boy, he operated two small radiotelescopes for student projects in Strasbourg. Now in Kiel he joined the DLØSHF group, also writing software for the telescope operations, and using the instruments for the observational projects of the astronomy students in our institute. Contact: koeppen@astrophysik.uni-kiel.de (Inst.Theoret.Physik u.Astrophysik, Univ. Kiel).

Creating a Rotation Curve of the Milky Way Galaxy Using the 21 cm Neutral Hydrogen Line

Shalyn Vanderhorst

(Student Paper - High School Junior: Mentor - Tom Crowley)

1. Introduction

The Galaxy Rotation Problem refers to an issue in astrophysics where the observed mass of a galaxy using experimental methods does not correlate to its theoretical mass using the known laws of physics. Keplerian physics states that in large systems, the rotational velocities of orbiting bodies decrease as their distance from the center of mass increases. For instance, in our own solar system, the outer planets take many years longer to complete a revolution around the Sun than the inner planets. However, this principle does not hold true for many galaxies, as their mass has been observed to revolve at the same rate regardless of their distance from the center of their respective galaxies. This discrepancy is best demonstrated by rotation curves, as seen in Figure 1, which are graphs that display the speed in which a tracer object is orbiting a galaxy versus its distance from the galactic center. By equating the centripetal and gravitational forces of each tracer object and plotting the results as a logarithmic function, scientists can determine the total amount of mass that resides in a galaxy as well as the mass distribution of said galaxy. Rotation curves grew in popularity as more advanced techniques to create them became widespread, allowing scientists to further investigate this gap in knowledge. One of the first and most influential rotation curves displaying the Galaxy Rotation Problem was published in 1971 by Vera Rubin and W Kent Ford of the galaxy NGC 5033, and used observational evidence from the 21 cm neutral hydrogen line. They sampled numerous other galaxies as well, and determined that their unusually fast rotation rates were all different to the speeds recorded using data from just observable matter [14].

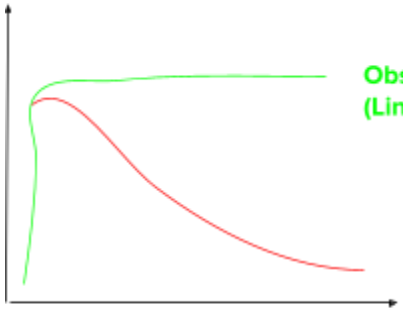

Figure 1: A schematic demonstrating the behavior of mass in the Milky Way, adapted from Source [24].

Line A shows the shape of most experimental rotation curves.

Line B shows the rotation curve where only visible matter is accounted for

The 21 cm neutral hydrogen line refers to areas in the Milky Way galaxy with a high concentration of radio objects, specifically neutral hydrogen, also known as h-one (HI). HI is a highly abundant isotope of hydrogen that resides in the interstellar medium, the area between stars, and is created by the spin flip transition. The spin flip transition occurs when an electron's spin goes from being aligned with its proton to unaligned, releasing energy at the characteristic frequency (1420 megahertz) and wavelength (21 cm) of HI, allowing scientists to determine the identity of the element using this information [29]. After its discovery, the 21 cm line became a staple tracer object in creating rotation curves because it can essentially map out the distribution of hydrogen in the galaxy. Being the most abundant element in all galaxies and the largest contributor to their mass, hydrogen is an ideal candidate to determine the total mass of a galaxy.

In order to detect this abundant HI, Ford and Rubin used hydrogen line spectroscopy.

Spectroscopy is a scientific technique where researchers measure the spectral lines produced when matter emits electromagnetic radiation, then record the frequency at which these spectral lines occur in order to identify the source of the radiation.

Eventually, spectral data was produced using the 21 cm neutral hydrogen line for HI in our own galaxy, the Milky Way, and future researchers used it to create rotation curves showing that our galaxy has a relatively consistent mass throughout as opposed to being concentrated at its central bulge. The influx of results showing unusual galactic rotation rates caused shockwaves in the astrophysics community as more scientists were alerted to the existence of the Galaxy Rotation Problem and searched for ways to solve it. The two main contending theories in this debate were Modified Newtonian Dynamics (MOND) and the dark matter hypothesis. MOND works to alter Newtonian physics at galactic scales and relies on numerous adjustments to Newton's well established theories. However, it has had minimal success in predicting the behavior of individual galaxies [15]. Dark matter on the other hand proposes that a halo of invisible, non baryonic matter encapsulates most galaxies, causing them to rotate uniformly. The dark matter hypothesis has had more success in predicting galactic behavior and correlating it with the amount of dark matter in a galaxy as different kinds of galaxies have been discovered [1]. Since dark matter is non-baryonic, meaning it is not composed of the same elementary particles as visible matter, it makes detection extremely difficult. Thus began the search to detect dark matter through observing its effects on surrounding structures, contributing to the growing relevance and use cases of rotation curves.

In order to properly study dark matter, adjustments to how rotation curves were made and what they were used for had to change. For instance, the data from individual rotation curves is now frequently conglomerated into unified rotation curves, which display more accurate properties of a galaxy's mass and the finer details of its structure [33]. Additionally, scientists can use rotation curves to extrapolate dozens of kiloparsecs (kpc) further into the galaxy than they can optically observe in order to study the behavior of the dark matter halo proposed to surround the Milky Way [3]. The dark matter halo is theorized to be made of Weakly Interacting Massive Particles (WIMPS) whose velocities can be determined by the gravitational potential energy equation, which requires the mass distribution of the galaxy to be known. Thus, using rotation curves to determine the location of WIMPS is crucial in giving credence to the theory of dark matter, greatly boosting the relevance of rotation curves in the scientific conversation. In summary, rotation curves have a crucial part in identifying the effects of dark matter on galaxies and observing the fine details of their structure, making it more important than ever to create useful rotation curves.

Rotation curves have been created in the past using varying levels of equipment and precision. The first rotation curve using the 21 cm HI line was created using a simple horn telescope and the tangent point method, where the circular velocity and galactocentric radius of an HI cloud are determined under the assumption that the end of the cloud's velocity vector is tangent to the galactic center [18]. The assumption that the tip of the cloud's velocity vector is also tangent to the center of the galaxy has been found to be incorrect in many cases in the Milky Way. Additionally, the tangent point method can only account for the inner portions of the Milky Way, with its accuracy greatly decreasing at distances greater than 8 kpc [8]. As a result, more modern studies tend to use sophisticated methods such as the creation of pseudo rotation curves that have the ability to map distances hundred of kpc further than the tangent point method can without losing accuracy [28].

Since the more modern methods of creating rotation curves require extensive equipment and mathematical precision, I decided to employ the tangent point method instead which is less sophisticated and more feasible with my available materials. This limited me to studying a small section of the rotation curve literature, as most

modern studies employ more advanced methods. One recent study, conducted by Nix and collaborators, used the tangent point method as well as built their own radio telescope using online plans from the Digital Signal Processing in Radio Astronomy (DSPIRA) website, affiliated with the University of West Virginia. They also built their own spectrometer in a dedicated software called GNU Radio to collect HI cloud signals. As previously stated, they used the tangent point method to determine a rotation curve for the Milky Way out to approximately 10 kpc using a sample of eight HI clouds [23]. However, the unadvanced nature of their spectrometer led to extraneous noise in their spectra and prevented data from being collected at 30 degrees galactic longitude, contributing to their rotation curve increasing at 5 kpc instead of flattening as the previous literature suggests. Additionally they used a horn shaped telescope that has less gain (signal quality) than a similarly sized parabolic dish which allows more illumination of the surface. Inputting distorted data such as this in a unified curve could decrease its overall accuracy.

Therefore, the goal of my project is to improve on the work of Nix and collaborators by using a more advanced spectrometer that collects radio frequencies at multiple decimal points of precision, as well as improve on the shape of their telescope by using a parabolic dish instead. I hypothesize that these adjustments will create more precise HI frequency data that has the ability to be included in unified rotation curves, thus progressing the study of dark matter.

2. Methods and Materials

2.1 Equipment

This study uses a parabolic-dish telescope provided by the Society for Amateur Radio Astronomers (SARA) which consists of a tripod, a 2.4 gHz wifi dish antenna, and an SMA connector. The SMA connector was attached to a Sawbird LNA directly in order to minimize the amount of signal loss while an Rtl-SDR USB plugin was connected to the telescope with a separate USB cable. The remaining ends of the USB cable and SMA connector were connected to a Windows laptop with a spectrometer and planetarium software installed.

The Low Noise Amplifier (LNA) and the Software Defined Radio (SDR) are two pieces of hardware that amplify signals and prepare them for processing in a spectrometer software. The spectrometer used for this study, called SDR #, works by performing Fourier analysis on radio signals in order to display them as signal vs frequency spectra. SDR # can also be used in conjunction with plugins that enhance its capabilities, such as the IF Average software plugin. IF Average was specifically made for radio astronomy and provides a spectrum showing the amount of hydrogen signals collected as well as more fine tuned calibration parameters for HI. These parameters include the ability to increase the number of signals processed by the spectrometer as well as setting the amount of gain of the telescope higher, making it an ideal choice for this study. An adjustable base for the telescope was also used, because it made it

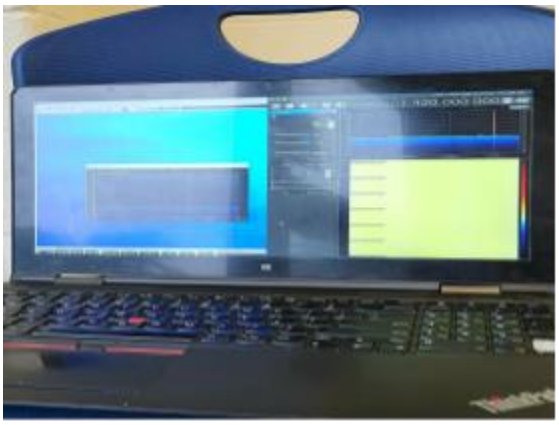

Figure 2:
Left (Behind): Radio Eyes application focusing on HI dense region.
Left (Front Program Window): IF Average displaying HI signals building
Right: SDR # tuned to find radio waves emitting 1420 mHz.

Figure 3: Telescope set up showing adjustable base, antenna, and level

easier to point to different locations in the sky and served as a compass for altitude and azimuth coordinates. Azimuth and altitude coordinates are used to identify objects relative to an observer's own reference frame and are dependent on one's location. It was crucial that I used azimuth and altitude coordinates to locate HI because the planetarium software I used, Radio Eyes, only gave the location and galactic longitudes of radio objects relative to my location. I used a level attached to the base of the telescope to accurately point to altitude values denoted by Radio Eyes and used a compass pointed parallel to the ground to locate azimuth values.

2.2 Observation Procedure

The Milky Way's position in the sky changes as it sets below the horizon and is dependent on the time in which it is observed. Thus, the times at which I observed neutral hydrogen had to be adjusted accordingly. For example, Daylight Savings Time, which began on March 12, 2023, allowed me to access the most extreme galactic longitudes, namely 10 degrees and 90 degrees, at approximately 8 a.m. Before this, these points could only be accessed at times earlier than seven in the morning and were thus inaccessible to me. Additionally, after Daylight Savings Time, the remaining seven HI clouds were able to be observed between the hours of 8 and 11 a.m. Beginning around noon, the Milky Way dipped too far below the horizon to observe the lower longitudes.

Figure 4: Example of HI spectrum taken at 20 degrees Galactic Longitude

Once the appropriate observation times were selected, I could begin collecting HI data. First, the LNA and SDR needed to be connected to the laptop with SDR # active and let neutralize for about 10 minutes. This allowed the sensitive equipment to perform more precisely. Next, the radio telescope needed to be calibrated by attaching a 50 ohm terminator to the LNA and performing a background scan using the IF Average plugin. The spectrometer needed to accumulate 902,000 signals before completing the scan, as that is the number of signals I set IF Average to accumulate using the Dynamic Averaging parameter. This number of signals created sufficiently strong signal strength in my HI spectra. The remaining parameters in IF Average were set to the following values: the FFT Resolution was set to 1024, the Intermediate Average was set to 1000, and Gain was set to 335. Note that calibration is not necessary for collecting HI, as the frequency picked up will be the same regardless of calibration. However, creating a reference scan during calibration is useful for making the signals clearer on the signal vs frequency spectrum.

Additionally, Radio Eyes was loaded alongside SDR # to display radio objects within various galactic quadrants. For this project, I only focused on Galactic Quadrant I, which encompasses galactic longitudes 10-90, because it experiences the least redshift relative to Earth's location and makes it so that the HI frequencies do not need to be adjusted for redshift mathematically. Redshift is the elongation of electromagnetic waves as they move away from an observer. In the case of HI, redshift causes their frequency values to decrease if they are indeed moving away from the Earth and increase if they are moving towards it.

Galactic Longitude (ℓ)	Observed Frequency
10± 5°	1420.5999046
20±5°	1420.5770038
30±5°	1420.5632634
40±5°	1420.5907443
50±5°	1420.572436
60±5°	1420.5357825
70±5°	1420.5128817
80±5°	1420.4899809
90±5°	1420.4716603

Figure 5: Table of collected frequencies and longitudes

I began observing by first selecting nine areas of activity within Quadrant 1 and adjusting the telescope to their elevation and azimuth coordinates as denoted by Radio Eyes. I let the signal build completely for about seven minutes which is the time necessary to complete the scan, allowing humps in the graph to become visible around 1420 mHz, as seen in Figure 4. Finally, I created a table showing the galactic longitudes and frequencies of each HI cloud, shown in Figure 5.

2.3 Calculating the Rotational Velocities and Radial Distances

After all the HI frequency data was collected, it was time for me to determine the rotational velocity and radial distance of each HI cloud. Distance and velocity are the x and y axes of a rotation curve respectively and are plotted to create the curve of the graph. The velocity (v) is found using the equation,

$$v = {}_{fef-0fo}\, c + v_e sin(\ell)$$

which was adapted from reference [23]. This equation is made of the sum of two components: the velocity of the HI cloud along Earth's line of sight with respect to Earth itself, which is encapsulated by $\frac{fe}{f-0}\frac{fo}{c}$ and the velocity

of the HI cloud along Earth's line of sight relative to the center of the Milky Way, found by $v_e sin(\ell)$. To calculate the velocity of HI along Earth's line of

sight, the frequency picked up by my radio telescope (f) was subtracted from the known frequency of HI (fe), 1420.4057517667 mHz. This value was divided by my observed frequency and multiplied by the speed of light, which is ~300,000 km/sec (c). To determine the rotational velocity around the Milky Way of HI along Earth's line of sight, Earth's average rotational speed around the galaxy (v_e) was added to the sine of my observed galactic longitude.

After the rotational speeds of all the HI clouds were calculated I then began solving for their distances. The distance of an HI cloud from the center of the Milky Way galaxy can be found using the equation $R_L = R_e sin(\ell)$,

where R_e is the distance from Earth to the center of the Milky Way, and ℓ is the galactic longitude the HI cloud was observed at. The velocity and distance equations were derived using simple

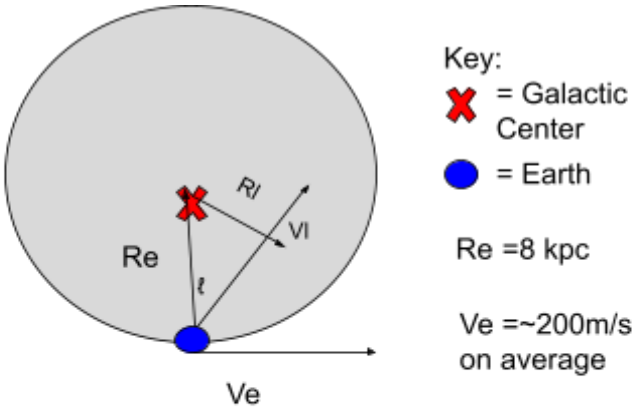

Figure 6: A schematic showing how the trigonometric values were derived. Rl is solved for using trigonometry while Re and Ve are already known values, according to reference [24]. Vl is equivalent to the velocity of the HI cloud along Earth's line of sight

trigonometry, which can be seen in Figure 6. Finally, the results were plotted into a logarithmic curve with radial distance on the x axis and orbital velocity on the y, creating the final rotation curve. Google Sheets was used to generate said scatter plot and apply the fit and error bars.

3. Results

In summary, I recorded the galactic frequencies and longitudes of nine HI clouds found in the 21 cm neutral hydrogen line. These values allowed me to mathematically determine the distance from the galactic center as well as the speed in which each HI cloud orbited the Milky Way Galaxy. Finally, I plotted these values into the final rotation curve using Google Sheets and applied error bars, as well as a logarithmic fit, as seen in Figure 7. I chose the logarithmic fit, because it correlates most tightly with the rotation curve data.

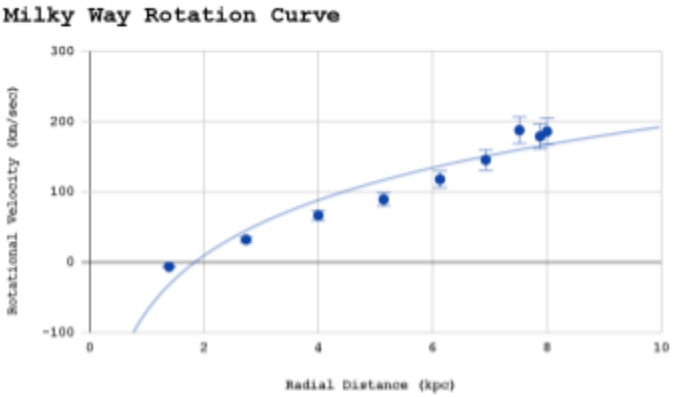

Figure 7: My curve using a logarithmic fit

3.1 Analysis

In order to determine how precise my curve was and thus how effective my improvements on Nix and collaborator's work was, I needed to compare the shape of my rotation curve to theirs as well as to similar literature. Thus, I selected the curve from reference [26] which was a similar study to mine in terms of methodology, as well as the curve created by Nix and collaborator from reference [23]

The curve from reference [23] was created by Nix and collaborators using a sample of eight HI clouds, a homemade spectrometer software that lacked precision, and no mathematical adjustments to the velocity of HI that made them closer to their true, real life values. Additionally, this study failed to record a frequency of HI at 30 degrees galactic longitude, which they stated to be the cause of their curve increasing at 5 kpc instead of flattening out like the curve from reference [26]. Note that Nix and collaborators had outlined this discrepancy with their data and suggested that future researchers use a more precise spectrometer to avoid the same issue.

The rotation curve from reference [26] however, had a sample of seventeen HI clouds, used a premade parabolic dish telescope and spectrometer software, and mathematically adjusted the velocities of the HI clouds to make them more precise. They achieved such precise rotational velocities by calculating the recessional velocity of each HI cloud, which is how quickly the cloud is moving away from the Earth, as well as removing the motion of the Earth and Sun from the calculations. These key corrections made their velocities more in line with how the HI clouds actually behave, giving their rotation curve a noticeably different shape to mine.

Between the two compared rotation curves, mine agrees most with the one created by Nix and collaborators, as the slopes of our two rotation curves tend to increase at 5 kpc instead of flattening out like the curve from reference [26].

My curve and those from references [26] and [23] differ the most in shape for values between 0 and 3 kpc. My graph has a relatively shallow slope, showing that the HI velocities minimally change at those distances, while the curves from the aforementioned literature drastically increase on that same interval, showing a sharp increase in HI speeds. Part of the reason for this discrepancy may be the precision of the radio frequencies I used and how they affect the values of the radial velocity. For instance, the curve from reference [23] used frequencies up to 2 decimal points of precision, with many at zero decimal points due to their relatively unadvanced spectrometer software. Furthermore, only one of the eight recorded frequencies had a value greater than the known frequency of HI, 1420.405751, causing this cloud to have a relatively small velocity and blue shift compared to the remaining seven HI clouds. Out of my nine HI clouds however, all nine had values greater than 1420.405751, causing all of

my clouds to have relatively low velocities and be blue shifted. This fact translated into my rotation curve in that it did not have a steep increase in velocity on the interval 4-7 kpc and instead gradually increased as radial distance increased. Reference [26] never explicitly gave a table of radio frequencies so it is difficult to ascertain the precision of their HI coordinates. However, they did provide a table of corrected recessional velocities of each HI cloud, making these velocities truer to life than mine or those of reference [23].

Overall, my curve differs in shape from the literature primarily due to the lower orbital velocity values of my HI clouds. Additionally, its shape is closer to the rotation curve of Nix and collaborators, meaning my adjustments to their methods were not enough to counteract the errors my blue shifted HI clouds caused in the velocity calculations. Simply put, due to the quality of my measured HI clouds, I was unable to improve on Nix and collaborator's work by creating a rotation curve more in line with the shape of the previous literature. However, I hypothesize that my precise frequencies can still undergo corrections similar to those from reference [26] in order to make them more useful in future research.

3.2 Corrections and Adjustments

In order to determine the uncertainty of the observed galactic longitudes, the beamwidth of my telescope needed to be found. My best estimate for its beamwidth was 15 degrees using the diffraction limit equation, adapted from reference [23], θ = 1. 22 d^{λ} the telescope.λMost horn antennas have a beam width between 5-10 degrees,d making my where is the wavelength of the radio wave, in this case 21 cm and is the diameter of uncertainty for the galactic longitudes slightly smaller than 5 degrees because I used a parabolic dish with a wider diameter.

4. Discussion

In summary, the goal of this experiment was to determine the galactic rotation curve of the Milky Way using the tangent point method and nine neutral hydrogen clouds as tracer objects. Much of the previous literature using the tangent point method didn't use modern and precise spectrometer software that produced HI frequencies up to seven decimal places. Additionally, previous studies tended to use horn shaped radio antennas, which have smaller illumination surfaces than parabolic dishes and can lead to lower gain values. Therefore, my data successfully filled a gap in the literature by creating a rotation curve using the tangent point method, an advanced spectrometer and software plugin, as well as a parabolic dish telescope. Despite improving on the work of Nix and collaborators by recording more precise HI frequency values, I was unable to improve on the shape of their rotation curve because of the impact my blue shifted HI clouds had on my orbital velocity values.

4.1 Implications

Dark matter is a burgeoning topic of astrophysics that continues to open new possibilities into the future of physics and human understanding of the universe. Rotation curves are at the cutting edge of dark matter research, as they help scientists determine the precise amounts of dark matter in galaxies as well as extrapolate further into galactic dark matter haloes than they can see with optical means. Therefore, the precise radio frequencies obtained in my experiment can be corrected using further mathematics and contribute to dark matter research by being input into unified rotation curves, shedding light into the mass distribution of the Milky Way.

4.2 Limitations

The Half Power Beam Width is the best estimate of a given telescope's beam width. However, the information necessary to determine it such as the resonance frequency and modal loss factor were unknown values for my telescope that are not within my scope to determine. Therefore, I had to best approximate the beam width as the angular resolution using the diffraction limit equation, as seen in reference [23].

Although my spectrometer was fairly advanced, it still received a fair amount of noise from surrounding cars, electronics, and buildings as evidenced by the tall white peaks in my spectra [see appendix]. This sometimes made

it difficult for HI signals to completely build, because the equipment was being distracted by objects on Earth at similar frequencies.

Furthermore, the most extreme galactic longitudes observed, namely 10 and 90 degrees, were fairly difficult to access due to their relatively high and low position respectively. This is evidenced by the relatively weak signal strength in their spectra, especially at Galactic Longitude 90. This made their frequency values more uncertain than the rest of my spectra.

Using the tangent point method to determine a rotation curve is relatively ineffective compared to modern methods. Specifically, it only tends to be accurate to galactic radii up to 8 kpc and loses accuracy at radii less than 4 kpc. This makes my rotation curve less precise than the literature that employs more advanced methods.

Rotation curves tend to be compared using visual analysis, where the behavior of a curve is described in descriptive terms instead of quantitative metrics. This is a standard practice in the literature even for the more precise curves. For instance, the rotation curve created in reference [23] was said to "increase past a radius of 5 kpc" and "flatten out at a speed of around 250 km/s." Terms such as these are not as useful in comparing rotation curves as comparing the mathematical values of the fit of the line, which would give a more useful metric. Due to this, the comparison of my curve to the literature could be improved by using statistical values instead of visual differences.

Due to the high level of mathematics required to calculate the recessional velocity of HI clouds and remove the effect of Earth's motion in my velocity calculations, I was unable to include these corrections in my rotation curve. Resultantly, my rotation curve has a slightly different shape to reference [26] and other literature that included these adjustments.

4.2 Future Research

Future research can be conducted on the exact relationship between telescope beam width, signal gain, and the precision in which they can collect radio frequency data, in order to advise future scientists on the ideal shaped radio telescopes for their purposes. By comparing different telescope shapes of similar sizes, it can be known which shape is ideal for the purpose of observing the 21 cm hydrogen line as well as other radio astronomy projects.

Furthermore, research can be conducted into the relationship between blue shift, red shift and the accuracy of rotation curves. Due to my data being blue shifted, my rotation curve varied drastically from those of the literature in terms of the orbital speeds of each HI cloud, suggesting that blue shifted tracer objects can decrease a rotation curve's overall accuracy. Therefore, research can be conducted that finds a way to minimize the number of blue shifted data points collected from Galactic Quadrant I and the best way to correct for it mathematically.
The field of astronomy is continually shifting towards studying dark matter. Therefore, I suggest that future researchers create unified rotation curves as well as pseudo rotation curves using my HI frequencies. This will allow researchers to better observe the mass distribution in the Milky Way galaxy as well as extrapolate further into the dark matter halo.

4.3 Conclusions

In conclusion, I hope that my research can be used in future unified rotation curves of the Milky Way galaxy in order to shed light on dark matter. This is a necessary step towards understanding the distribution of dark matter in our own galaxy and can lead the way towards mapping the dark matter halo. Additionally, I hope that my work will serve as a guide for future researchers to conduct similar experiments and investigate the questions I

proposed for future endeavors. That way, they will be able to improve on my methods and propel dark matter research forward.

5. References

1. *100 Years of Rotating Galaxies - Vera C. Rubin*. (n.d.). Retrieved April 20, 2023, from ned.ipac.caltech.edu/level5/Sept04/Rubin/Rubin1.html
2. *A History of Dark Matter- Gianfranco Bertone & Dan Hooper*. (n.d.). Retrieved April 12, 2023, from ned.ipac.caltech.edu/level5/Sept16/Bertone/Bertone4.html
3. Bahcall, & A, N. (2017). Vera C Rubin 1928–2016. In *OUP Academic*. dx.doi.org/10.1093/astrogeo/atx054
4. Bhattacharjee, P., Chaudhury, S., & Kundu, S. (2014). ROTATION CURVE OF THE MILKY WAY OUT TO ∼200 kpc. *The Astrophysical Journal*, *785*(1), 63.

https://doi.org/10.1088/0004-637x/785/1/63

5. Blitz, L. (n.d.). *1 The Millimeter Wave Observatory is operated by the Elec-*. Retrieved January 9, 2023, from https://adsabs.harvard.edu/pdf/1979ApJ...231L.115B
6. Chaudhury1, S., Kundu1, S., & Majumdar3, S. (n.d.). *√8π2 "Z dΨ2 +*. Retrieved January 22, 2023, from https://arxiv.org/pdf/1210.2328.pdf
7. Chemin, L., Renaud, F., & Soubiran, C. (2015). Incorrect rotation curve of the Milky Way. *Astronomy & Astrophysics*, *578*, A14. https://doi.org/10.1051/0004-6361/201526040
8. Chiu, C. K., & Strigari, L. E. (2020). *Testing the Accuracy of the Tangent Point Method for Determining the Milky Way's Inner Rotation Curve - IOPscience*. IOP

Publishing. iopscience.iop.org/article/10.3847/2515-5172/abbad8

9. *Dark Energy, Dark Matter | Science Mission Directorate*. (n.d.). Retrieved September 9, 2022, from science.nasa.gov/astrophysics/focus-areas/what-is-dark-energy
10. *Dark Matter*. (n.d.). Retrieved September 28, 2022, from abyss.uoregon.edu/~js/cosmo/lectures/lec17.html
11. *DARK MATTER, MAGNETIC FIELDS, AND THE ROTATION CURVE OF THE*

MILKY WAY - IOPscience. (2012). IOP Publishing. iopscience.iop.org/article/10.1088/2041-8205/755/2/L23/meta

12. *EXISTENCE AND NATURE OF DARK MATTER IN THE UNIVERSE*. (n.d.).

Retrieved January 9, 2023, from escholarship.org/uc/item/2hz008rs#main

13. Fich, Michel, Blitz, Leo, Stark, & A., A. (n.d.). The Rotation Curve of the Milky Way to 2R 0. In *NASA/ADS*. Retrieved March 22, 2023, from ui.adsabs.harvard.edu/abs/1989ApJ...342..272F/abstract
14. Ford, W. K., & Rubin, V. C. (n.d.). *>■ 700- south #*. Retrieved April 23, 2023, from https://articles.adsabs.harvard.edu/cgi-bin/nph-iarticle_query?db_key=AST&bibcode=1971AJ.....76...22F&letter=0&classic=YES&defaultprint=YES&whole_paper

=YES&page=22&epage=22&plate=1&eplate=1&send=Send+PDF&filetype=.pdf

15. Galaxy mass models: MOND versus dark matter haloes. (2014). In *OUP Academic*. dx.doi.org/10.1093/mnras/stu100

16. Galaxy rotation curve. (2022). In *Wikipedia: The Free Encyclopedia*. Wikimedia Foundation, Inc. en.wikipedia.org/wiki/Galaxy_rotation_curve
17. Gotame, R. (n.d.). Rotation Curve Method for Determining the Mass of Spiral Galaxies. In *Physics Feed*. Retrieved January 22, 2023, from physicsfeed.com/post/rotation-curve-method-determining-mass-spiral-galaxies/
18. Hulst, van de, C., H., Muller, A., C., Oort, & H., J. (n.d.). The spiral structure of the outer part of the Galactic System derived from the hydrogen emission at 21 cm wavelength. In *NASA/ADS*. Retrieved January 22, 2023, from ui.adsabs.harvard.edu/abs/1954BAN....12..117V/abstract
19. *Hydrogen Clouds detected with 21 cm Line Emission - PhysicsOpenLab*. (2020). physicsopenlab.org/2020/10/03/hydrogen-clouds-detected-with-21-cm-line-emiss ion/
20. Kalberla, P. M. W. (n.d.). *Þ1=2, and equation (2) becomes*. Retrieved January 22, 2023, from https://iopscience.iop.org/article/10.1086/374330/pdf
21. Levine, S., E., Heiles, Carl, Blitz, & Leo. (n.d.). The Milky Way Rotation Curve and Its Vertical Derivatives: Inside the Solar Circle. In *NASA/ADS*. Retrieved March 22, 2023, from ui.adsabs.harvard.edu/abs/2008ApJ...679.1288L/abstract
22. Ludwig, G. O. (2021). Galactic rotation curve and dark matter according to gravitomagnetism. *The European Physical Journal C*, *81*(2). https://doi.org/10.1140/epjc/s10052-021-08967-3
23. *Measuring the mass of the Milky Way using observations of radio waves emitted by neutral hydrogen | JUEPPEQ: Journal of Undergraduate Engineering Physics and Physics Experiments at Queen's*. (2021). ojs.library.queensu.ca/index.php/JUEPPEQ/article/view/14774
24. *Milky Way structure detected with the 21 cm Neutral Hydrogen Emission PhysicsOpenLab*. (2020). physicsopenlab.org/2020/09/08/milky-way-structure-detected-with-the-21-cm-neu tral-hydrogen-emission/
25. Pato1, M. (n.d.). *galkin: a new compilation of the Milky Way rotation curve data*. Retrieved January 22, 2023, from https://arxiv.org/pdf/1703.00020.pdf
26. *[PDF] The Hydrogen 21-cm Line and Its Applications to Radio Astrophysics | Semantic Scholar*. (n.d.). Retrieved September 9, 2022, from https://www.semanticscholar.org/paper/The-Hydrogen-21-cm-Line-and-Its-Applic ations-to-Liu/e8f9a72231c288cba4f348e030e0e94a3709fe63
27. *Rotation Curve | COSMOS*. (n.d.). Retrieved January 9, 2023, from astronomy.swin.edu.au/cosmos/R/Rotation+Curve
28. Rotation Curve of the Milky Way and the Dark Matter Density. (2020). In *MDPI*. Multidisciplinary Digital Publishing Institute. www.mdpi.com/2075-4434/8/2/37
29. Storey, J. W. V., Ashley, M. C. B., Naray, M., & Lloyd, J. (1994). 21 cm line of atomic hydrogen. In *ResearchGate*. www.researchgate.net/publication/253458921_21_cm_line_of_atomic_hydrogen
30. *The Circular Velocity Curve of the Milky Way from 5 to 25 kpc - IOPscience*. (2019). IOP Publishing. iopscience.iop.org/article/10.3847/1538-4357/aaf648/meta
31. The Circular Velocity Curve of the Milky Way from 5 to 25 kpc using luminous red giant branch star. (n.d.). In *arXiv.org*. Retrieved January 9, 2023, from arxiv.org/abs/2212.10393v1

32. Trimble, V. (1987). Existence and Nature of Dark Matter in the Universe. *Annual Review of Astronomy and Astrophysics*, *25*(1), 425–472. https://doi.org/10.1146/annurev.aa.25.090187.002233
33. Unified Rotation Curve of the Galaxy -- Decomposition into de Vaucouleurs Bulge, Disk, Dark Halo, and the... (2008). In *ResearchGate*.
www.researchgate.net/publication/23417476_Unified_Rotation_Curve_of_the_G alaxy_--_Decomposition_into_de_Vaucouleurs_Bulge_Disk_Dark_Halo_and_the _9-kpc_Rotation_Dip_--
34. *Vera Rubin on Dark Matter: A Factor of Ten | AMNH*. (n.d.). Retrieved April 23, 2023, from https://www.amnh.org/learn-teach/curriculum-collections/cosmic-horizons-book/v era-rubin-dark-matter
35. Walter1, F., Brinks2, E., Bigiel1, F., Kennicutt, R. C., D., M., & Leroy1, A. K. (n.d.). *∼ D <*. Retrieved November 25, 2022, from https://arxiv.org/pdf/0810.2125v1.pdf
36. Zwicky, A. (n.d.). *A History of Dark Matter Gianfranco Bertone1 and Dan Hooper2,3 1GRAPPA, University of Amsterdam, Netherlands*. Retrieved January 23, 2023, from https://arxiv.org/pdf/1605.04909.pdf

6. Appendix

All HI Spectra https://docs.google.com/document/d/1BOIqgbUp78NVAC-VFmNknYD6iDpCZwH0XHlibRZ_Jis/edit?usp=drivesdk

Observation Reports

Asteroid C8FF042 Entry Event – November 19, 2022

James Van Prooyen

This is an observation report of the earth entry event of Asteroid C8FF042 (also referred to as 2022 WJ1) as observed using a Bi-Static HF Radar we call the Michigan Space Fence (MSF). Shown below is plot of the event:

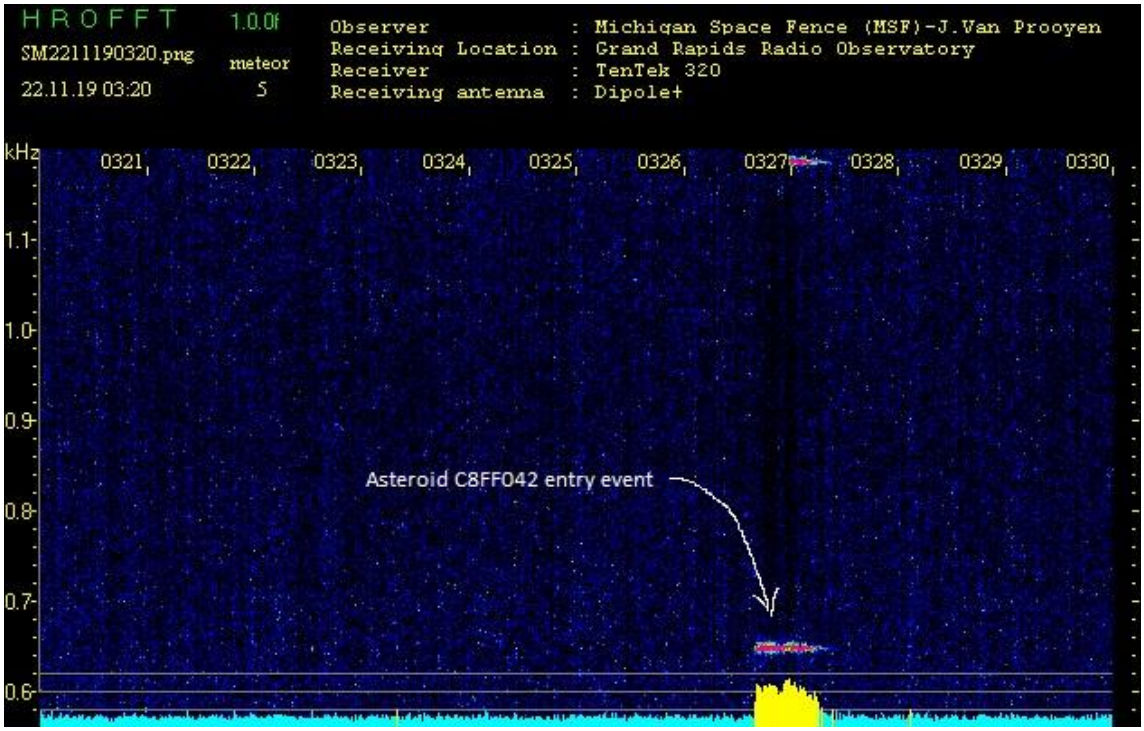

In the next plot we show what "may be" a second event that could be related to C8FF042,

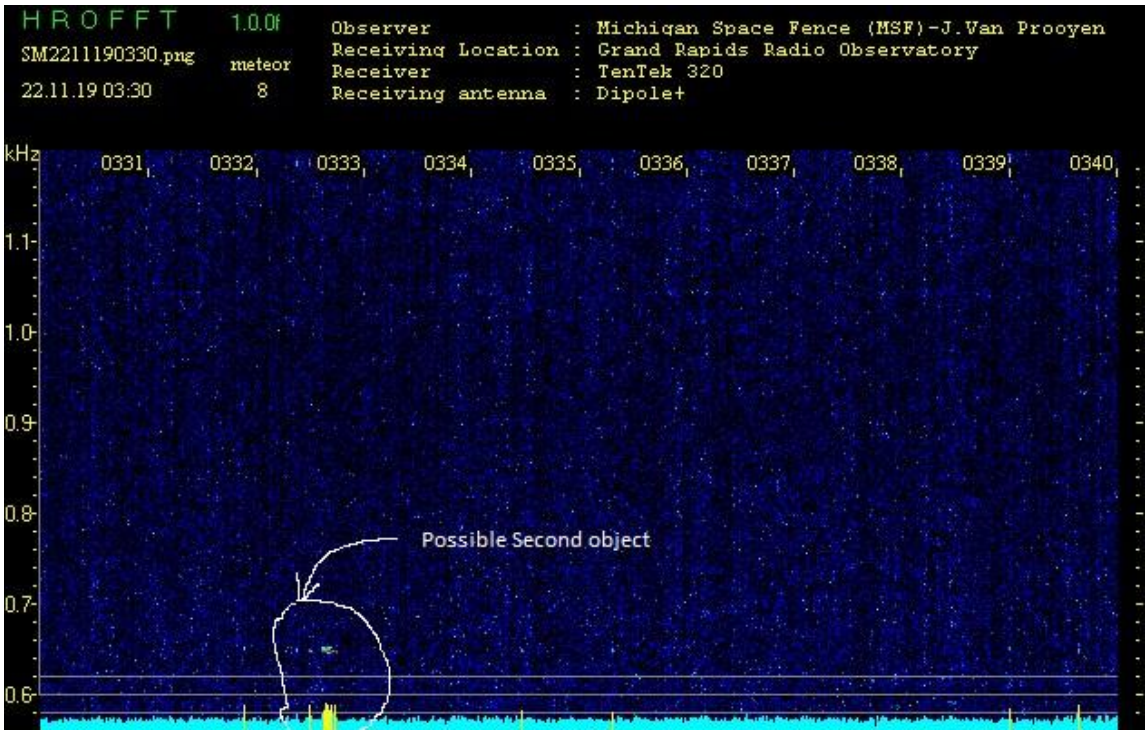

There are no additional reports that would support this, and efforts to contact people who made the discovery of the object have had no response.

Here is the MSF Beam overlaid on the Heat map of the event from the IMO database.

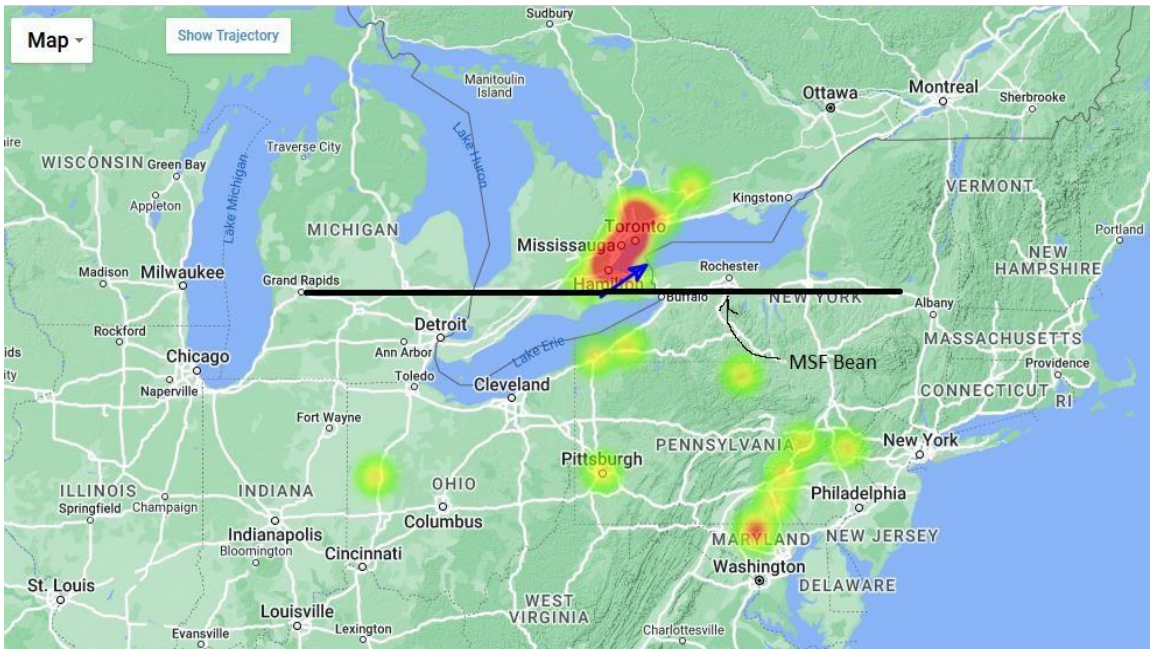

MSF – Michigan Space Fence
A Bi-Static HF Radar looking East from Grand Rapids Michigan across Ontario (Canada) and New York State. It operates 24x7 and is used to count day-time fire ball events. It has been in continues operation for ~4 years, first light was in 2016.

Reference:
2022 WJ1 - Wikipedia https://en.wikipedia.org/wiki/2022_WJ1

The IMO Fireball Report of the event may be found here:
https://fireball.amsmeteors.org/members/imo_view/event/2022/8984

Enjoy

James Van Prooyen - N8PQK Grand Rapids
Radio Observatory grro@sbcglobal.net

Methanol maser line 6.7 GHz observations
by Dimitry Fedorov UA3AVR

This report comprises results obtained for 6.7 GHz methanol maser line (transition $5_1 \rightarrow 6_0$, A^+ molecule type [1]) in last two months using a small dish radio telescope. Observed line belongs to Class II masers, i.e. when a molecular cloud is pumped to inverse state mainly by the infrared radiation from nearby stellar objects, not by collisions.

Setup data

Dish size D = 1.8 m;
Telescope characteristics:
Sensitivity (G, forward gain) – 0.63 mK/Jy;
System temperature $T_{sys} \approx 150$ K (measured, see below);
Source automatic tracking during the integration time.

Outdoor downconverter: Terrasat 6.4-7.1 GHz
RX module (LO 5.7 GHz) + LNA (NF=1.1 dB)
Indoor IF receiver: USRP B200mini,
Receiver resolution – 5 kHz by noise bandwidth (<0.2 km/s in VLSR), total bandwidth – 1.5 MHz;
Location near Moscow (N56.146254, E37.496530).
Dish sensitivity (G, forward gain) was calculated using the formula [2]

$$\mathrm{G} = \eta_A \frac{\pi D^2}{8\,k} \qquad (1)$$

where k – the Boltzmann constant, η_A= 0.68 – the aperture efficiency, calculated from the feed far field pattern using Comsol 3D RF module.

The indoor IF receiver USRP B200mini is controlled using LabVIEW software with on-fly averaging of spectrum during the integration time (no intermediate data are stored), see more details about the receiver and post processing procedures in [3].

T_{sys} measurements

The system temperature was measured by the Y-factor method using the formula:

$$T_{sys} = \frac{T_{hot} - Y\,T_{cold}}{Y - 1} \qquad (2)$$

where $Y=P_{hot}/P_{cold}$, P_{hot} and P_{cold} are the receiver response in power units when the antenna beam sees radiating objects with T_{hot} and T_{cold} temperatures, respectively. Approximate values of temperatures are:

T_{hot} ≈ 280 K when antenna is directed to the warm brickwall (see right, it is assumed that the noise temperature of such brickwall is somewhat colder than ambient temperature ≈ 290 K);

T_{cold} ≈ 10 K when antenna is directed to the sky with elevation about 30-40 deg.

Measured Y-factor = 4.3 dB (2.69 as a power ratio), and we have T_{sys} ≈ 150 K from the formula (2). The receiver noise contributes ≈ 95 K to T_{sys}; therefore, ground and surrounding objects contribute ≈ 55 K due to the dish spillover.

Results

Here are the line spectrums received for several masers. They can be compared to professional results from Ibaraki database [4]. All observation were made with the observation time ≈ 1 hour (except the last Cepheus A spectrum with 2 hours of integration)..

- W3(OH) maser (G133.94+1.04). Expected peak flux is >3000 Jy, but received peak flux do not exceed 2000 Jy. Nevertheless, this is outstandingly stable and strong maser. The peak velocity and line width correspond to expected ones. This maser source can be applied as a beacon for receiver checks. Showed spectrum is received 2022-05-27:

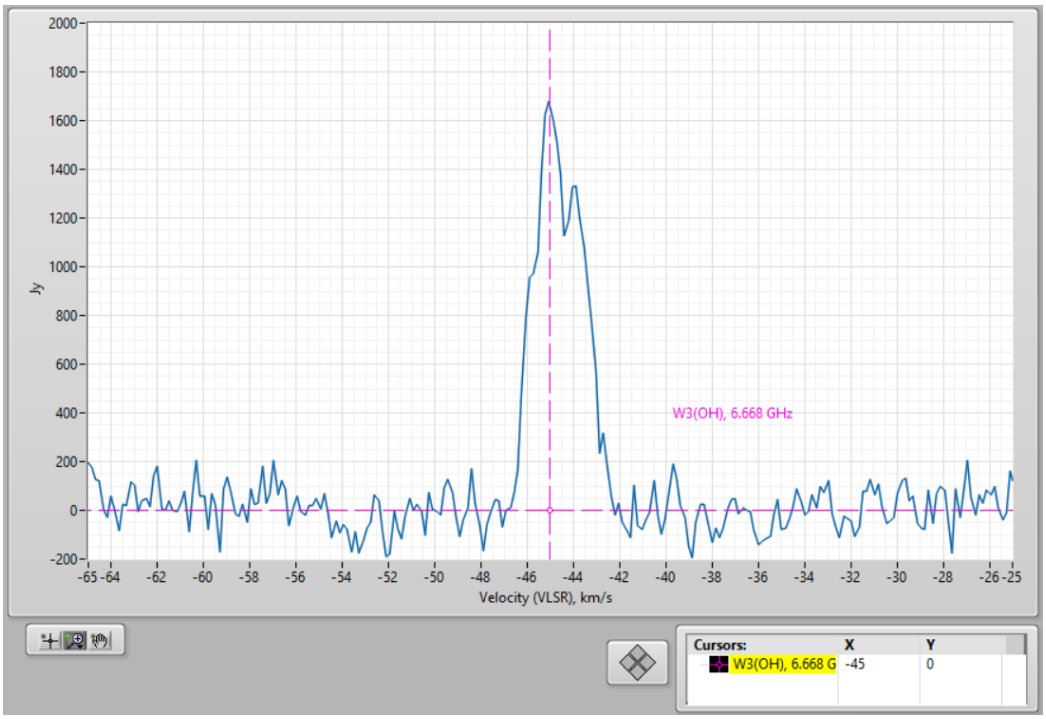

- Maser line form the object G188.94+0.89. The peak flux, velocity and line width correspond to expected ones. The spectrum received 2022-05-31:

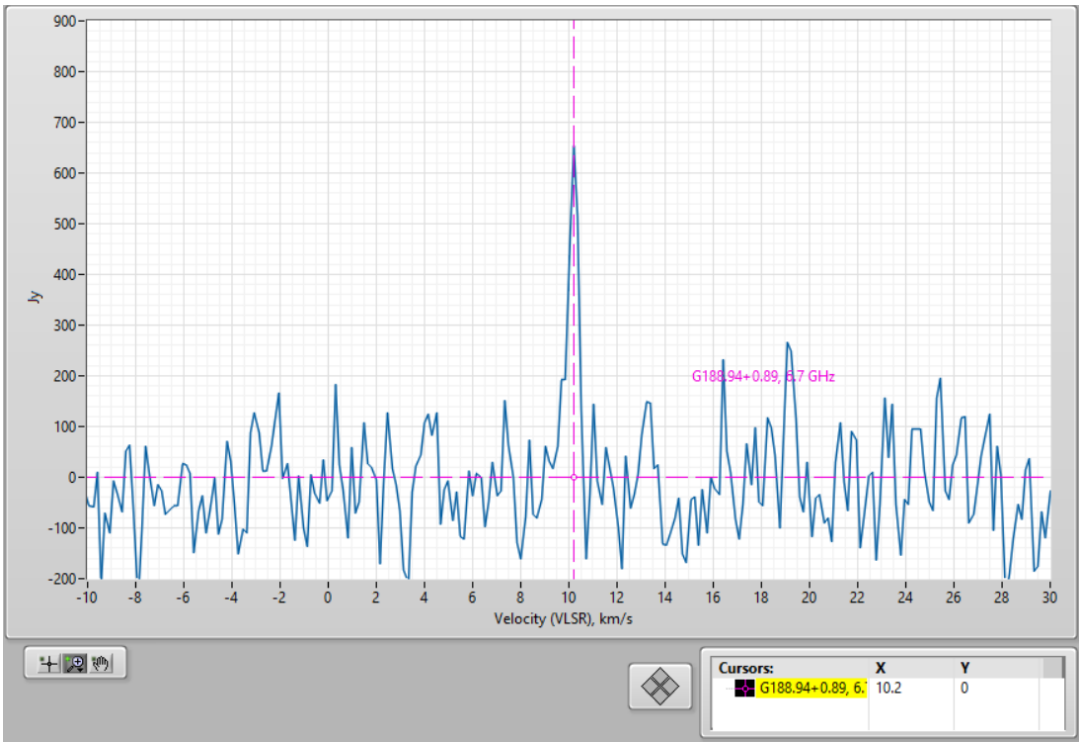

Similar spectrum was received several days later, 2023-06-03:

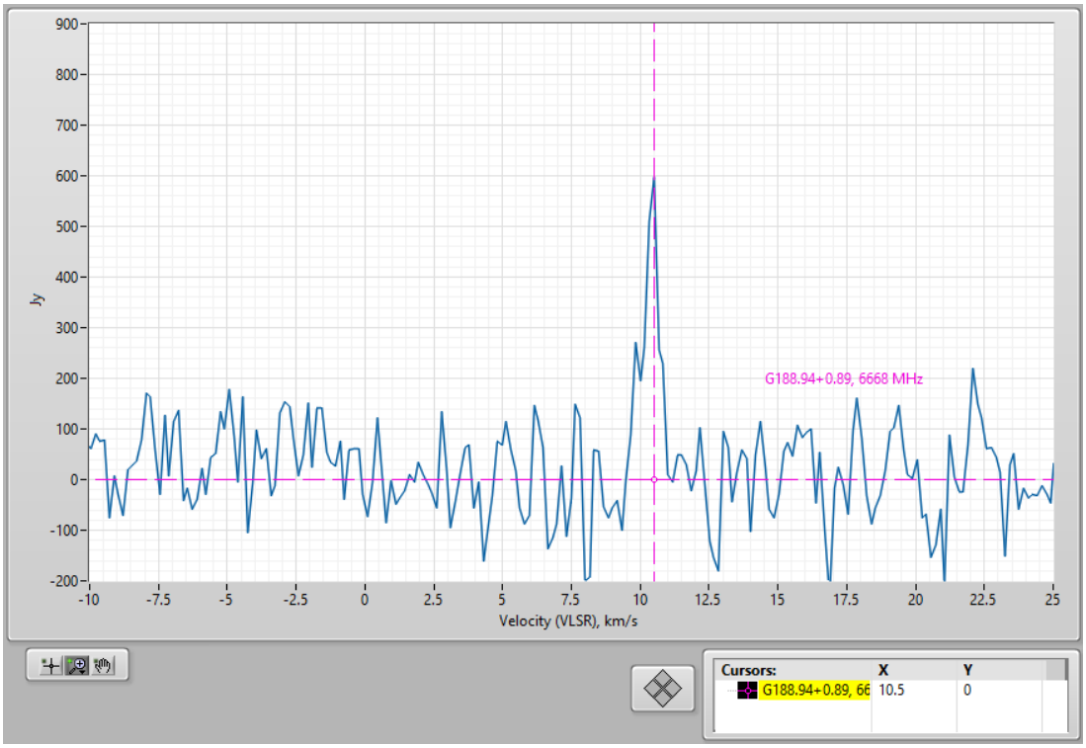

- Cepheus A maser (G109.86+2.10). This maser is significantly variable and may have two well distinctive peaks. The peak fluxes, velocities and line widths correspond to expected ones. The spectrum received 2022-04-15 (with my old receiver with T_{sys}>200 K):

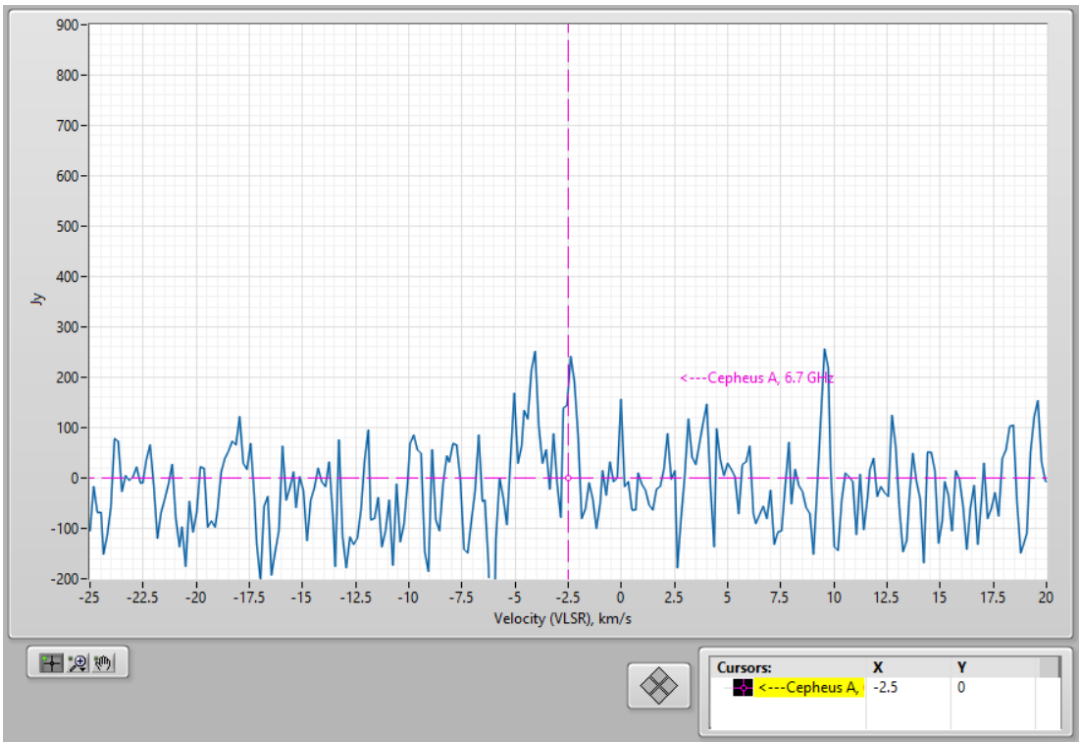

Next, the two line spectrum was observed again 2023-06-04,

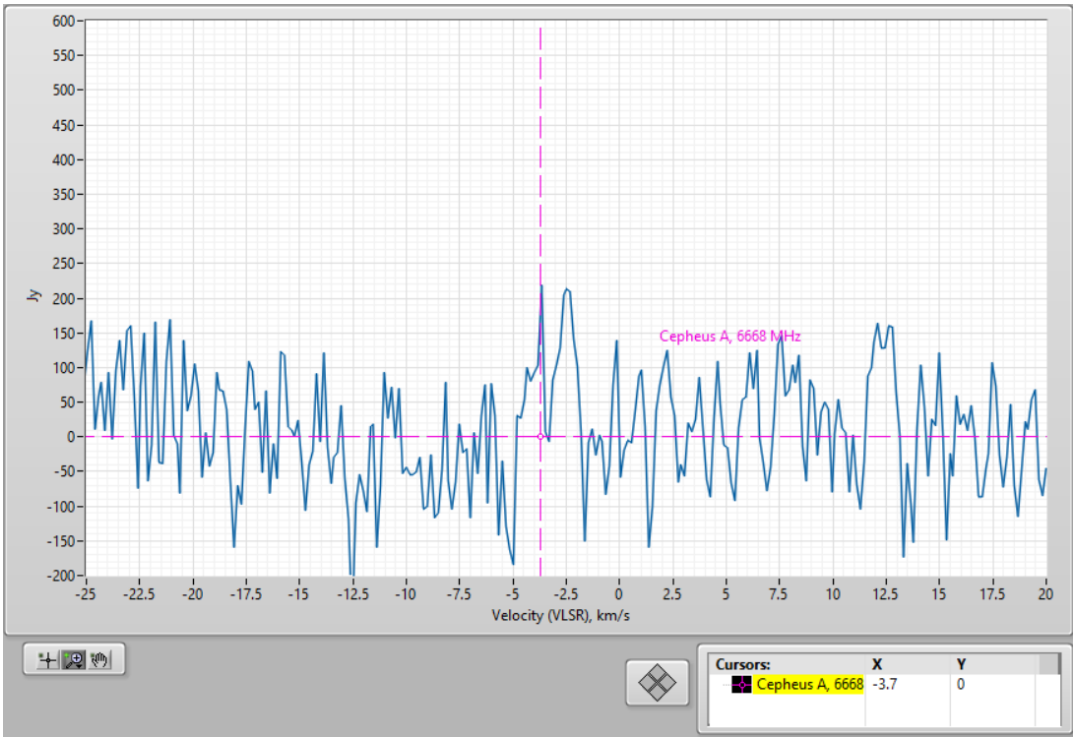

but the measurements several days after (2023-06-08) have given only one fairly seen line with a bit higher peak flux. The integration time is about 2 hours. The peak velocity of observed line is close to 4 km/s and corresponds to usually weaker line of this maser (see spectrums at http://vlbi.sci.ibaraki.ac.jp/iMet/data/109.8+21/):

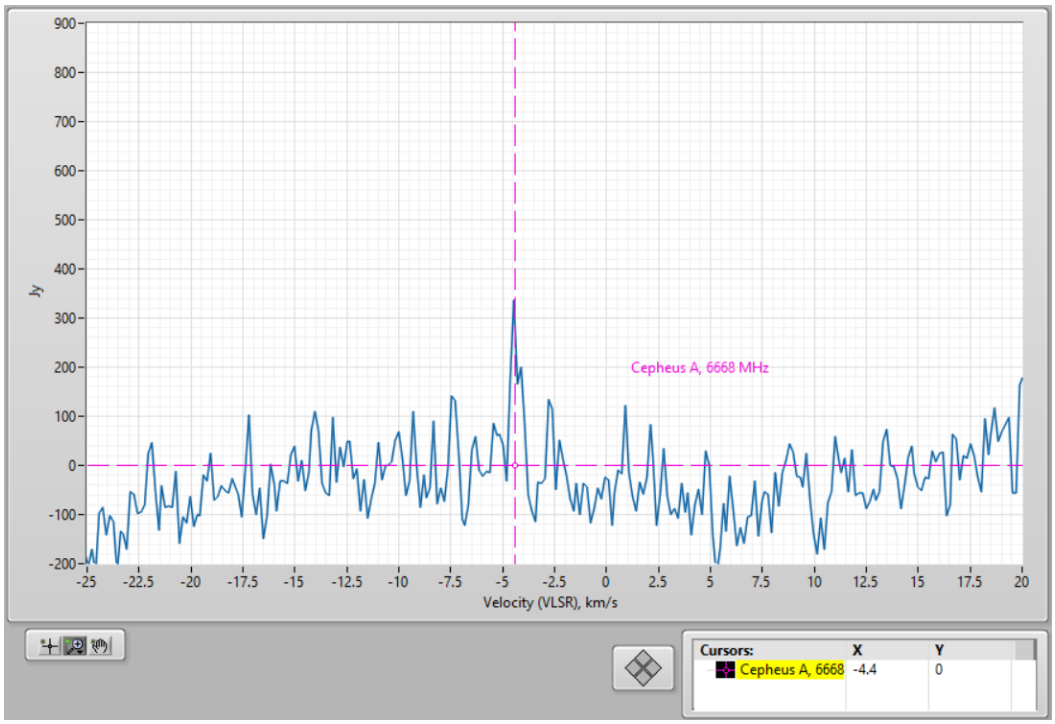

Acknowledgments

to Eduard Mol for references to Ibaraki database iMet;
to Alex Nersesian K6VHF for help with downconverter.

References

[1] H.S.P. Mueller, K.M. Menten, H. Maeder, Accurate rest frequencies of methanol maser and dark cloud lines, arXiv:astro-ph/0408094v2, https://arxiv.org/abs/astro-ph/0408094v2.
[2] T.L. Wilson, K. Rohlfs, S. Hüttemeister, *Tools of Radio Astronomy*, 6th ed, Springer, 2013, see page 173, eq. (7.25).
[3] D. Fedorov UA3AVR, *Methanol maser lines 12 GHz observations*, Radio Astronomy, Journal of the Society of Amateur Radio Astronomers, September – October 2022, page 71.
[4] Ibaraki methanol maser line 6.7 GHz database iMet, http://vlbi.sci.ibaraki.ac.jp/iMet/ (data are retrieved by galactic coordinate identifiers).

About the author

Dimitry Fedorov was first licensed as radio amateur since 1982, as UA3AVR since 1983. In 1990 graduated as MS in electronics in Moscow Power Engineering University. Now works as research and development engineer in wireless industry, LTE/5G NR, RF and microwave modules development. Previous scientific experience in nuclear and particle physics, worked in Moscow State University, Institute of Nuclear Physics and Universität Tübingen, Institut für Theoretische Physik, see profile blog at https://www.researchgate.net/profile/Dimitry-Fedorov-2. Radio Astronomy hobby since 2012, mainly in applications for weak signals reception. You can contact the author at ua3avr@yandex.ru.

Journal Archives and Other Promotions

The rich and diverse legacy of member contributed content is available in the SARA Journal Archives. Table of contents for journals is available online at: SARA-Journal-Master-Index.xlsx (live.com)

The entire set of The Journal of The Society of Amateur Radio Astronomers is available by online download. It goes from the beginning of 1981 to the end of 2022 (over 6000 pages of SARA history!)

All SARA journals and conference proceedings are available through the previous calendar year.

SARA Store (radio-astronomy.org/store.)

SARA offers the above USB drives, DVDs, printed Proceedings and Proceedings on USB drive and other items at the SARA Store: http://www.radio-astronomy.org/e-store. Proceeds from sales go to support the student grant program. Members receive an additional 10% discount on orders over $50 US. Payments can be made by sending payment by PayPal to treas@radio-astronomy.org or by mailing a check or money order to SARA, c/o Brian O'Rourke, 337 Meadow Ridge Rd, Troy, VA 22974-3256

SARA Online Discussion Group
SARA members participate in the online forum at http://groups.google.com/group/sara-list. This is an invaluable resource for any amateur radio astronomer.

SARA Conferences
SARA organizes multiple conferences each year. Participants give talks, share ideas, attend seminars, and get hands-on experience. For more information, visit http://www.radio-astronomy.org/meetings.

What is Radio Astronomy?

Radio Astronomy is just what the name implies…. Astronomy observed at radio wavelengths instead of optical. But why do radio astronomy? Radio astronomy has expanded the knowledge of the universe about as much since its discovery in 1932 as optical has since humans first looked up at the sky. (The sky in the different frequencies or colors of radio are as different and varied as all of the flowers on Earth. Each frequency has its own information about what is happening in the universe.) This knowledge has been gained by both professional astronomers as well as amateurs with amateurs contributing to this day.

Do I need a big dish and expensive equipment?
No. Complete beginner projects are available at the SARA store at very reasonable prices. You can monitor the Sun's effects upon our planet with SuperSID. This information is gathered for Stanford for research into our ionosphere and radio signal propagation. Another project is the detection the hydrogen line just like Dr. Ewen had done in 1951 for a fraction of the cost using the Scope in a Box kit.

That said, radio astronomy is like optical astronomy in that you can spend as much as you want to. Many amateurs push the lower boundaries of cost by using very low-cost receivers and low-noise low-cost amplifiers that were not available even a few years ago. (See the Scope in a Box kit in the store for examples of both.)

Is everything 'plug and play' and boring?
The kits mentioned above are a starting point which are mostly plug-and-play… that gets you started. After you have mastered the basics, where you go from there depends upon your interests. Monitoring pulsars is done by amateurs. (One even noticed a pulsar glitch before the professionals!) These amateurs are pushing the boundaries of what can be done. Papers are being published and discussion had about pulsar detection as well detection of a MASER with a 50 inch dish. Techniques on new detection methods are posted in the SARA forum and elsewhere. You are free to build your own equipment to receive the signals as well as software to collect and analyze the data.

What is SETI?
SETI is the Search for Extra-Terrestrial Intelligence. Some amateurs scan the sky and search for signals that might be from aliens. To date no one has received a definitive alien signal (professional or amateur), but the search continues. The search has resulted not just in better receiving equipment but also wide and lively discussions about how aliens might communicate and how they might be trying to contact us. Some of these techniques have interesting ideas for our own communication techniques here on Earth!

What should I do to get started?
You should start with reading our Introduction to Radio Astronomy and joining our online SARA Forum. Look at the SARA store to get a project to get your feet wet without much expense and minimal risk. We will work with you so you can succeed.

Administrative

Officers, directors, and additional SARA contacts

The Society of Amateur Radio Astronomers is an all-volunteer organization. The best way to reach people on this page is by email with SARA in the subject line SARA Officers.

President: Dr. Rich Russel, AC0UB, https://www.radio-astronomy.org/contact/President
Vice President: Jay Wilson, https://www.radio-astronomy.org/contact/Vicepresident
Secretary: Bruce Randall, NT4RT, https://www.radio-astronomy.org/contact/Secretary
Treasurer: Brian O'Rourke, K4UL, https://www.radio-astronomy.org/contact/Treasurer
Past President: Dennis Farr
Founder Emeritus and Director: Jeffrey M. Lichtman, KI4GIY, jeff@radioastronomysupplies.com

Board of Directors

Name	Term expires	Email
Ed Harfmann	2024	edharfmann@comcast.net
Dr. Wolfgang Herrmann	2023	messbetrieb@astropeiler.de
Tom Jacobs	2023	tdj0@bellsouth.net
Charles Osborne	2023	k4cso@twc.com
Bob Stricklin	2024	bstrick@n5brg.com
Steve Tzikas	2024	Tzikas@alum.rpi.edu
Jon Wallace	2023	wallacefj@comcast.net
David Westman	2024	david.westman@engineeringretirees.org

Other SARA Contacts

All Officers	http://www.radio-astronomy.org/contact-sara	
All Directors and Officers	http://www.radio-astronomy.org/contact/All-Directors-and-Officers	
Eastern Conference Coordinator	http://www.radio-astronomy.org/contact/Annual-Meeting	
All Radio Astronomy Editors	http://www.radio-astronomy.org/contact/Newsletter-Editor	
Radio Astronomy Editor	Dr. Richard A. Russel	drrichrussel@netscape.net
Contributing Editor	Whitham D. Reeve	whitreeve@gmail.com
Educational Outreach	http://www.radio-astronomy.org/contact/Educational-Outreach	
Grant Committee	Tom Crowley	grants@radio-astronomy.org
Membership Chair	http://www.radio-astronomy.org/contact/Membership-Chair	
Technical Queries (David Westman)	http://www.radio-astronomy.org/contact/Technical-Queries	
Webmaster	Ciprian (Chip) Sufitchi, N2YO	webmaster@radio-astronomy.org

Resources

Great Projects to Get Started in Radio Astronomy

Radio Observing Program

The Astronomical League (AL) is starting a radio astronomy observing program. If you observe one category, you get a Bronze certificate. Silver pin is two categories with one being personally built. Gold pin level is at least four categories. (Silver and Gold level require AL membership which many clubs have membership. For the bronze level, you need not be a member of AL.)

Categories include
1) SID
2) Sun (aka IBT)
3) Jupiter (aka Radio Jove)
4) Meteor back-scatter
5) Galactic radio sources

This program is a collaboration between NRAO and AL. Steve Boerner is the Lead Coordinator and a SARA member.

For more information:
Steve Boerner
2017 Lake Clay Drive
Chesterfield, MO 63017
Email: sboerner@charter.net
Phone: 636-537-2495
http://www.astroleague.org/programs/radio-astronomy-observing-program

Radio Jove

The Radio Jove Project monitors the storms of Jupiter, solar activity and the galactic background. The radio telescope can be purchased as a kit, or you can order it assembled. They have a terrific user group you can join.
http://radiojove.gsfc.nasa.gov/

INSPIRE Program

The INSPIRE program uses build-it-yourself radio telescope kits to measure and record VLF emissions such as tweeks, whistlers, sferics, and chorus along with man-made emissions. This is a very portable unit that can be easily transported to remote sites for observations.
http://theinspireproject.org/default.asp?contentID=27

SARA/Stanford SuperSID

Stanford Solar Center and the Society of Amateur Radio Astronomers have teamed up to produce and distribute the SuperSID (Sudden Ionospheric Disturbance) monitor. The monitor utilizes a simple pre-amp to magnify the VLF radio signals which are then fed into a high definition sound card. This design allows the user to monitor and record multiple frequencies simultaneously. The unit uses a compact 1-meter loop antenna that can be used indoors or outside. This is an ideal project for the radio astronomer that has limited space. To request a unit, send an e-mail to supersid@radio-astronomy.org

Radio Astronomy Online Resources

SARA YouTube Videos: https://www.youtube.com/channel/UC-SzptAQZ-20c9CkRb9ZPxw/videos	Pisgah Astronomical Research Institute: www.pari.edu
AJ4CO Observatory – Radio Astronomy Website: http://www.aj4co.org/	A New Radio Telescope for Mexico - ORION 2021 01 20. Dr. Stan Kurtz https://www.youtube.com/watch?v=Q9aBWr1aBVc
Radio Astronomy calculators https://www.aj4co.org/Calculators/Calculators.html	National Radio Astronomy Observatory http://www.nrao.edu
Introduction to Amateur Radio Astronomy (presentation) http://www.aj4co.org/Publications/Intro%20to%20Amateur%20Radio%20Astronomy,%20Typinski%20(AAC,%202016)%20v2.pdf	NRAO Essential Radio Astronomy Course http://www.cv.nrao.edu/course/astr534/ERA.shtml
RF Associates Richard Flagg, rf@hawaii.rr.com 1721-1 Young Street, Honolulu, HI 96826	Exotic Ions and Molecules in Interstellar Space -- ORION 2020 10 21. Dr. Bob Compton https://www.youtube.com/watch?v=r6cKhp23SUo&t=5s
RFSpace, Inc. http://www.rfspace.com	The Radio JOVE Project & NASA Citizen Science – ORION 2020.6.17. Dr. Chuck Higgins https://www.youtube.com/watch?v=s6eWAxJywp8&t=5s
CALLISTO Receiver & e-CALLISTO http://www.reeve.com/Solar/e-CALLISTO/e-callisto.htm	UK Radio Astronomy Association http://www.ukraa.com/
Deep Space Exploration Society http://DSES.science	CALLISTO software and data archive: www.e-callisto.org
Deep Space Object Astrophotography Part 1 -- ORION 2021 02 17. George Sradnov https://www.youtube.com/watch?v=Pm_Rs17KIyQ	Radio Jove Spectrograph Users Group http://www.radiojove.org/SUG/
European Radio Astronomy Club http://www.eracnet.org	Radio Sky Publishing http://radiosky.com
British Astronomical Association – Radio Astronomy Group http://www.britastro.org/baa/	The Arecibo Radio Telescope; It's History, Collapse, and Future - ORION 2020.12.16. Dr. Stan Kurtz, Dr. David Fields https://www.youtube.com/watch?v=rBZlPOLNX9E
Forum and Discussion Group http://groups.google.com/group/sara-list	Shirleys Bay Radio Astronomy Consortium marcus@propulsionpolymers.com
GNU Radio https://www.gnuradio.org/	SARA Twitter feed https://twitter.com/RadioAstronomy1
SETI League http://www.setileague.org	SARA Web Site http://radio-astronomy.org
NRAO Essential Radio Astronomy Course http://www.cv.nrao.edu/course/astr534/ERA.shtml	Simple Aurora Monitor: Magnetometer http://www.reeve.com/SAMDescription.htm
NASA Radio JOVE Project http://radiojove.gsfc.nasa.gov Archive: http://radiojove.org/archive.html https://groups.io/g/radio-jove	Stanford Solar Center http://solar-center.stanford.edu/SID/
National Radio Astronomy Observatory http://www.nrao.edu	

For Sale, Trade and Wanted

At the SARA online store: radio-astronomy.org/store.

SARA Polo Shirts

New SARA shirts have arrived.

We now have a good selection of X, XX, and XXX shirts available in all colors including white!

Shirts are $20 at the conference and $25 shipped.

Contact the treasurer at treas@radio-astronomy.org for availability and shipping.

Scope in a Box

radio-astronomy.org/store.

Kit of parts and software to build a working Radio Telescope to detect Hydrogen Line emissions. Available to USA addresses only at this time.

SuperSID Complete Kit
radio-astronomy.org/store.

SARA Publication, Journals and Conference Proceedings (various prices)
radio-astronomy.org/store.

SARA Journal Online Download
radio-astronomy.org/store.

The USB drive covers the society journal "Radio Astronomy" from the founding of the organization in 1981 thru 2020. Articles cover a wide range of topics including: cosmic radiation, pulsars, quasars, meteor detection, solar observing, Jupiter, Radio Jove, gamma ray bursts, the Itty Bitty Telescope (IBT), dark matter, black holes, the Jansky antenna, methanol masers, mapping at 408 MHz and more. This CD contains all of the above and more with over 4800 pages of articles on radio astronomy. Also included is a copy of Grote Reber's handwritten, 34 page document "Carriage and Mirror Detail" of his historic antenna now on display at the National Radio Astronomy Observatory (NRAO) in Greenbank, WV. You also get an electronic copy of the 109 page "Basics of Radio Astronomy" from JPL Goldstone-Apple Valley Radio Telescope. Also included is the NRAO 40-foot radio telescope "Operators Manual", which by the way, you get to operate if you attend the Eastern SARA conference in July.

SARA Advertisements

There is no charge to place an ad in Radio Astronomy; but you must be a current SARA member. Ads must be pertinent to radio astronomy and are subject to the editor's approval and alteration for brevity. Please send your "For Sale," "Trade," or "Wanted" ads to edit@radio-astronomy.org. Please include email and/or telephone contact information. Please keep your ad text to a reasonable length. Ads run for one bimonthly issue unless you request otherwise.

Radio-Astro-Machine, zzblac@gmail.com
Elevation rotation adapter plate for Scope in a Box and custom machining. For further information visit https://radio-astro-machine.wixsite.com/my-site or send an email.

Typinski Radio Astronomy, Inc., info@typinski.com
Antenna systems and feed line components for HF radio astronomy

Jeff Kruth, WA3ZKR, kmec@aol.com
RF components from HF to MMW, various types including mixers, RF switches, amplifiers, oscillators, coaxial components, waveguide components, etc. I have a very large collection of stuff and the facilities to test and provide data. Please email with your needs and I will see if I have something for you. Have fun!

Stuart and Lorraine Rumley, sales@valontechnology.com
The Valon Technology 2100 Downconverter, when combined with our 5009 frequency synthesizer module, provides a high-performance, compact receiver downconverter system. Applications include hydrogen line studies at 1420MHz and radio astronomy in the protected 30MHz segment of the 21 cm band. For more information visit http://www.valontechnology.com/2100downconverter.html or send an email.

Radio2Space, filippo.bradaschia@primalucelab.com
SPIDER radio telescopes and turn-key-systems designed specifically for education.
https://www.radio2space.com
We developed our SPIDER radio telescopes as turn-key-system just to avoid the problem you perfectly highlighted in your website: "Purchasing a radio telescope isn't like buying an optical telescope. They are harder to find, and usually require assembly and software troubleshooting. In some cases, a radio telescope must be built from components." Our SPIDER radio telescopes are not designed for amateurs that prefer to build a radio telescope but to schools, universities, museums, and other science institutes that needs for a complete and ready-to-use system, just like the optical telescopes they can normally buy!

Membership Information

Annual SARA dues Individual $20, Classroom $20, Student $5 (US funds) anywhere in the world. Membership includes a subscription to Radio Astronomy, the bimonthly Journal of The Society of Amateur Radio Astronomers, delivered electronically (via a secure web link, emailed to you as each new issue is posted). We regret that printing and postage costs prevent SARA from providing hardcopy subscriptions to our Journal.

We would appreciate the following information included with your check or money order, made payable to SARA:

Name: _____

Email Address : _____
(required for electronic Journal delivery)

Ham call sign: _____ (if applicable)

Address: _____

City: _____

State: _____

Zip: _____

Country: _____

Phone: _____

Please include a note of your interests. Send your application for membership, along with your remittance, to our Treasurer.

For further information, see our website at:
http://radio-astronomy.org/membership

How to get started?

SARA has a made a kit of software and parts to detect the Hydrogen line signal from space. This is an excellent method to get started in radio astronomy. It teaches the principles of antenna design, signal detection, and signal processing. Read more about this and other projects on our web site.

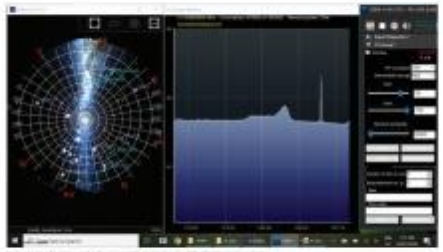

Society of Amateur Radio Astronomers, Inc.
Founded 1981

Membership supported, nonprofit [501(c) (3)]
Educational and Radio Astronomy Organization

Knowledge through Common Research, Education and Mentoring

SARA members have been privileged to use this forty foot diameter drift-scan hydrogen line radio telescope every year at their annual meeting in Green Bank.

http://radio-astronomy.org

Why Radio Astronomy?

Because about sixty five percent of our current knowledge of the universe has stemmed from radio astronomy alone. The discovery of quasars, pulsars, black holes, the 3K background from the "Big Bang" and the discovery of biochemical hydrogen/carbon molecules are all the result of professional radio astronomy.

The Society of Amateur Radio Astronomers

SARA was founded in 1981, with the purpose of educating those interested in pursuing amateur radio astronomy.

The society is open to all, wishing to participate with others, worldwide.

SARA members have many interests, some are as follows:

SARA Areas of Study and Research:

- Solar Radio Astronomy
- Galactic Radio Astronomy
- Meteor Detection
- Jupiter
- SETI
- Gamma Ray/High Energy Pulse
- Detection
- Antennas
- Design of Hardware / Software

The members of the society offer a friendly mentor atmosphere. All questions and inquiries are answered in a constructive manner. No question is silly!

SARA offers its members an electronic bi-monthly journal entitled Radio Astronomy. Within the journal, members report on their research and observations. In addition, members receive updates on the professional radio astronomy community and, society news.

Once a year SARA meets for a three-day conference at the Green Bank Observatory in Green Bank West Va.

There is also a spring conference held at various cities in the Western USA. Previous meeting have been at the VLA in Socorro, NM and at Stanford University.

How do I get started?

Just as a long journey begins with the first step, the project you elect must start with a clear idea of your objectives. Do you wish to study the sun? Jupiter? Make meteor counts? Do you wish to engage in imaging radio astronomy? What you decide will not only determine the type of equipment you will need, but also the local radio spectrum.

How do amateurs do radio astronomy?

Radio astronomy by amateurs is conducted using antennas of various shapes and sizes, from smaller parabolic dishes to simple wire antennas. These antennas are connected to receivers and most of these receivers are software defined radios these days. Data from the receivers are collected by computers, and the received signals will be displayed as charts, graphs or maybe even sky maps. As diverse as the observed objects, so is are the instruments and tools used. SARA members will always be supportive to find good solutions for what one wishes to observe.

Is amateur radio astronomy instrumentation expensive?

Technical information freely circulated in our monthly journal helps amateurs to obtain good low noise equipment from off the shelf assemblies, or to build their own units. The actual cash investment in radio astronomy equipment need not exceed that of any other hobby.

What are amateurs actually looking for in the received data?

The aim of the radio amateur is to find something new and unusual. Just as an amateur optical observer hopes to notice a supernova or a new comet, so does an amateur radio observer hope to notice a new radio source, or one whose radiation has changed appreciably.

The Reber Telescope at NRAO. Constructed by Grote Reber in 1937 in his back yard in Wheaton, Illinois

SARA Members discussing the IBT (Itty Bitty Telescope)